



UNIVERSITAT POLITÈCNICA
DE CATALUNYA
BARCELONATECH

Synthesis and characterization of polycarbonates from epoxidized vegetable oils, propylene oxide and carbon dioxide

Farra Wahida binti Shaarani

ADVERTIMENT La consulta d'aquesta tesi queda condicionada a l'acceptació de les següents condicions d'ús: La difusió d'aquesta tesi per mitjà del repositori institucional UPCommons (<http://upcommons.upc.edu/tesis>) i el repositori cooperatiu TDX (<http://www.tdx.cat/>) ha estat autoritzada pels titulars dels drets de propietat intel·lectual **únicament per a usos privats** emmarcats en activitats d'investigació i docència. No s'autoritza la seva reproducció amb finalitats de lucre ni la seva difusió i posada a disposició des d'un lloc aliè al servei UPCommons o TDX. No s'autoritza la presentació del seu contingut en una finestra o marc aliè a UPCommons (*framing*). Aquesta reserva de drets afecta tant al resum de presentació de la tesi com als seus continguts. En la utilització o cita de parts de la tesi és obligat indicar el nom de la persona autora.

ADVERTENCIA La consulta de esta tesis queda condicionada a la aceptación de las siguientes condiciones de uso: La difusión de esta tesis por medio del repositorio institucional UPCommons (<http://upcommons.upc.edu/tesis>) y el repositorio cooperativo TDR (<http://www.tdx.cat/?locale-attribute=es>) ha sido autorizada por los titulares de los derechos de propiedad intelectual **únicamente para usos privados enmarcados** en actividades de investigación y docencia. No se autoriza su reproducción con finalidades de lucro ni su difusión y puesta a disposición desde un sitio ajeno al servicio UPCommons No se autoriza la presentación de su contenido en una ventana o marco ajeno a UPCommons (*framing*). Esta reserva de derechos afecta tanto al resumen de presentación de la tesis como a sus contenidos. En la utilización o cita de partes de la tesis es obligado indicar el nombre de la persona autora.

WARNING On having consulted this thesis you're accepting the following use conditions: Spreading this thesis by the institutional repository UPCommons (<http://upcommons.upc.edu/tesis>) and the cooperative repository TDX (<http://www.tdx.cat/?locale-attribute=en>) has been authorized by the titular of the intellectual property rights **only for private uses** placed in investigation and teaching activities. Reproduction with lucrative aims is not authorized neither its spreading nor availability from a site foreign to the UPCommons service. Introducing its content in a window or frame foreign to the UPCommons service is not authorized (*framing*). These rights affect to the presentation summary of the thesis as well as to its contents. In the using or citation of parts of the thesis it's obliged to indicate the name of the author.



UNIVERSITAT POLITÈCNICA
DE CATALUNYA
BARCELONATECH

Synthesis and Characterization of Polycarbonates from Epoxidized Vegetable Oils, Propylene Oxide and Carbon Dioxide

Dissertation submitted to the
Polytechnic University of Catalonia, Barcelona Tech
In Partial Fulfilment of the Requirements for the
Degree of Doctor of Philosophy
in **Chemical Engineering**

Author:

Farra Wahida binti Shaarani

Main Director:

Prof. Dr. Jordi Bou Serra

Department of Chemical Engineering

February 2021

ACKNOWLEDGEMENT

First and foremost, I would like to offer my unreserved gratitude and praises to Almighty God who has bestowed upon me His generous blessing and grace during the course of this study.

This doctoral thesis is in its current form due to the assistance and encouragement of my supervisor. My deepest gratitude to Professor Dr. Jordi Bou Serra for his whole-hearted involvement, inspiration and constant support during the entire period of research work. All the suggestions, constructive criticisms and careful review from you helped shape and improve this dissertation.

I wish to acknowledge Universiti Kuala Lumpur for providing the administrative and financial support for me to undertake this study. I would also like acknowledge the monetary funding received from Majlis Amanah Rakyat (MARA) programme. I also like to convey my appreciation towards the Spanish Ministry of Economy and Competitiveness for the financial assistance that I have benefitted over the course of my study.

I would also like to put forward my gratitude to the all the present and past members of Department of Chemical Engineering, Universitat Politècnica de Catalunya Barcelona Tech (ETSEIB) namely Professor Dr. Antxon Martinez De Ilarduya Saez De Asteasu, Dr. Marti Hortós Lobera, Miss Laura de Sousa and all the numerous people whose names have not been mentioned for their co-operation and help during my tenure in Department of Chemical Engineering, ETSEIB.

I wish to express my gratitude towards my wonderful parents and my family including my siblings and my in-laws for their understanding and support. Last but not least, my highest gratitude and appreciation towards my husband who has always been the love of my life and my pillar of strength throughout the course of this study.

ABSTRACT

The current research is primarily focused on the preparation of a polycarbonate using epoxidized linseed oil (ELO) and epoxidized soybean oil (ESO) as feedstocks. The presence of unsaturation in vegetable oil structure enables chemical modifications to introduce epoxy group which further used to synthesize polycarbonate via catalytic copolymerization with carbon dioxide (CO₂). In this study, with the presence of heterogeneous catalyst a mixture of epoxidized vegetable oil and propylene oxide (PO) were reacted with CO₂. The produced polymeric products were characterized using Fourier Transform Infra-Red (FTIR) Spectroscopy, Proton Nuclear Magnetic Resonance (¹H NMR) spectroscopy and Gel Permeation Chromatography (GPC). Synthesis of polycarbonate via this pathway helps to lessen the reliance on petroleum-based feedstocks and besides employing renewable raw materials meets the 7th principle of 12 Principles of Green Chemistry that contributes to sustainability in chemistry.

The research work is divided into four phases. The first phase comprises preliminary studies whereby preparation of a heterogeneous catalyst for the copolymerization of epoxide with CO₂ was made. Catalyst screening tests showed that cobalt-zinc double metal cyanide (Co-Zn DMC), a heterogenous catalyst commonly employed in the copolymerization reaction was feasible for cyclohexene oxide (CHO)/CO₂ and PO/CO₂ copolymerization. Then *in-situ* epoxidation of unsaturated fatty acids using selected vegetable oils were carried out to modify vegetable oil to epoxidized vegetable oil. The molar ratio of 0.4:0.1:1.7 (organic acid: double bonds: hydrogen peroxide) were applied and the epoxidation reaction took place at 70°C for five hours. No formation of polymer was observed from the terpolymerization of epoxidized olive oil (EEO),

epoxidized palm oil (EPaO) and epoxidized sunflower oil (ESFO) most likely due to the low content of epoxy group of the epoxide oils used. However, from the preliminary studies a promising result were obtained from both ELO and ESO whereby a polymer has been successfully developed from the copolymerization reaction.

The second phase of the work is focused on the copolymerization of ESO, PO and CO₂ catalyzed by Co-Zn DMC. Products comprises of mixture of poly(propylene carbonate), cyclic carbonate and polyether unit. The M_n of the polymeric products recorded is 6498 g. mol⁻¹ with the percentage incorporation of ESO in the polymer is only 7.8%.

The third phase of the work is dedicated on the development of a poly(carbonate-co-ether) using ELO as the starting material. The terpolymerization reaction was conducted at fixed CO₂ pressure of 5 MPa and various catalyst loading, reaction temperature and reaction time. At CO₂ pressure of 5 MPa, reaction temperature of 60 °C, reaction time of 24 h and catalyst loading of 0.2 g, the resultant polymer with maximum M_n of 6.21 x 10⁵ g.mol⁻¹ and PDI of 1.05 was recorded.

Finally, the ability of the synthesized polymer to degrade was study under aerobic condition. The aerobic biodegradation of the test materials was determined under controlled composting conditions by analysis of evolved CO₂ using an in-house built direct measurement respirometric (DMR) system. Results from this study disclose that 44.6% of PC-ELO and 51.8% of PC-ESO were degraded at the end of trial period. Both polymers were able to degrade most likely due to the co-monomer employed in the copolymerization reaction are renewable and bio based.

RESUMEN

La investigación que se describe se centra principalmente en la preparación de policarbonatos utilizando aceite de linaza epoxidado (ELO) y aceite de soja epoxidado (ESO) como materias primas. La presencia de insaturación en la estructura del aceite vegetal permite modificaciones químicas para introducir un grupo epoxi que luego se usa para sintetizar los policarbonatos mediante copolimerización catalítica con dióxido de carbono (CO_2). En este estudio, con la presencia de un catalizador heterogéneo se hizo reaccionar una mezcla de aceite vegetal epoxidado y óxido de propileno (PO) con CO_2 . Los productos poliméricos producidos se caracterizaron utilizando espectroscopía de infrarrojos por transformada de Fourier (FTIR), espectroscopía de resonancia magnética nuclear de protones (^1H NMR) y cromatografía de permeación en gel (GPC). La síntesis de policarbonato a través de esta vía ayuda a disminuir la dependencia de materias primas a base de petróleo y, además de emplear materias primas renovables, cumple con el séptimo principio de los 12 principios de la química verde que contribuye a la sostenibilidad en la química.

El trabajo de investigación se divide en cuatro fases. La primera fase comprende estudios preliminares mediante los cuales se realizó la preparación de un catalizador heterogéneo para la copolimerización del epóxido con CO_2 . Las pruebas de selección de catalizadores mostraron que el cianuro doble metálico de cobalto-zinc (Co-Zn DMC), un catalizador heterogéneo comúnmente empleado en la reacción de copolimerización, era factible para la copolimerización de óxido de ciclohexeno (CHO) / CO_2 y PO / CO_2 . Luego se llevó a cabo la epoxidación in situ de ácidos grasos insaturados utilizando aceites vegetales seleccionados para modificar el triglicérido en

aceite vegetal epoxidado. Se aplicó la relación molar de 0,4: 0,1: 1,7 (ácido orgánico: dobles enlaces: peróxido de hidrógeno) y la reacción de epoxidación tuvo lugar a 70°C durante cinco horas. No se observó formación de polímero a partir de la terpolimerización de aceite de oliva epoxidado (EEO), aceite de palma epoxidado (EPaO) y aceite de girasol epoxidado (ESFO) muy probablemente debido al bajo contenido de grupos epoxi. Sin embargo, de los estudios preliminares se obtuvo un resultado prometedor tanto de ELO como de ESO mediante el cual se ha desarrollado con éxito un polímero a partir de la reacción de copolimerización.

La segunda fase del trabajo se centra en la copolimerización de ESO, PO y CO₂ catalizada por Co-Zn DMC. Los productos se componen de una mezcla de poli (carbonato de propileno), carbonato cíclico y unidad de poliéter. El M_n de los productos poliméricos registrados es 6498 g.mol⁻¹ con el porcentaje de incorporación de ESO en el polímero es solo del 7,8%.

La tercera fase del trabajo está dedicada al desarrollo de un poli (carbonato-co-éter) utilizando ELO como material de partida. La reacción de terpolimerización se llevó a cabo a una presión fija de CO₂ de 5 MPa y varias cargas de catalizador, temperatura de reacción y tiempo de reacción. A una presión de CO₂ de 5 MPa, una temperatura de reacción de 60°C, un tiempo de reacción de 24 h y una carga de catalizador de 0,2 g, se registró el polímero resultante con un M_n máximo de 6,21 x 10⁵ g.mol⁻¹.

Finalmente, se estudió la capacidad de degradación del polímero sintetizado en condiciones aeróbicas. La biodegradación aeróbica de los materiales de prueba se determinó en condiciones controladas de compostaje mediante el análisis del CO₂ desprendido utilizando un sistema

respirométrico de medición directa (DMR) de construcción propia. Los resultados de este estudio revelan que el 44,6% de PC-ELO y el 51,8% de PC-ESO se degradaron al final del período de prueba. Ambos polímeros pudieron degradarse muy probablemente debido a que el comonomero empleado en la reacción de copolimerización es renovable y de base biológica.

TABLE OF CONTENTS

Contents

ACKNOWLEDGEMENT	i
ABSTRACT.....	ii
RESUMEN	iv
List of Figures	xii
List of Schemes.....	xv
List of Tables	xvi
List of Appendices	xviii
Abbreviations and Symbols	xix
CHAPTER 1 : INTRODUCTION	1
1.1 Introduction	1
1.2. Objectives.....	6
1.3. Thesis organization	7
CHAPTER 2 : LITERATURE REVIEW	10
2.1 Polycarbonates	10
2.2 Mechanism of epoxide/CO ₂ copolymerization	12
2.3 Catalysts for copolymerization of epoxides with CO ₂	14
2.3.1 Double metal cyanide complex (DMCC) catalyst.....	19

2.3.2	The structure of DMCC Catalyst and Mechanism for copolymerization	22
2.4	Renewable Raw Materials for Polymers	23
2.4.1	Vegetable Oil as Renewable Raw Materials for Polymers	27
2.4.2	Vegetable Oils used in Industry	34
2.4.3	Copolymerization of Vegetable Oils-based Epoxides with CO ₂	43
2.5	Degradation of plastics	47
2.6	Biodegradation	48
2.6.1	Polymer biodegradation	49
2.6.2	Mechanism of Biodegradation	50
2.6.3	Techniques for Evaluation of Biodegradation	52
2.6.4	International standards related to biodegradation and composting	55
2.7	Summary of Literature Review	60
CHAPTER 3 : Preparation of Heterogeneous Catalysts and the Selection of Potential Epoxidized Vegetable Oil for Bio-based Polycarbonate Production via Copolymerization Reaction		62
3.1.	Introduction	62
3.2	Materials and methods	65
3.2.1	Materials	65
3.2.2	Methods	66
3.3	Results and discussion	71
3.3.1	Product analysis and characterization	71

3.3.2	GPC Analysis.....	73
3.3.3	Characterization of Co-Zn DMC catalyst.....	74
3.3.4	Proton Nuclear Magnetic Resonance (¹ H NMR) Analysis.....	78
3.3.5	Epoxidized Vegetable Oil.....	81
3.3.6	Copolymerization of EVO and CO ₂ with Co-Zn DMC.....	87
3.4	Conclusions.....	88
CHAPTER 4 : Synthesis of Vegetable-Oil based Polymer by Terpolymerization of Epoxidized Soybean Oil, Propylene Oxide and Carbon Dioxide.....		
		90
4.1	Abstract.....	91
4.2	Introduction.....	91
4.3	Experimental.....	94
4.3.1	Material.....	94
4.3.2	Preparation of the Catalyst.....	95
4.3.3	Polymerization of ESO, PO and CO ₂	96
4.3.4	Characterizations.....	96
4.3.5	Solubility Test.....	97
4.4	Results and Discussion.....	97
4.4.1	IR of Co-Zn DMC Catalyst.....	97
4.4.2	Properties and Characterization of Terpolymerization Products.....	99
4.4.3	Analysis of Products.....	100

4.5 Conclusions and outlook.....	106
Acknowledgment	107
Appendix C4: Supplementary material.....	108
CHAPTER 5 : Synthesis of Bio-based Poly(carbonate-co-ether) by means of Catalytic Polymerization of Epoxidized Linseed Oil, Propylene Oxide and Carbon Dioxide	
5.1 Abstract	112
5.2 Introduction	112
5.3. Experimental section.....	117
5.3.1. Materials	117
5.3.2. Preparation of the catalyst	117
5.3.3. Polymerization of ELO, PO and CO ₂	118
5.3.4. Characterizations	120
5.4 Results and discussion	120
5.4.1 Co-Zn DMC catalyst	120
5.4.2. Characterization of ELO.....	123
5.4.3. Polymerization of ELO, PO and CO ₂	126
5.4.4. Effect of Operating Conditions	132
5.5 Conclusions.....	134
Acknowledgments.....	135
Appendix C5: Supplementary material.....	136

CHAPTER 6 : Aerobic Biodegradation of Bio-based Poly(carbonate)-co-ether	140
6.1 Abstract	141
6.2 Introduction.....	141
6.3. Experimental	144
6.3.1 Preparation of poly(carbonate)-co-ether.....	144
6.3.2 Biodegradation study.....	148
6.3.3. Data Analysis	152
6.4. Results and Discussion.....	153
6.4.1. Biodegradation environment.....	153
6.4.2. Physical characterizations	156
6.4.3. Aerobic Biodegradation of test materials	157
6.5. Conclusions	166
Acknowledgement	167
Appendix C6. Supplementary material.....	168
CHAPTER 7 : CONCLUSIONS AND RECOMMENDATIONS.....	170
7.1 Conclusions	170
7.2 Recommendations	172
List of Publications and Conferences	174
References.....	176

List of Figures

Figure 1. 1. Examples of bio-based polymers and fossil-based polymers which are biodegradable and non-biodegradable (European Bioplastics, 2019)	2
Figure 2.1. General structure of Polycarbonate	11
Figure 2.2. Flow diagram for synthesis of DMCC catalysts (Ionescu, 2005)	21
Figure 2.3. Plausible structure of DMCC catalyst (Liu et al., 2020)	23
Figure 2.4. Life cycle of polymers based on vegetable oils (Seniha Güner et al., 2006)	25
Figure 2.5. Global production capacities of bioplastic in 2019 (by region) (European Bioplastics, 2019)	26
Figure 2.6. Ripe olive fruit (Krist and Bauer, 2020).....	38
Figure 2.7. Chemical structure of olive oil (Molekuul.be, 2020)	40
Figure 2.8. Chemical structure of palm oil (Clark and Hoong, 2014)	41
Figure 2.9. Chemical structure of sunflower oil (Michelle, 2020)	43
Figure 2.10. Parameters affecting the biodegradation of polymers (Artham and Doble, 2008)...	50
Figure 2.11. Schematic of polymer biodegradation mechanism (Leejarkpai et al., 2011)	51
Figure 3.1. IR spectra of $K_3[Co(CN)_6]$ and Co-Zn DMC catalyst.....	75
Figure 3.2. (a) and (b) SEM images of Co-Zn DMC.....	76
Figure 3.3. Thermogravimetric analysis of Co–Zn DMC complex.....	77
Figure 3. 4. 1H NMR spectrum of PCHC1	78
Figure 3.5. 1H NMR spectrum of PPC1.....	80

Figure 3.6. FTIR spectra of OO and EOO	82
Figure 3.7. FTIR spectra of PaO and EPaO	83
Figure 3.8. FTIR spectra of SFO and ESFO	83
Figure 3.9. FTIR spectra of LO and ELO	84
Figure 3.10. FTIR spectra of SO and ESO	85
Figure 4.1. General structure of polycarbonate	94
Figure 4.2. Structure of ESO.....	95
Figure 4.3. IR spectra of $K_3Co(CN)_6$ and Co-Zn DMC catalyst	98
Figure 4.4. FTIR spectrum for sample prepared at $T = 80^\circ C$ and $t = 6h$ (entry no. 5 in Table 4.1)	102
Figure 4.5. 1H NMR spectra for sample prepared at $T = 80^\circ C$ and $t = 6h$ (entry no. 5 in Table 4.1)	103
Figure 5.1. Illustration of flaxseed plant (<i>Linum usitatissimum</i>) (Schneider, 2014)	114
Figure 5.2. Schematic diagram of the experimental setup for polymerization of ELO, PO and CO_2	119
Figure 5.3. Plausible structure of Co-Zn DMC catalyst (Liu et al., 2020)	121
Figure 5.4. IR spectra of $K_3Co(CN)_6$ and Co-Zn DMC catalyst	123
Figure 5.5. FTIR Spectrum of ELO	124
Figure 5.6. 1H NMR Spectrum of ELO	125
Figure 5.7. FTIR spectrum of purified ELO 60 (prepared at $T = 60^\circ C$ and $t = 24 h$ and catalyst loading = 0.20 g).....	129

Figure 5.8. Comparison of ^1H NMR spectra for ELO monomer and crude ELO 60	130
Figure 6.1. Schematic diagram of the experimental apparatus	150
Figure 6.2. Biodegradation test parameters as a function of time.	156
Figure 6.3. Production of CO_2 per g of volatile solids in inoculum bioreactor	159
Figure 6.4. Cumulative CO_2 evolution of cellulose bioreactor.....	160
Figure 6.5. Biodegradation of cellulose bioreactor.....	160
Figure 6.6. Cumulative CO_2 evolution of LO, ELO and PC-ELO test materials	161
Figure 6.7. Biodegradation of LO, ELO and PC-ELO test materials.....	162
Figure 6.8. Cumulative CO_2 evolution of SO, ESO and PC-ESO test materials.....	163
Figure 6.9. Mineralization of SO, ESO and PC-ESO test materials.....	163
Figure 6.10. Hydrolyzable functional groups commonly found in biodegradable polymers (Kale et al., 2007)	166

List of Schemes

Scheme 2.1. Industrial routes to poly(bisphenol-A carbonate) (Taherimehr and Pescarmona, 2014)	11
Scheme 2.2. Products of epoxide/CO ₂ copolymerization (Taherimehr and Pescarmona, 2014) .	12
Scheme 2.3. Catalytic cycle of CO ₂ /epoxide copolymerization (Trott et al., 2016).....	14
Scheme 2.4. General strategies for the synthesis of plant oil – based polymers (Ronda et al., 2011)	33
Scheme 2.5. Synthesis of bio-based polycarbonate from soybean oil and CO ₂ (Cui et al., 2019)	45
Scheme 2.6. Synthesis of EMU and its copolymerization with CO ₂ (Zhang et al., 2014)	47
Scheme 3.1. (a) Copolymerization of CHO and CO ₂ and (b) copolymerization of PO and CO ₂ (Kothandaraman et al., 2019).....	72
Scheme 3.2. Conversion of double bond via epoxidation and ring opening (Hazmi et al., 2013)	81
Scheme 4.1. Copolymerization of CO ₂ and epoxide	101
Scheme 5.1. Epoxidation procedure for linseed oil (Khandelwal et al., 2018)	115
Scheme 5.2. General mechanism of Polycarbonates production	116

List of Tables

Table 2.1. Catalytic system for copolymerization of CO ₂ /epoxide	16
Table 2.2. Formulas and structures of the most important fatty acids (Xia and Larock, 2010) ...	28
Table 2.3. Fatty acid compositions of the common vegetable oils (Zhang et al., 2017)	29
Table 2.4. Main FTIR bands and corresponding functional groups of oils (Karak, 2012; Seniha Güner et al., 2006)	30
Table 2.5. Assignment of signals of ¹ H NMR spectra for the fatty acids (Seniha Güner et al., 2006)	31
Table 2.6. World soybean production (%) in the year of 2019 (The American Soybean Association, 2020).	35
Table 2.7. Physical properties of soybean oil (Krist and Bauer, 2020)	36
Table 2.8. Physical properties of linseed oil (Krist and Bauer, 2020)	37
Table 2.9. Physical properties of olive oil (Krist and Bauer, 2020)	39
Table 2.10. Physical properties of palm oil (Krist and Bauer, 2020)	41
Table 2.11. Physical properties of sunflower oil (Krist and Bauer, 2020)	42
Table 2.12. Types and causes of polymer degradation (Kumar et al., 2009)	48
Table 2.13. ASTM standards related to composting and biodegradation (Rudnik, 2019)	56
Table 2.14. EN standards related to biodegradation and composting.....	57
Table 2.15. ISO standards on biodegradation of plastics (Funabashi et al., 2009).....	58

Table 3.1. Preparation conditions of polycarbonate samples by using different types of monomers and catalyst.....	73
Table 3.2. Molecular weights and PDI of PCHC and PPC samples.....	74
Table 3.3. Summary for ¹ H NMR spectrum of PCHC1	79
Table 3.4. Summary for ¹ H NMR spectrum of PPC1.....	80
Table 3.5. FTIR peaks and their assignment measured for pure oil and epoxidized oil.....	86
Table 3.6. Data of the preliminary experiments	88
Table 4.1. Data on the terpolymerization of ESO, PO and CO ₂ under Co-Zn DMC catalyst	100
Table 4.2. Percentage incorporation of ESO and amount of cyclic carbonate in the terpolymerization products	105
Table 5.1. FTIR assignment of ELO (Salih et al., 2015).....	124
Table 5.2. Assignment of signals of ¹ H NMR spectra for the ELO (Jebrane et al., 2017).....	126
Table 5.3. Percentage incorporation of ELO and amount of cyclic carbonate in the polymeric products.....	131
Table 5.4. Study of reaction parameters in semi-batch reactor.....	133
Table 6.1. Parameters/Operating conditions for polymerization reaction	146
Table 6.2. Detailed composition of 1 L of mineral solution.....	151
Table 6.3. Characteristics of the samples used in the trials of the experimental apparatus.....	157
Table 6.4. Properties of PC-ELO and PC-ESO	165

List of Appendices

Appendix C4.1. FTIR spectrums of resultant polymers prepared at different reaction temperature	108
Appendix C4.2. FTIR spectrums of resultant polymers prepared at different reaction time	109
Appendix C4.3. ¹ H NMR spectrums of terpolymerization products in CDCl ₃ over the range of reaction temperature.....	109
Appendix C4.4. ¹ H NMR spectrums of terpolymerization products in CDCl ₃ over the range of reaction time.....	110
Appendix C5.1. ¹ H NMR spectrum of terpolymerization products in CDCl ₃ over the range of reaction temperature.....	136
Appendix C5.2. ¹ H NMR spectrum of terpolymerization products in CDCl ₃ over the range of reaction time.....	137
Appendix C5.3. ¹ H NMR spectrum of terpolymerization products in CDCl ₃ over the range of catalyst loading	138
Appendix C5.4. GPC spectrum of ELO 80.....	139
Appendix C6.1. ¹ H NMR spectra for PC-ELO and ELO	168
Appendix C6.2. ¹ H NMR spectra for PC-ESO and ESO.....	168
Appendix C6.3. DSC spectrum for PC-ELO	169
Appendix C6.4. DSC spectrum for PC-ESO	169

Abbreviations and Symbols

Abbreviations and symbols are presented in an alphabetical order.

Abbreviations

a.u.	Arbitrary unit
ASTM	American Society for Testing and Materials
BPA	bisphenol-A
BPA-PC	poly(bisphenol-A carbonate)
CEN	European Committee for Standardization
CHO	Cyclohexene oxide
CMR	Cumulative measurement respirometric system
CO ₂	Carbon Dioxide
Co-Zn DMC	Cobalt-Zinc Double Metal Cyanide
C _{TOT}	Proportion of total organic carbon in the total mass of test material
DAS	Data acquisition system
DB	Double bond
DMC	Double metal cyanide (complexes)
DMCC	Double Metal Cyanide Complex
DMR	Direct measurement respirometric system
DMSO	Dimethyl sulfoxide
<i>e.g.</i>	For example
ELO	Epoxidized Linseed Oil
EMU	Epoxy methyl 10-undecenoate
EOO	Epoxidized Olive Oil
EPaO	Epoxidized Palm Oil
ESO	Epoxidized Soybean Oil

EU	European Union
EVO	Epoxidized Vegetable Oil
FA	Formic acid
FTIR	Fourier-transform infrared spectroscopy
GMR	Gravimetric measurement respirometry
GPC	Gel permeation chromatography
¹ H NMR	Proton nuclear magnetic resonance
HFIP	Hexafluoroisopropanol
<i>i.e.</i>	That is
IR	Infra-Red
ISO	International Organization for Standardization
LO	Linseed Oil
MWD	Molecular Weight Distribution
<i>n/a</i>	Not available
NDIR	Non-dispersive infrared gas analyzer
OO	Olive Oil
PaO	Palm Oil
PBS	Polybutylene succinate
PC	Polycarbonate
PCHC	Poly(cyclohexene carbonate)
PCL	Polycaprolactone
PDI	Polydispersity index ratio
PET	Polyethylene
PFA	Peroxoformic acid
PHA	Polyhydroxyalkanoates
PO	Propylene Oxide
PPC	Poly(propylene carbonate)
ppm	parts per million
RH	relative humidity
SEM	Scanning Electron Microscopy
SFO	Sunflower Oil

SO	Soybean Oil
SOTE	Soybean oil – based terminal epoxide
SO ₂	Sulfur Dioxide
TGA	Thermogravimetric analysis
Th(CO ₂)	Theoretical amount of evolved carbon dioxide
TOC	Total organic carbon
UV	Ultra-Visible
VO	Vegetable Oil

Symbols

M _n	Number average of molecular weight	g.mol ⁻¹
M _w	Number weight average molecular weight	g.mol ⁻¹
M _z	Z average molecular weight	g.mol ⁻¹
T _g	Glass transition temperature	°C
T _m	melting temperature	°C

CHAPTER 1 : INTRODUCTION

1.1 Introduction

In this modern era, usage of advanced material such as polymers have become indispensable. Polymers can be found everywhere, from households to industry. Its vast applications include diverse sectors such as construction, transportation, packaging, healthcare and electronics. In Europe, the last 50 years have witnessed a continuous growth in the production of plastic. It was reported that in the year of 2014, the plastic production reached 311 million tonnes and was projected to double by 2035 and might even quadruple by 2050 (World Economic Forum LLC, 2016). Most of these plastics/polymers are derived from non-renewable fossil feedstocks (e.g. natural gas, oil or coal). Considering their low biodegradability in the environment, there have been public concerns about a potentially huge environmental accumulation and pollution problem that could persist for centuries. According to the report published by Plastic Europe, approximately 27.1 million tonnes of post-consumer plastics waste ended in the official waste streams in the year of 2016 in Europe alone (PlasticsEurope, 2018).

Plastic waste recycling has been one of the strategies taken to solve the problem concerning waste disposal, however it is very difficult to recover all the used plastic. Therefore, another strategy is to replace petroleum-based products with the use of biodegradable plastics. By definition, a biodegradable polymer refers to the materials whose physical and chemical properties undergo deterioration and completely degrade when exposed to microorganisms, in the presence of oxygen (aerobic processes that produce CO₂), without oxygen (anaerobic processes that produce methane) and with water (both processes). On the other hand, bio-based polymers are materials

which are produced from renewable resources. Bio-based polymers can be biodegradable (*e.g.*, polylactic acid (PLA), polyhydroxyalkanoates (PHA), polybutylene succinate (PBS) and starch) or nondegradable (*e.g.*, bio-polyethylene (PET)). Similarly, while many bio-based polymers are biodegradable, not all biodegradable polymers are bio-based (*e.g.*, polycaprolactone (PCL) and poly(butylene adipate-co-terephthalate) (PBAT)) (Babu et al., 2013; European Bioplastics, 2019). Figure 1.1 shows examples of bio-based polymers and fossil-based polymers which are biodegradable and non-biodegradable.

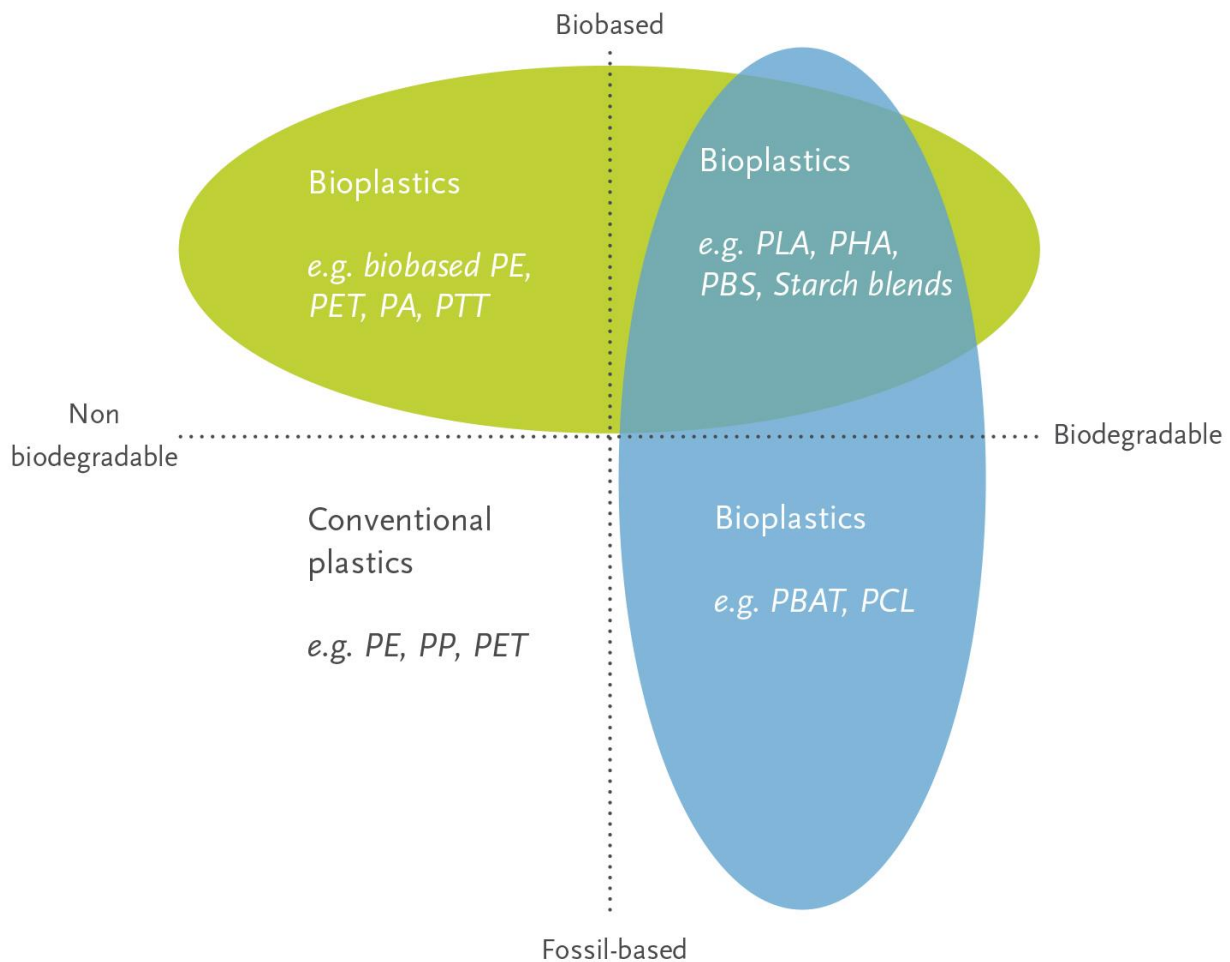


Figure 1. 1. Examples of bio-based polymers and fossil-based polymers which are biodegradable and non-biodegradable (European Bioplastics, 2019)

Utilization of renewable resources in the development of polymeric material is perceived as an elegant solution to overcome the dependency on finite petroleum resources and the volatility of its prices. In addition, concerns on environmental issues such as global warming and non-degradable nature of most synthetic polymers have triggered for scientific research in order to alleviate the dependency of the society on polymers derived from petroleum-based feedstocks. Efforts are made on a global scale to develop innovative technologies to transform natural resources into novel monomers and polymers. Some of these technologies have already generated competitive industrial products with properties comparable to conventional petrochemical polymers.

Among different polymeric materials, polycarbonate (PC) from renewable resources have been explored extensively. Traditionally, PC is synthesized via condensation of bisphenol-A (BPA) and phosgene (COCl_2). The product is an amorphous polymer with high impact strength, toughness, heat resistance and transparency. These exceptional properties made them a versatile material with substantial industrial significance. Despite the excellent properties exhibit by BPA-PC, usage of both monomers in production of BPA-PC have triggered anxiety owing to phosgene being a highly toxic volatile compound and BPA may cause negative health effects due to leaching out of the polymer when in contact with food (US Food and Drug Administration, 2014). Moreover, both monomers used are petroleum-based compounds and, recently, efforts have been made to replace them, at least partially, with renewable and bio-based monomers (Hauenstein et al., 2016).

Copolymerization of carbon dioxide (CO₂) with epoxide have been an alternative route to manufacture PC. This method was first discovered by Inoue and co-workers (1969) in the late 1960s whereby copolymerization was performed using an equimolar reaction mixture of diethyl zinc and water as catalyst at room temperature with 30 – 50 atm CO₂ pressure. This has successfully produced an alternating copolymer of aliphatic PC with a high molecular weight of 50,000 – 150,000. This pathway appears to be an attractive one since it circumvents the use of very toxic and hazardous phosgene in the traditional polycondensation by substitution with CO₂.

As a main greenhouse gas, the utilization of CO₂ may as well help to curb although not fully but partially the global warming phenomenon. At present the CO₂ emission rate are being reported to reach 35 billion tonnes per year with the main sources from electricity generation, transportation and industrial processes such as oil refineries, ammonia and ethylene oxide processes, cement production, and steel and iron industries (Muthuraj and Mekonnen, 2018) (Cuéllar-Franca and Azapagic, 2015). Besides, deforestation activities also have been reported to contribute the release of CO₂ to the atmosphere. Rebecca Lindsey (2020), stated that the CO₂ build-up in the atmosphere has escalate to more than 409 ppm today from a concentration of 270 ppm at the birth of the industrial revolution (Raupach et al., 2007). The Intergovernmental Panel on Climate Change (IPCC) forecasted that by the year of 2100, the CO₂ concentration level in the atmosphere may reach 570 ppm and consequently this may cause the rise in sea level and earth surface temperature by 3.8 m and 1.9°C, respectively. The ever-increasing trend of CO₂ level in the atmosphere has prompted enormous effort among the society to mitigate the accumulation of CO₂ in the atmosphere. Amongst the commonly accepted approaches are direct reduction of CO₂ emission from the source, CO₂ capture and storage, and transformation of CO₂ into building block

for platform chemicals and fuels (Saeidi et al., 2014). The efficient conversion of CO₂ into high value-added chemical products has enticed global interest from both academic research and industrial production. According to Lu and Darensbourg (2012), in recent decades there are over than 20 reactions involving CO₂ as a starting material have been developed. Among the reactions are the synthesis of urea, inorganic carbonates, methanol, salicylic acid and organic carbonates. Although the amount of CO₂ consumed (approximately 3.7 Gt annually) in these processes is relatively small in comparison with the overall amount of CO₂ generated, nevertheless this approach potentially provides access to more environmentally benign routes to producing chemicals otherwise made from the reagents detrimental to the environment. With regards to the copolymerization of CO₂ with epoxide, the use of CO₂ does carry several other benefits such as its low toxicity and general abundance, most inexpensive and non-flammable. However, epoxide/CO₂ copolymerization systems focus mainly on petroleum derivatives monomers such as propylene oxide (Cheng et al., 2018; Du et al., 2020; Huang et al., 2020; Pinilla-de Dios et al., 2017; Qiang et al., 2015; Tran et al., 2020; Zhu et al., 2018), cyclohexene oxide (Anderson and Kozak, 2019; Chen et al., 2019; Hartweg and Sundermeyer, 2019; Kernbichl and Rieger, 2020; Raman et al., 2020; Shao et al., 2020; Veronese et al., 2020) and to a lesser extent styrene oxide (Honda et al., 2020; Wu et al., 2011; Wu et al., 2013).

The motivation of this doctoral thesis is therefore to explore the potential of utilizing epoxidized vegetable oil in copolymerization with CO₂, which produces biodegradable polycarbonates and polyether. The chemical transformation of epoxidized vegetable oils into a polymeric product is a promising strategy to produce renewable and environmentally friendly materials that can substitute petroleum-based polymers. This strategy also helps in the

development of sustainable green technology to produce wide varieties of value-added chemicals and industrial products. Also, research on the synthesis of polymer from epoxidized vegetable oils has gained considerable interest because polymer obtained is biodegradable as compared to polymer derived from petroleum-based monomer.

1.2. Objectives

Based on the previous approach and background presented in this chapter, this doctoral work aims mainly to synthesize bio-based polycarbonates from natural products. The main objectives of this research work are:

- i. to synthesize polycarbonates from epoxidized derivatives of vegetable oil, via catalytic copolymerization with CO₂ at high pressures. Vegetable oils employed in this study can be divided into three categories as per following:
 - a) vegetable oils with a high number of epoxy groups in the molecule such as soybean oil and linseed oil
 - b) vegetable oils with a moderate number of epoxy groups in the molecule namely sunflower oil and olive oil
 - c) vegetable oil with a low number of epoxy groups in the molecule in particular palm oil.
- ii. to investigate the effect of temperature, time and catalyst loading on the polymerization reaction.

- iii. to analyse the synthesized polymers which includes physical-chemical characterization:
 - validation of the synthesis of polymeric material via *Infra-Red (IR) Spectroscopy* and *Proton Nuclear Magnetic Resonance (¹H NMR) spectroscopic* analyses
 - determination of molecular weight distribution (MWD) by *Gel Permeation Chromatography (GPC)*

- iv. to determine the degradation ability of synthesized polymeric material by CO₂ evolution (according to standardized procedures ISO 14855) (International Organization for Standardization, 2012)

1.3. Thesis organization

This dissertation comprises a total of seven chapters and has been organized as per following:

Chapter 1 impart the introduction, list of objectives of this doctoral research work and organization of the dissertation.

Chapter 2 provide readers with information on the history and development of copolymerization reaction of epoxides with CO₂, current research findings related to the topics published by other researchers and state of the art concerning biodegradation study.

Chapter 3 elaborates the preliminary experiments conducted. The objectives of the preliminary study were to select a specific catalyst to be used in the copolymerization reaction and to identify potential vegetable oil-based epoxide as co-monomer in the catalytic polymerization reaction with CO₂. Prior to copolymerization reaction, three different types of catalysts were synthesized and tested in the copolymerization reaction of CHO/CO₂ and PO/CO₂. Three vegetable oils namely olive oil, palm oil and sunflower oil were transformed into epoxidized vegetable oil via *in situ* epoxidation reaction. The prepared epoxidized oils were tested in the screening experiments together with additional two commercial epoxidized oil obtained from the industry. The purpose of the screening experiments was to evaluate the practicality of these oil as the co-monomer in the copolymerization with CO₂.

Chapter 4 presents the main results obtain in the synthesis of vegetable-oil based polymer by terpolymerization of ESO, PO and CO₂. Results from the FTIR spectroscopy, ¹H NMR spectroscopy and GPC are presented in this chapter.

Chapter 5 discusses the main results obtained in the synthesis of bio-based poly(carbonate-co-ether) by means of catalytic polymerization of ELO, PO and CO₂. The effect of parameters such as catalyst loading, reaction temperature and reaction time on the properties of the resultant polymer are studied.

Chapter 6 report the main results obtained in the aerobic biodegradation study of bio-based polycarbonate via CO₂ evolution. The methods of biodegradation study follow the ISO 14855.

Chapter 7 provides the overall conclusions and list of recommendations for the future studies.

CHAPTER 2 : LITERATURE REVIEW

2.1 Polycarbonates

Polycarbonates (PCs) are a class of thermoplastic polymers with carbonate linkages in their chemical structure. Depending on the structure of the R groups, they are categorized as aliphatic or aromatic polycarbonate (PC). The general structure of PC is shown in Figure 2.1. Most of the polycarbonate available in the market is made of bisphenol-A owing to the durability, good mechanical properties, ease of moulding and its transparency. At present, there are two different industrial routes for the synthesis of high molecular weight poly(bisphenol-A carbonate) (BPA-PC). The first route involves the interfacial reaction between phosgene and the sodium salt of bisphenol-A (BPA) in a heterogeneous system. The second route consists of a melt-phase transesterification between a BPA and diphenyl carbonate (Scheme 2.1). However, the conventional methods of BPA-PC production have some drawbacks. From the environmental point of view, the first path is detrimental owing to the consumption of the hazardous dichloromethane (as solvent) and phosgene, with huge amounts of sodium chloride is produced as a side product. Meanwhile, the second route consumes excessive amount of energy since high temperature is required to remove phenol which is the product of high boiling condensation in this polymerization reaction (Ang et al., 2015). In addition, because of its potential toxicity as a human carcinogen BPA has also come under scrutiny. According to a report published by the Centers for Disease Control and Prevention, more than 90% of Americans have BPA in their urine, possibly from plastic bottle and cans.

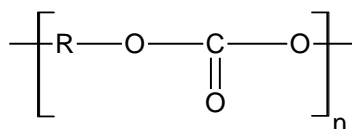
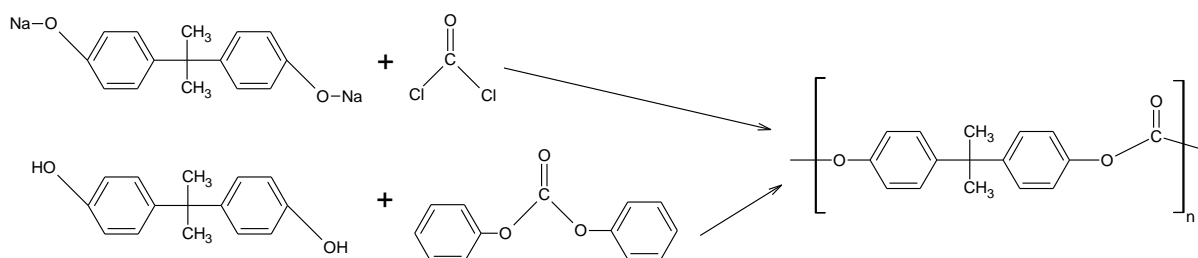


Figure 2.1. General structure of Polycarbonate



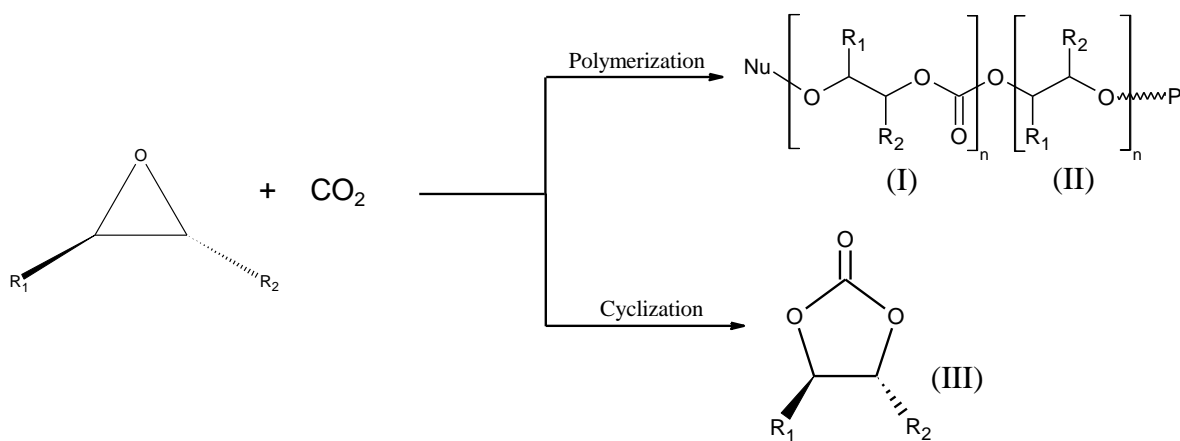
Scheme 2.1. Industrial routes to poly(bisphenol-A carbonate) (Taherimehr and Pescarmona, 2014)

Alternatively, a different method to synthesized PCs was discovered by Dr. Shohei Inoue and co-workers in the year of 1969. They have successfully synthesized an aliphatic PC specifically poly(propylene carbonate) (PPC) from propylene oxide (PO) and CO₂ by using diethyl zinc (ZnEt₂) and water as catalyst (Inoue et al., 1969). This approach is known to offers a few advantages in comparison to the existing industrial processes. For example, copolymerization of epoxide and CO₂ is a chain growth process meanwhile BPA-PC involves step-growth mechanisms. Hypothetically, better control of molecular weight with good selectivity can be achieved via copolymerization of epoxide and CO₂. This means that there is potential to get high molecular weights via this method without the necessity for the monomer conversions to approach unity. In

addition, in the copolymerization reaction the monomers involve do not possess safety hazards as compared to the current industrial process based on phosgene (Ang et al., 2015). Moreover, copolymerization reaction which involves CO₂ is deemed as green chemistry since CO₂ used is a renewable material.

2.2 Mechanism of epoxide/CO₂ copolymerization

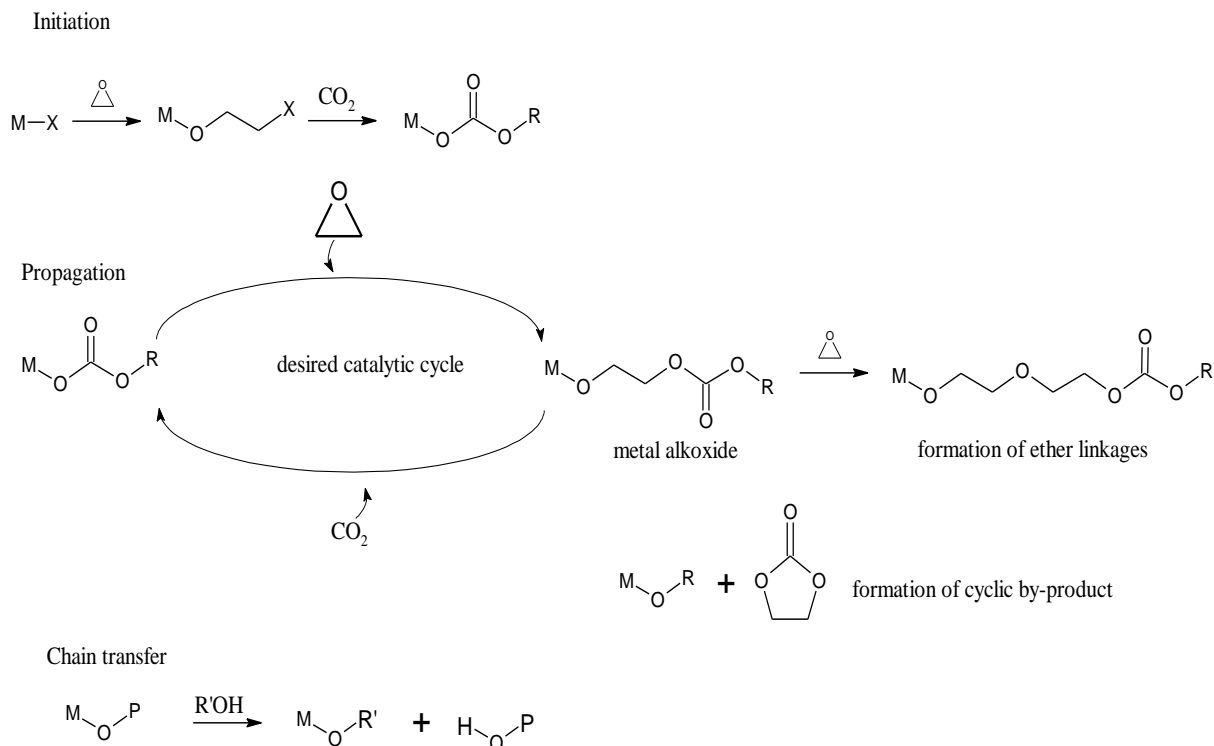
As shown in Scheme 2.2, the copolymerization between epoxide and CO₂ can generate two main types of products either polycarbonates (I) or cyclic carbonates (III) depending on the catalytic system applied and the copolymerization conditions. Ideally, an alternating insertion of epoxide and CO₂ may take place which result in the formation of polycarbonate. Nevertheless, this ideal case is often flawed by the consecutive addition of epoxides or backbiting reactions leading to undesired ether linkages in the backbone. The latter also produces cyclic carbonates that will compromise yield of the aliphatic polycarbonate. The consecutive insertion of two CO₂ molecules has never been observed as this is strongly disfavoured from a thermodynamic perspective (Coates and Moore, 2004b).



Scheme 2.2. Products of epoxide/CO₂ copolymerization (Taherimehr and Pescarmona, 2014)

Researchers in this field have proposed different mechanisms for the reaction of CO₂ with epoxides depending on the nature of the catalytic system, but also on the substrate and on the reaction conditions. Generally, the addition of CO₂ to epoxides is carried out in the presence of a catalytic system that can initiate the reaction by activating either the epoxide or CO₂, or both simultaneously. Frequently, epoxide is being activated by the interaction of the oxygen atom with a Lewis acid (an electron-pair acceptor), followed by a nucleophilic (an electron pair donor) attack of a carbonate group or ligand (X) that causes the opening of the epoxide ring to form a metal alkoxide intermediate as shown in Scheme 2.3.

Then CO₂ inserts into the metal alkoxide intermediate to form a metal carbonate species during chain propagation. This carbonate species can either evolve towards the cyclic carbonate or propagate by further addition of epoxide and CO₂ with formation of a polycarbonate. Instead of CO₂ insertion, metal alkoxide may as well attack an epoxide molecule thus resulting in the formation of ether linkages in the polymer chain. These linkages cause an alteration to the polymer properties but somehow it could be beneficial depending on the area of application. Regardless it reduces the CO₂ sequestered in the polymer backbone (Langanke et al., 2014; Lee et al., 2012). Traces of water, alcohol or acid in the polymerization medium can initiate a chain transfer which will lessen the molecular weights of the polycarbonate produced.



Scheme 2.3. Catalytic cycle of CO₂/epoxide copolymerization (Trott et al., 2016)

2.3 Catalysts for copolymerization of epoxides with CO₂

Following Inoue's discovery in the year of 1969 (Inoue et al., 1969), numerous amounts of catalysts have been designed for the copolymerization of epoxide with CO₂ (Anderson and Kozak, 2019; Ang et al., 2015; Kember et al., 2011; Lu and Darensbourg, 2012; Mandal, 2020; Pescarmona and Taherimehr, 2012; Trott et al., 2016). Generally, these catalysts are categorized into two main classes which are homogeneous and heterogeneous depending on their solubility in the reaction media. If the catalysts are in the same phase as reactants, they are called homogeneous catalysts and on the contrary they are called heterogeneous catalysts if the phase of the catalyst differs from the phase of the reactants (Bahramian and Dehghani, 2016). Both homogeneous and heterogeneous catalysts have their own pros and cons when applied in the copolymerization

reaction. For instance, homogeneous catalyst such as zinc phenoxide (Darensbourg et al., 2000) , zinc (β -diiminates) (Ren et al., 2015) and salen-based cobalt (III) complexes (Cohen et al., 2005; Ren et al., 2009) have high catalytic activity and selectivity for CO₂/epoxides copolymerization. On the other hand, such homogeneous catalysts demand a complex synthesis procedure and stringent conditions for polymerization. Furthermore, the catalyst separation from the reaction mixture is rather difficult despite of its effectiveness in most cases (Sankar et al., 2015). Meanwhile heterogeneous catalysts such as ZnEt₂/protonic compounds (Inoue et al., 1969), rare earth-based catalysts (Liu et al., 2001), and zinc dicarboxylate (Pescarmona and Taherimehr, 2012) can catalyze CO₂-PO copolymerization with high M_n and M_w, but in turn they often suffer from low productivities of 10–200 g polymer/g catalyst (Dai et al., 2016; Zhang et al., 2011). Table 2.1 gives the summary of catalytic system previously used by researchers in the copolymerization of CO₂ with different types of epoxides.

Table 2.1. Catalytic system for copolymerization of CO₂/epoxide

Catalyst	Epoxide	Products	Molecular Weight	References
MgCo heterodinuclear complex	CHO	PCHC	$M_n = 1.24 \text{ kg/mol}$	(Deacy et al., 2020)
SalenCr ^{III} Cl bis(triphenylphosphine)iminium chloride as cocatalyst	CHO	poly(cyclohexene carbonate sulfite) Terpolymerization of SO ₂ , CO ₂ with CHO.	$M_n = 9.52 \times 10^3$ g/mol	(Zhi et al., 2019)
Zinc organyls	CHO	Poly(ether)carbonates	79.3 kg/mol	(Wulf et al., 2018)
ZnEt ₂ -glycerine- Y(CCl ₃ COO) ₃ ternary catalyst	PO	poly(propylene carbonate) (PPC)	$M_n = 20 \times 10^4$ g/mol	(Cheng et al., 2018)
SalenCoCl/PPNCl	Soybean oil-based terminal epoxides	Polycarbonates soybean oil-based polycarbonate	$M_n = 5100 \text{ g/mol}$	(Chang et al., 2017)
Double metal cyanide (DMC) catalyst	1,2-epoxydecane	poly(1-decene-co-carbonate)	$M_w = 15 \text{ kDa}$	(Jin et al., 2017)

Catalyst	Epoxide	Products	Molecular Weight	References
SalenCr ^{III} Cl	cyclohexene oxide (CHO) and alpha-pinene oxide	aliphatic polycarbonate (Terpolymer)	$M_n = 1.04 \times 10^4$ g/mol	(Zhi et al., 2017)
Zinc glutarate - (ZnGA)	PO	Poly(propylene carbonate) (PPC)	$M_n = 99$ kDa	(Marbach et al., 2017)
Zinc Glutarate	epichlorohydrin	poly(ECH/CO ₂)	$M_n = 2.7$ to 17.1 kDa	(Sudakar et al., 2016)
ZnGA/DMC composite	PO	poly(propylene carbonate)	$M_w = 3.8 \times 10^5$ g/mol	(Meng et al., 2016)
β -diiminate zinc catalyst (bdi)Zn(OAc).	Limonene oxide	poly(limonene carbonate)	$M_n = 108.6$ kDa	(Hauenstein et al., 2016)
Zn-Co DMC and Zn-Fe DMC	PO	poly (propylene carbonate) (PPC)	$M_n = 4.3429 \times 10^3$ $M_n = 8.9259 \times 10^3$	(Dai et al., 2016)
Schiff Base Complex	CHO	poly(cyclohexenylene carbonate) (PCHC)	$M_n = 1.85 \times 10^4$ g.mol ⁻¹ .	(Fan et al., 2015)

Catalyst	Epoxide	Products	Molecular Weight	References
Zinc adipate/tertiary amines complex	PO	poly (propylene carbonate)	$M_n = 259\ 000$ kg/mol	(Tang et al., 2013)
Double metal cyanide	Ethylene oxide (EO)	poly(carbonate-ether)s	$M_n = 2.7-247$ kg/mol	(Gu et al., 2013)

2.3.1 Double metal cyanide complex (DMCC) catalyst

DMCC also known as Prussian blue analogues is a powerful heterogeneous catalyst which has been widely used in the synthesis of chemical products as well as in the separation of gas. Utilization of DMCC catalyst has been reported in numerous chemical reactions such as in the hydrolysis or alcoholysis of the plant oil to obtain biodiesel (Satyarthi et al., 2011), Prins condensation reactions (Patil et al., 2007), synthesis of dimethyl carbonate via transesterification of propylene carbonate with methanol (Srivastava et al., 2006) and hydroamination reaction (Peeters et al., 2013). However, DMCC is generally recognized for the ring-opening polymerization of epoxides, especially PO (Yu et al., 2014; Zhang et al., 2007). It is commonly used to synthesize poly(propylene oxide) polyols which have moderate and high molecular weights. In the year of 1985, Kruper et al. (Kruper and Swart, 1985) has successfully applied Zn-Co (III) DMCC to CO₂/epoxide copolymerization. Ever since substantial amount of studies have been conducted on its preparation and application to manufacture CO₂-based copolymers (Guo and Lin, 2014; Sebastian and Darbha, 2015; Shi et al., 2018; Subhani et al., 2016; Varghese et al., 2013; Zhang et al., 2015b). Various DMCC catalysts have also been developed and reported used in the copolymerization of CS₂/epoxides (Zhang et al., 2008), cyclic anhydrides/epoxides (Suh et al., 2010) as well as CO₂/cyclic anhydrides/epoxides terpolymerization (Sun et al., 2010) and the results obtained gave fairly satisfying catalytic activity.

As being implied by their name, DMCC catalyst attributes two different metal centers, one coordinating via the carbon atom of the CN⁻ ligand and the other via the nitrogen atom. A typical formula of DMCC catalyst is denoted as M^{II}_u[M(CN)_n]_v · xM^{II}X_w · yL · zH₂O (M^{II} = Zn²⁺, Fe²⁺, Ni²⁺, Co²⁺ etc.; M = Co²⁺, Co³⁺, Fe²⁺, Fe³⁺, etc.; X = Cl⁻, Br⁻, I⁻ and OAc⁻, etc.; L is an electron-

donating complexing agent). It is nonstoichiometric since x , y and z varied subjected to the methods and batches of preparation. Traditionally, preparation method of the DMCC catalyst is via precipitation reactions of aqueous solutions of water-soluble metal salts, $M^{II}X_w$, and water-soluble metal cyanide salts. A water-soluble complexing agent (L) is intermixed during the preparation of the DMCC catalyst (Zhang et al., 2007) and this procedure is often conducted at temperature around 25°C to 40°C. As an example, the most promising catalyst in this class namely Zn-Co (III) DMCC catalyst can be prepared by the reaction between zinc chloride ($ZnCl_2$) and potassium hexacyanocobaltate ($K_3[Co(CN)_6]$) in aqueous form and the chemical reaction is depicted in Equation 2.1. The zinc hexacyanocobaltate $Zn_3[Co(CN)_6]_2$ precipitated as a white suspension. Then a complexing agent such as salts, alcohols and solvents were normally added to the resulting suspension leading to a formation of solid complex catalyst. This is further followed by multiple washing and centrifugation stages to allow for the removal of the excess potassium ions which known to have an adverse effect on the copolymerization of CO_2 and epoxides (Zhang et al., 2015b). The washing process usually are done by using a mixture of complexing agent and water and finally in pure complexing agent. Finally, the catalyst is dried at moderate temperature and under vacuum condition. Figure 2.2 illustrates the preparation scheme of Zn-Co (III) DMCC catalyst by the reaction of an aqueous solution of $K_3[Co(CN)_6]$ with an aqueous solution of $ZnCl_2$.



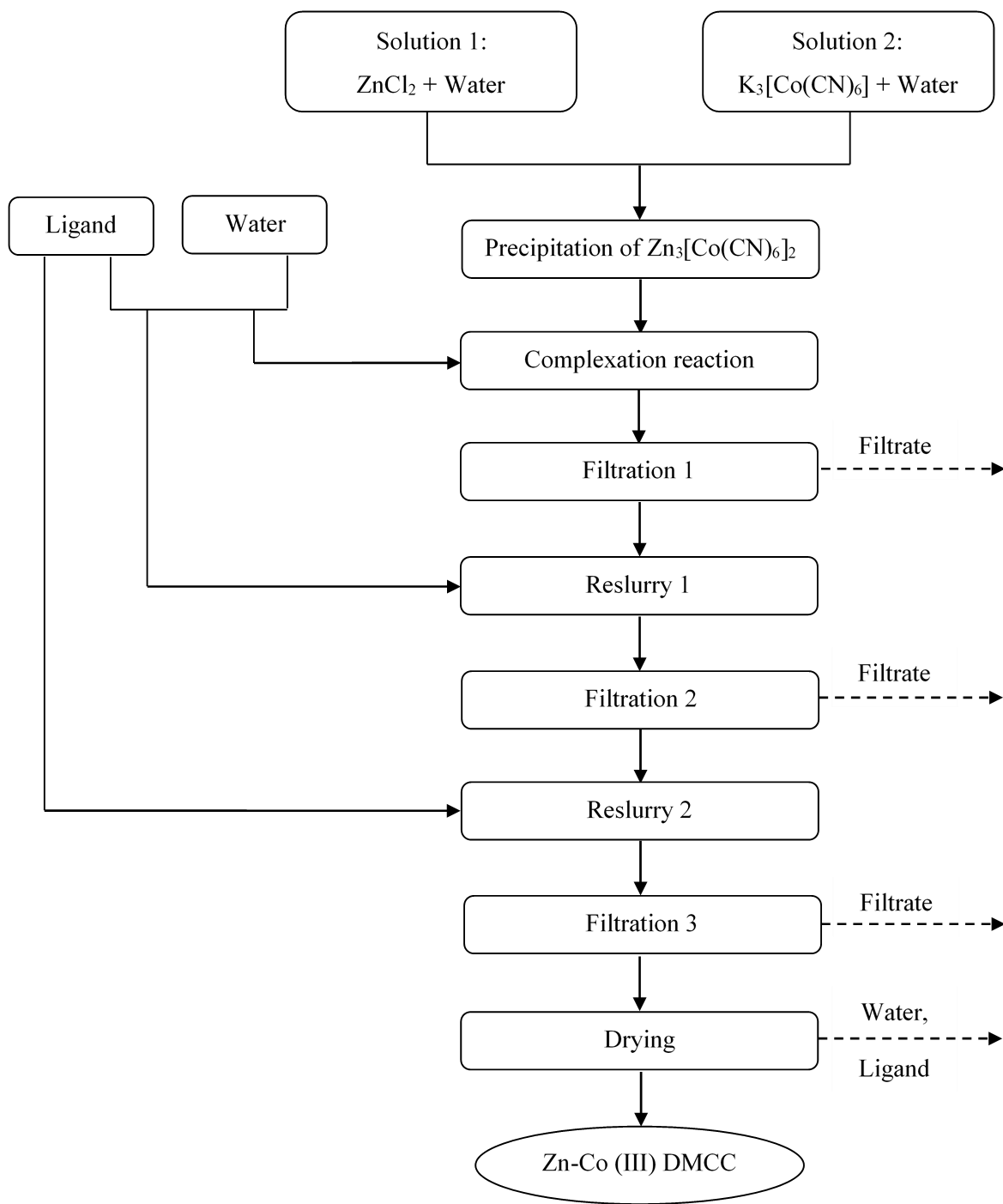


Figure 2.2. Flow diagram for synthesis of DMCC catalysts (Ionescu, 2005)

2.3.2 The structure of DMCC Catalyst and Mechanism for copolymerization

The bulky structure of Zn-Co (III) DMCC is proposed as in Figure 2.3. In general, the external metal M^{II} is linked with the inner metal M by a number of cyano-bridges ($M - C \equiv N - M^{II}$, with M^{II} usually a divalent metal ions such as Zn^{2+} , Fe^{2+} , Co^{2+} , Ni^{2+} , etc., M normally transition metal ions such as Fe^{2+} , Fe^{3+} , Co^{3+} , Ni^{2+} , etc.). The structure of these compounds is often cubic with a rock salt type ordering of $[M^{II}]^{v+}$ and $[M(CN)_6]^{w-}$, in which the $[M(CN)_6]^{w-}$ positions are only partially occupied to maintain charge neutrality (Marquez et al., 2017). As stated by Peeters et al. (2013) one third of the $[Co(CN)_6]^{3-}$ sites are vacant in the cubic $Zn_3[Co(CN)_6]_2$ to maintain framework neutrality. Despite of these vacancies increase the micropore volume, the pores are usually too small ($< 5 \text{ \AA}$) to allow diffusion of reactants and products, resulting in organic reactions mostly taking place on the external surface of the catalyst.

Due to its unsaturated coordinated structure, the external metal M^{II} on the surface of this catalyst acts as the active site for polymerizations (Luo et al., 2016). Even though most of the mechanisms proposed for the reaction of CO_2 with epoxides have been derived from studies of homogeneous catalytic systems, nevertheless heterogeneous catalysts are considered to follow similar pathways (Klaus et al., 2011). In the case of copolymerization of CO_2 /epoxide with Zn-Co (III) DMCC catalyst, the reaction commences once the epoxide molecule is coordinated at the Lewis acidic metal center (i.e.: Zn^{2+}) followed by the subsequent nucleophilic attack which leads to ring opening of the epoxide and formation of a metal bound alkoxide. Later CO_2 inserts into the metal alkoxide intermediate to form a metal carbonate species. This carbonate species can either evolve towards the cyclic carbonate or propagate by further addition of epoxide and CO_2 with formation of a polycarbonate.

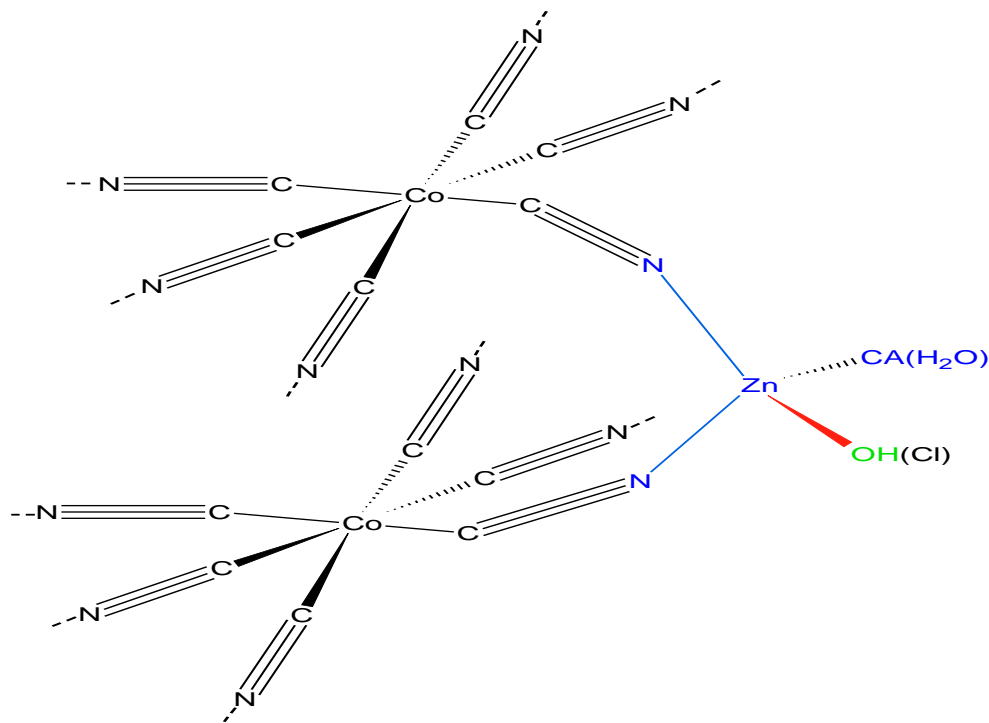


Figure 2.3. Plausible structure of DMCC catalyst (Liu et al., 2020)

2.4 Renewable Raw Materials for Polymers

Plastic is a synthetic material made from a wide range of organic polymers including synthetic, semi-synthetic, or natural materials that are physically malleable at elevated temperature and can be moulded into a variety of shapes and sizes. It was first manufactured from synthetic components in the year of 1907 and was called Bakelite named after Belgian - American chemist who created it, Leo Hendrik Baekeland (Baekeland, 1909). In those days, it was used for its electrical insulation properties. These days, synthetic plastics have been utilized in various fields of applications owing to their outstanding economic viabilities and physicochemical properties such as the availability, flexibility, durability, and light weight. The annual global production of plastics surpassed 300 million metric tons in the year of 2015 and is expected to exceed 500 million

metric tons by 2050. According to Geyer et al. (2017), from 1950 to 2015 the cumulative production of plastics are approximately 8300 million metric tons and the plastic waste generated is estimated to be 6300 metric tons. From the total of waste produced, only 9 percent has been recycled, 12 percent was incinerated whilst the remaining 79 percent is pile-up in landfills of in the environment. If the current developments persist, it is forecasted by the year 2050 approximately 12,000 metric tons of plastic waste will be accumulated in the landfills. It is well known that most polymers are derived from petroleum, therefore they are likely to be resistant to biodegradation.

Due to the oscillation of oil prices and the problem of the accumulation of waste, which has led to hard environmental policies, polymers from renewable resources may become a sustainable solution (Badia et al., 2017). Therefore, recent years have witnessed an increasing demand for the replacement of petroleum-derivate polymeric materials with bio-renewable polymers. Gandini (2011) stated that bio-renewable resources such as sugars, polysaccharides, lignins, plant oils, pine resin derivatives, and furans have been exploited in the development of different types of bio-renewable polymeric materials. Renewable feedstock, such as the biomass from plant-derived resources, represents a promising opportunity to produce polymeric materials. Vegetable oil has both economic and environmental advantages over petroleum-based materials, making it the most attractive alternative to replace fossil resources. Every year a massive amount of biomass is renewed in nature, specifically ~1011 tons, however only 3.5% are presently used by mankind (Li et al., 2009). Currently, the interest given to these materials is swiftly expanding, since vegetable oils are promising monomers for polymer chemistry as a result of their competitive cost, natural abundance and reactive functionalities. Furthermore, polymer derived from vegetable

oils are biodegradable. The life cycle of polymers-based vegetable oils is illustrated in Figure 2.3, according to which the biomass from plant-derived resources is extracted to yield the vegetable oil. Then, the oil is subjected to chemical modification with the objective of enhancing its reactivity towards a given type of polymerization approach (Gandini, 2008). The polymers are then made available to the consumers and once used, they become waste, which after degradation and assimilation is reused as biomass and the cycle starts again.

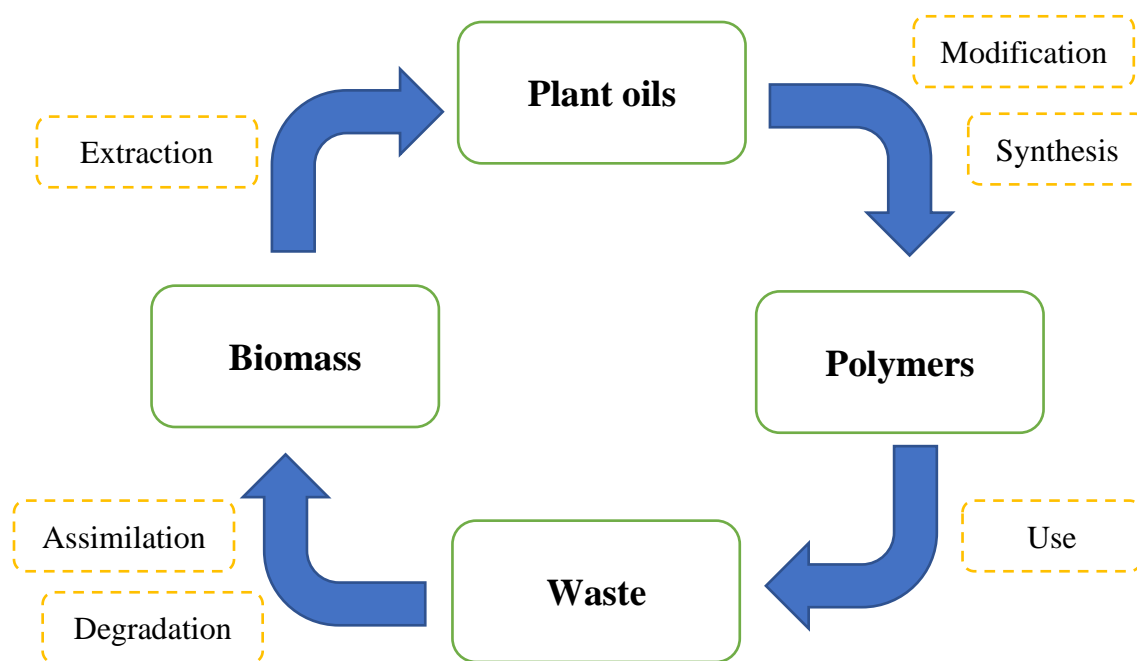


Figure 2.4. Life cycle of polymers based on vegetable oils (Seniha Güner et al., 2006)

According to the most recent market data compiled by European Bioplastics in collaboration with the research institute nova-Institute, the worldwide production of biobased plastics in the year of 2019 was estimated at 2.11 million metric tons of which 1.2 million tons were nonbiodegradable and the remaining biodegradable. Although the amount of biobased

plastics produced was less than 1% of the total plastic market, the global biopolymer market is likely to expand rapidly (projected to reach 2.43 million tonnes in 2024) to meet government regulations and consumer demand for safe, eco-friendly packing materials for food items around the world. Figure 2.4 depicts the global production capacities of bioplastic in 2019 by region. Asia has become the main production hub with 45 percent of bioplastics were produced in that region followed by Europe with one fourth of the global bioplastics production capacity is in this continent.

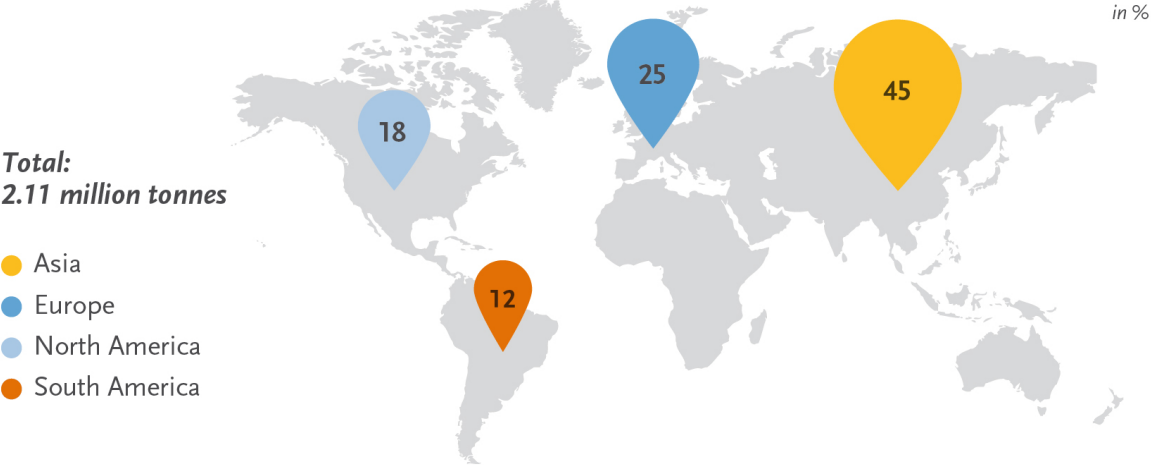
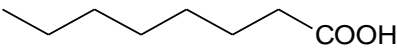
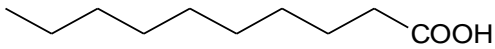
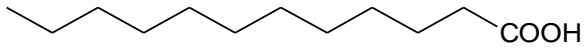
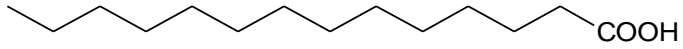
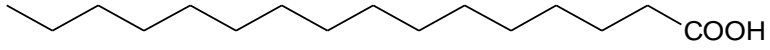
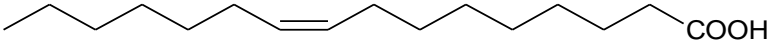
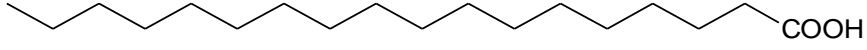
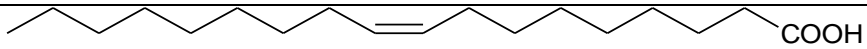
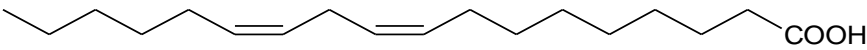
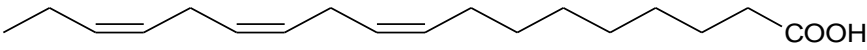
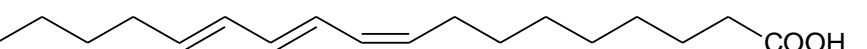
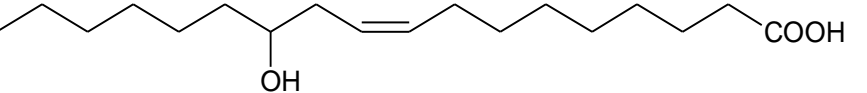
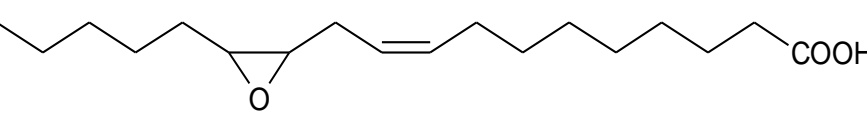


Figure 2.5. Global production capacities of bioplastic in 2019 (by region) (European Bioplastics, 2019)

2.4.1 Vegetable Oil as Renewable Raw Materials for Polymers

Vegetable oils are esters made of glycerine and various fatty acids containing from eight to 24 carbon atoms and between zero to seven carbon-carbon double bonds. In most vegetable oils, carbon-carbon double bonds are found between the 9th and 16th carbon atom. These naturally occurring carbon-carbon double bonds are most often non-conjugated and therefore are less reactive. This is owing to radicals are trapped by allyl hydrogen located in the methylene group between the double bonds (Karak, 2012; Petrović, 2008). Nevertheless, conjugated double bonds are present in some of the vegetable oil such as tung oil and as a result, these oils show high polymerization activity. Other important reactive sites such as ester group, hydroxyl group and epoxy groups also presence in some special oil (Miao et al., 2014). For instance, ricinoleic acid has one hydroxyl group located on the 12th carbon atom and it is the most abundant fatty acid in castor oil meanwhile vernolic acid has an epoxy group and is high in vernonia oil (Liang et al., 2018). Table 2.2 provides the structures of the most common fatty acids found in vegetable oils.

Table 2.2. Formulas and structures of the most important fatty acids (Xia and Larock, 2010)

Fatty Acid	Formula	Structure
Caprylic	C ₈ H ₁₆ O ₂	
Capric	C ₁₀ H ₂₀ O ₂	
Lauric	C ₁₂ H ₂₄ O ₂	
Myristic	C ₁₄ H ₂₈ O ₂	
Palmitic	C ₁₆ H ₃₂ O ₂	
Palmitoleic	C ₁₆ H ₃₀ O ₂	
Stearic	C ₁₈ H ₃₆ O ₂	
Oleic	C ₁₈ H ₃₄ O ₂	
Linoleic	C ₁₈ H ₃₂ O ₂	
Linolenic	C ₁₈ H ₃₀ O ₂	
α -Eleostearic	C ₁₈ H ₃₀ O ₂	
Ricinoleic	C ₁₈ H ₃₄ O ₃	
Vernolic	C ₁₈ H ₃₂ O ₃	

Listed in Table 2.3 is the fatty acid compositions of the most common vegetable oils. As shown from the table, different vegetable oils have different composition of fatty acids depending on the plant and growing conditions.

Table 2.3. Fatty acid compositions of the common vegetable oils (Zhang et al., 2017)

	Double bonds	Fatty acid composition (%)				
		C 16:0	C 18:0	C 18:1	C 18:2	C 18:3
Castor	3.0	2.0	1.0	7.0	3.0	0.5
Corn	4.5	10.9	2.0	25.4	59.6	1.2
Linseed	6.6	6.0	4.0	22.0	16.0	52.0
Olive	2.8	9.0	2.7	80.3	6.3	0.7
Palm	1.7	44.4	4.1	39.3	10.0	0.4
Soybean	4.6	10.6	4.0	23.3	53.7	7.6
Rapeseed	3.8	3.8	1.2	18.5	14.5	11.0
Sunflower	4.7	7.0	4.5	18.7	67.5	0.8
Canola	3.9	4.0	1.8	60.9	21.0	8.8
Cottonseed	3.9	21.6	2.6	18.6	54.4	0.7
Peanut	3.4	11.1	2.4	46.7	32.0	-

As other chemical compounds, the chemical structure of vegetable oils can be evaluated by using various spectroscopic techniques such as Ultra Visible (UV), FTIR, NMR spectroscopies and mass spectrometry. IR spectroscopy is widely used to determine the different functional groups present in the fatty acids. The FTIR spectral data of the oils indicate the presence of important linkages, such as ester groups, double bonds and other characteristic peaks. Table 2.4 gives the absorption bands and the corresponding function/groups commonly assigned to vegetable oil.

Table 2.4. Main FTIR bands and corresponding functional groups of oils (Karak, 2012; Seniha Güner et al., 2006)

Band (cm⁻¹)	Functional groups
3400–3500	-OH functions corresponding to free glycerol and/or residual moisture
3000–3010	Unsaturated C—H stretching vibration
2850–2925	CH ₂ asymmetric and symmetric stretching vibration
1735–1740	C=O stretching vibration of ester
1590–1650	C—C stretching vibration of C=C
1150–1250	C—O—C stretching vibration with aliphatic and aromatic moieties
980–990	C—C stretching vibration
730–750	Out of plane aromatic C—H bending vibration

Another sophisticated tool for determining the structure of vegetable oil is NMR spectroscopy. NMR spectroscopy can distinguish between different types of proton and carbon nuclei in the structure of the oil. Additionally, it is possible to determine the fatty acid content of vegetable oil from the NMR data. Table 2.5 provides the assignment of the pertinent peaks for the protons present in fatty acids.

Table 2.5. Assignment of signals of ^1H NMR spectra for the fatty acids (Seniha Güner et al., 2006)

^1H chemical shift (ppm)	Protons
0.88	($\text{CH}_3-(\text{CH}_2)_n-\text{CH}=\text{CH}$ -where $n > 3$)
0.97	($\text{CH}_3-\text{CH}_2-\text{CH}=\text{CH}$ -)
1.2 – 1.3	$-\text{CH}_2-$
1.6	$-\text{CH}_2-\text{C}=\text{O}$
2.0	$-\text{CH}_2-\text{CH}_2-\text{CH}=\text{CH}$ -
2.3	$-\text{CH}_2-\text{C}=\text{O}$
2.8	$-\text{CH}_2-\text{CH}=\text{CH}$ -
4.1 – 4.3	Protons of the glyceride moiety
5.3	$-\text{CH}=\text{CH}$ -

To date, various types of vegetable oils such as canola, castor, linseed, palm, rapeseed, safflower, soybean and sunflower have been widely used in the production of bio-based polymer (Belgacem and Gandini, 2008; Dai et al., 2020; Ghasemlou et al., 2019; Lamm et al., 2019; Miao et al., 2013; Miao et al., 2014; Parada Hernandez et al., 2019; Zhang et al., 2017) and these bio-based polymers have been applied in various field as illustrated in Figure 2.5.

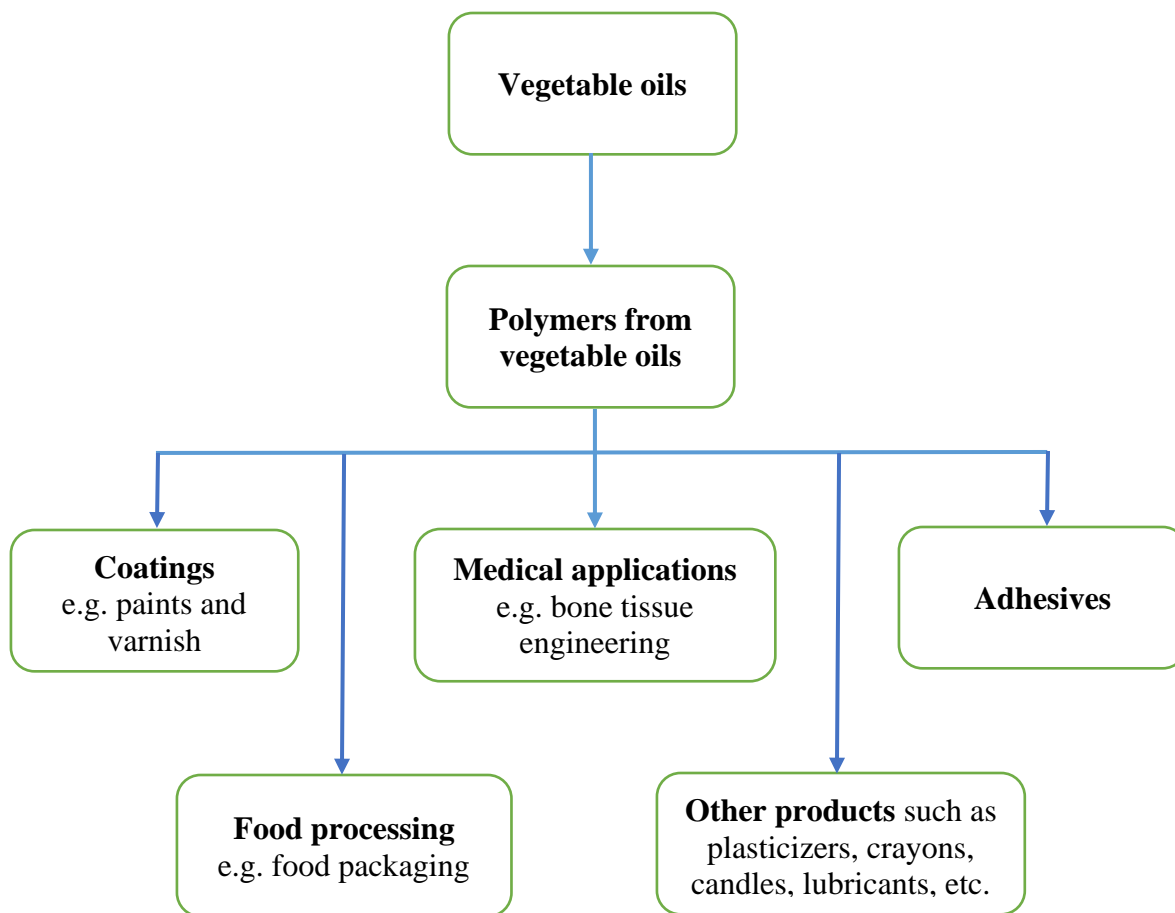
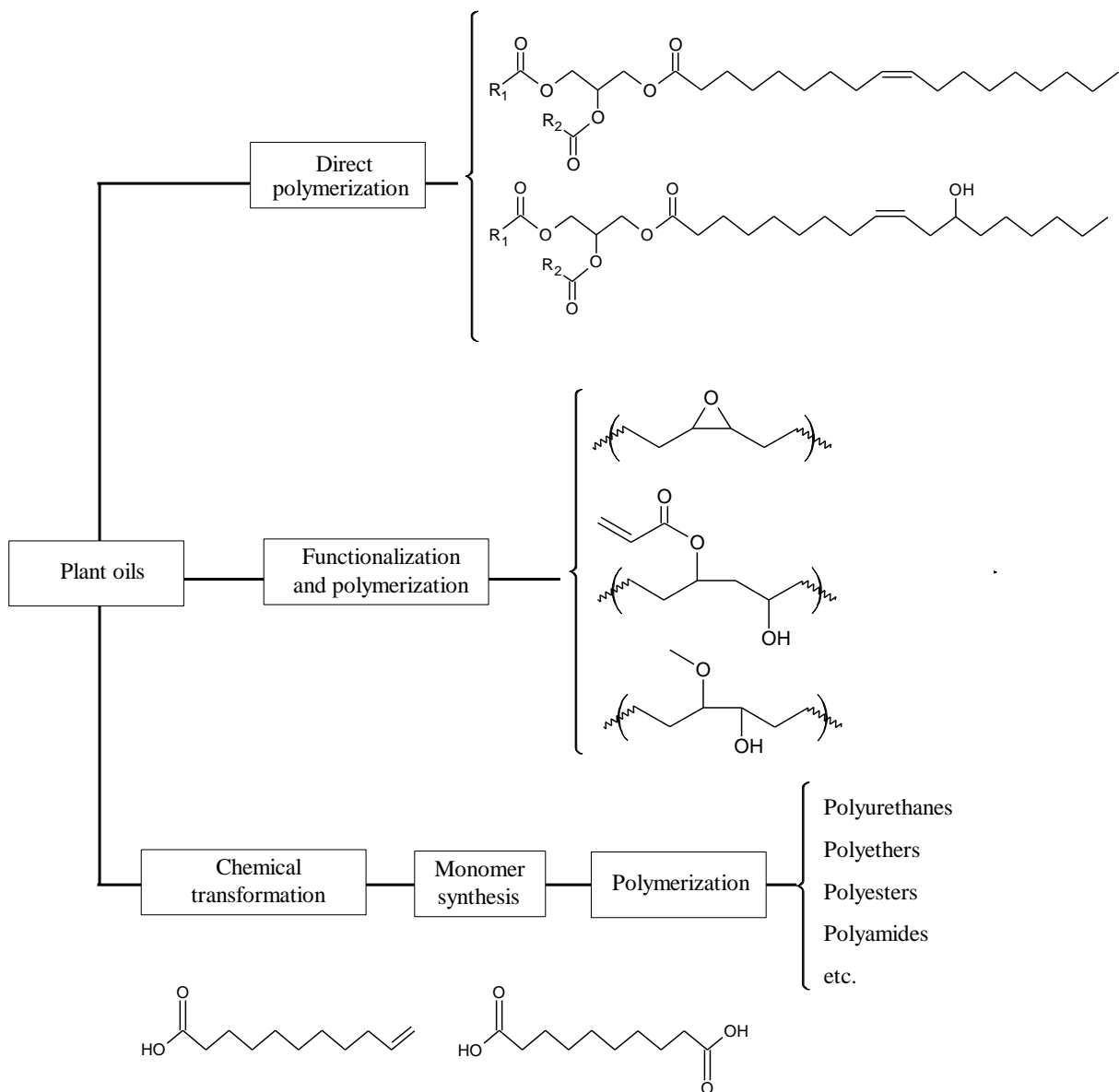


Figure 2.5. Applications of bio-based polymers made from vegetable oils (Abbasi et al., 2019)

Generally, polymers can be synthesized from vegetable oils via three main routes as presented in Scheme 2.5. The first route is the direct polymerization through the double bonds or other reactive functional groups present in the fatty acid chain. Second route involve the chemical modification of the double bonds with the aim to introduce functional groups which are easier to polymerize and the third route is the chemical transformation of plant oils to produce platform chemicals which can be used to produce monomers for the polymer synthesis.



Scheme 2.4. General strategies for the synthesis of plant oil – based polymers (Ronda et al., 2011)

2.4.2 Vegetable Oils used in Industry

A brief description of vegetable oils used in this research work is described in the following sub-section.

2.4.2.1 Soybean Oil

Soybean (*Glycine max* (L.) Merrill.) is one of the most cultivated grains in the world. It belongs to the family Leguminosae and subfamily Papilionaceae. Cultivation of soybean is dominated mainly by four countries namely Brazil, the United States, Argentina, and China whereby production in these countries alone accounts for almost 90% of the world's output. Table 2.6 shows the world soybean production (%) in the year of 2019 (The American Soybean Association, 2020). Soybean is the most important source of protein as well as vegetable oil. Primarily in Asia and other parts of the world, the seeds of soybean have been used to prepare a variety of fresh, fermented and dried foods. Besides its use for domestic purposes, soy oil finds diverse uses in industries related to production of pharmaceuticals, plastics, papers, inks, paints, varnishes, pesticides and cosmetics (Gupta, 2011).

Table 2.6. World soybean production (%) in the year of 2019 (The American Soybean Association, 2020).

Country	Production (Million Metric Tons)	Production (%)
Brazil	126.0	37.0
United States	96.8	28.0
Argentina	54.0	16.0
China	18.1	5.0
Paraguay	9.9	3.0
India	9.3	3.0
Canada	6.0	2.0
Other	21.7	6.0
Total	341.8	100

In recent years, soybean oil has garnered global interest from the government, industry and researchers as a promising renewable source for the biodiesel production (Changmai et al., 2020; Colombo et al., 2019; Faria et al., 2020; Hosseini et al., 2019; Laskar et al., 2020; Murillo et al., 2019; Yongphet et al., 2020) and polymeric material primarily in the synthesis of polyurethanes (Acik et al., 2018; Alagi et al., 2018; Lee and Deng, 2015; Mizera and Ryszkowska, 2016; Wang et al., 2009). Listed in Table 2.7 are the physical properties of soybean oil while its chemical structure is depicted in Figure 2.6.

Table 2.7. Physical properties of soybean oil (Krist and Bauer, 2020)

Density	0.916–0.922
Refractive index	1.4747–1.4765
Acid number	0.3–3.0
Iodine number	fluctuates, usually 124–136
Saponification number	189–195
Unsaponifiable	0.5–2%
Flash point	282 °C
Point of solidification	–8 to –16 °C

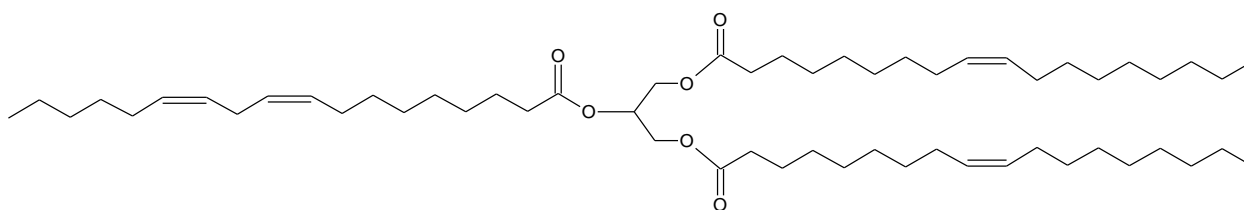


Figure 2.6. Chemical structure of soybean oil (Zhang et al., 2015a)

2.4.2.2 Linseed Oil

Linseed oil (*Linum usitatissimum*) is extracted from dry flax seeds through pressing, occasionally followed by solvent extraction. It is also called flaxseed oil and is one of the most unsaturated vegetable oils. The world's biggest producers are Kazakhstan, Canada, Russia, China, India, and the USA (Food and Agriculture Organizations of the United Nations, 2020). The colour of linseed oil is reported to vary depending on the pressing method i.e. golden yellow (cold pressed oil) and yellowish brown (unpressed oil). Refined oil is light yellow to golden yellow. Linseed oil

is a drying oil, meaning it can polymerize into a solid form. It is most widely used in the paint and varnish industry (Adekunle, 2015; Frances et al., 2020; İşeri-Çağlar et al., 2014; Otabor et al., 2019). Linseed oil is a slow-drying liquid with good preservative properties and water resistance. Table 2.8 gives the list of some important properties of linseed oil. The chemical structure of linseed oil is illustrated in Figure 2.7 and more description on linseed oil is given in Chapter Five (section 5.1).

Table 2.8. Physical properties of linseed oil (Krist and Bauer, 2020)

Density	0.930 to 0.936
Refractive index	1.472 to 1.485
Acid number	<4.0
Iodine number	170 to 204
Peroxide number	<20
Saponification number	188 to 196
Unsaponifiable	<2%

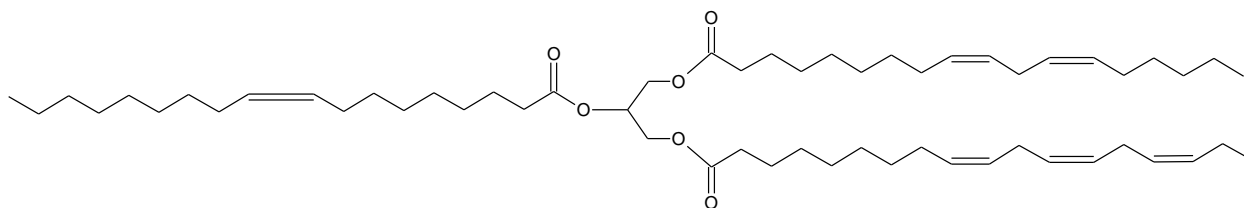


Figure 2.7. Chemical structure of linseed oil (Khandelwal et al., 2018)

2.4.2.3 Olive Oil

Olive tree (*Olea europaea* L. (Oleaceae)), favours porous, calciferous soil that is well-aired and well-drained, so that there is no stagnant moisture. It tolerates heat but is very frost-susceptible in cold winters. Generally, it grows best in a subtropical transition Mediterranean climate with dry, hot summers and cool, wet winters. Olive trees can grow up to 10–16 m tall and can reach an age of 1000 years. Olive oil is the oil obtained from the ripe stone fruit of *Olea europaea* (Figure 2.5) by cold pressing or other appropriate mechanical methods. It is frequently used in cooking, for frying foods or as a salad dressing. In the year of 2019, the production of olive oil has been reported as 3.12 million metric tons with majority of them are being produced by Mediterranean countries (Shahbandeh, 2020). Spain being the main world producer, followed by Italy, Greece, Turkey, Morocco, and Tunisia.



Figure 2.6. Ripe olive fruit (Krist and Bauer, 2020)

Olive oil is incomparable to other types of vegetable oils with regards to its grade variations and qualities. The types of olive oil are graded depending on the methods of harvesting and extraction with the best oil is the so-called virgin oil (*Oleum virginicum*). Each type of olive oil is unique by which it differs in flavour, odour, colour and their amount of free fatty acids. Like many other vegetable oils, olive oil is used to produce lubricants and soap, and as lamp oil (Bickel, 2012). Properties of olive oil is listed in Table 2.9 whereas the chemical structure of olive oil with an average of three double bonds is demonstrated in Figure 2.6.

Table 2.9. Physical properties of olive oil (Krist and Bauer, 2020)

Density	0.914–0.919
Refractive index	1.468–1.471
Acid number	2.0 maximum
Iodine number	78–90
Saponification number	187–196
Hydroxyl value	4–12
Unsaponifiable	0.5–1.3%
Flash point	225 °C
Ignition point	343 °C

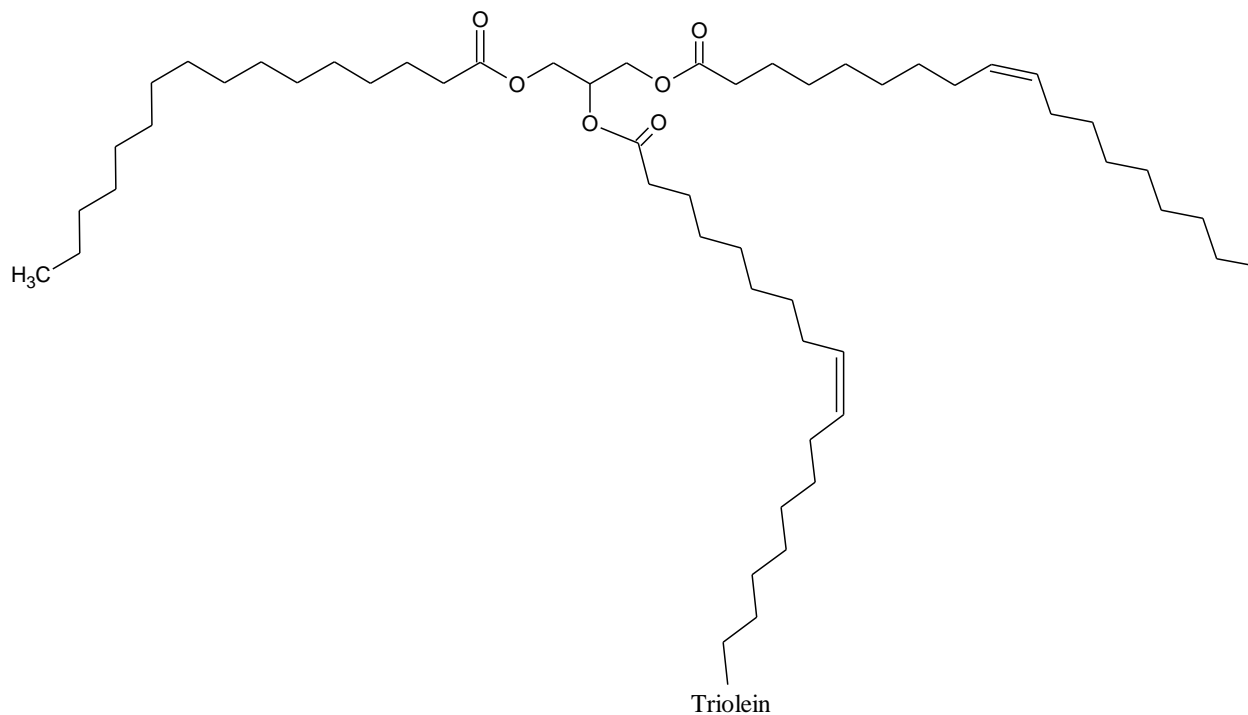


Figure 2.7. Chemical structure of olive oil (Molekuul.be, 2020)

2.4.2.4 Palm Oil

Oil Palm tree (*Elaeis guineensis*) is one of the major crops planted in South East Asian Countries mainly in Indonesia, Malaysia and Thailand. Indonesia is the leading producer of palm oil, followed by Malaysia by which both countries account for 84% of the worlds palm production. At present, 4.49 million hectares of land in Malaysia is under oil palm cultivation; producing 17.73 million tonnes of palm oil and 2.13 tonnes of palm kernel oil. Malaysia is one the largest producers and exporters of palm oil in the world, accounting for 11% of the world's oils and fats production and 27% of export trade of oils and fats. Two types of oils are being produce by the oil palm namely crude palm oil (CPO) from the fibrous mesocarp and crude palm kernel oil (CPKO) from the kernels. Even though both oils originate from the same fruit, palm oil is chemically and nutritionally different from palm kernel oil. In its virgin form, the oil is bright orange-red due to

the high content of carotene. These oils are widely used in food and other industries such as detergents and cosmetics. Palm oil has a balanced fatty acid composition in which the level of saturated fatty acids is almost equal to that of the unsaturated fatty acids. Palmitic acid (44%-45%) and oleic acid (39%-40%) are the major component acids, with linoleic acid (10%-11%) and only a trace amount of linolenic acid. The low level of linoleic acid and virtual absence of linolenic acid make the oil relatively stable to oxidative deterioration (MPOB, 2011). Basic properties of palm oil are reported in Table 2.10 whilst the chemical structure of palm oil bearing an average of two double bonds is depicted in Figure 2.7.

Table 2.10. Physical properties of palm oil (Krist and Bauer, 2020)

Density (50/20 °C)	0.891–0.899
Refractive index	1.449–1.456
Iodine number	49–55
Saponification number	190–209
Unsaponifiable	0–1.2%
Melting point	33–40 °C

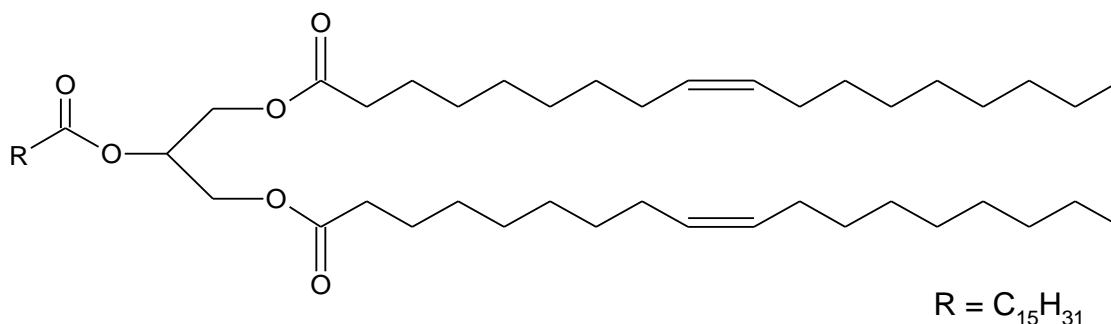


Figure 2.8. Chemical structure of palm oil (Clark and Hoong, 2014)

2.4.2.5 Sunflower Oil

Sunflowers (*Helianthus annuus*) grow in fertile, moist, well-drained soils containing heavy mulch (Zainal et al., 2018). Sunflower is a valuable oilseed crop. It is grown in over 26 million hectares in the world with an approximate production of 45 million metric tons (Konyalı, 2017). Originating from North America, this plant was subsequently introduced to several other world regions including Europe. Currently the major producing countries are Ukraine, Russia, European Union and Argentina. It is grown for its edible oil and fruits (seeds) both for human and livestock consumption. It is a semi-drying oil and its tendency to yellow is less than that of linseed oil, although it dries more slowly and has a softer finish.

As listed in Table 2.3, sunflower oil has an average of 4.7 double bonds, and this make it as an attractive candidate to be used as precursor for new polymeric material. Table 2.11 provides the physical properties of sunflower oil and its chemical structure is shown in Figure 2.8.

Table 2.11. Physical properties of sunflower oil (Krist and Bauer, 2020)

Density	20 °C: 0.918–0.923 15 °C: 0.922–0.926
Refractive index	25 °C: 1472–1476 40 °C: 1467–1469
Acid number	0.6
Iodine number	118–145
Saponification number	186–194
Point of solidification	–16 to –18 °C
Unsaponifiable	0–1.5%

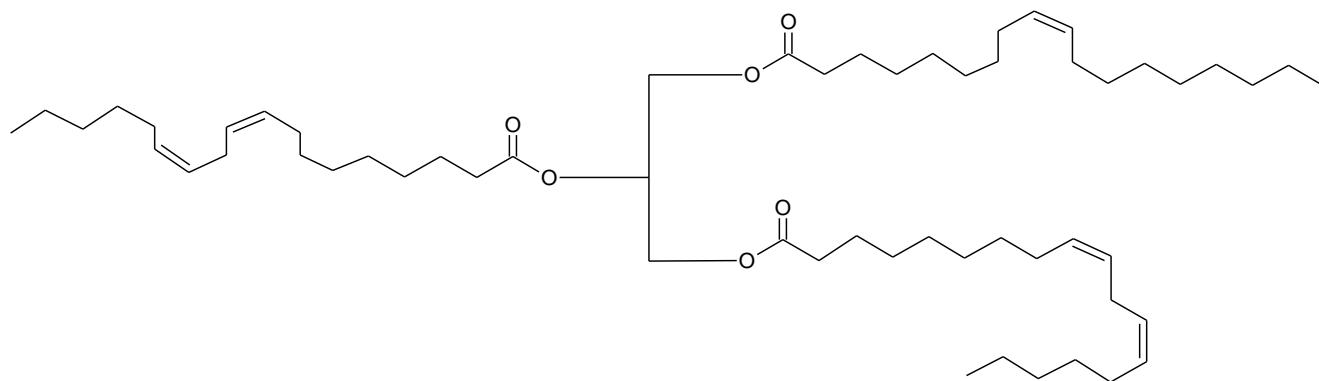
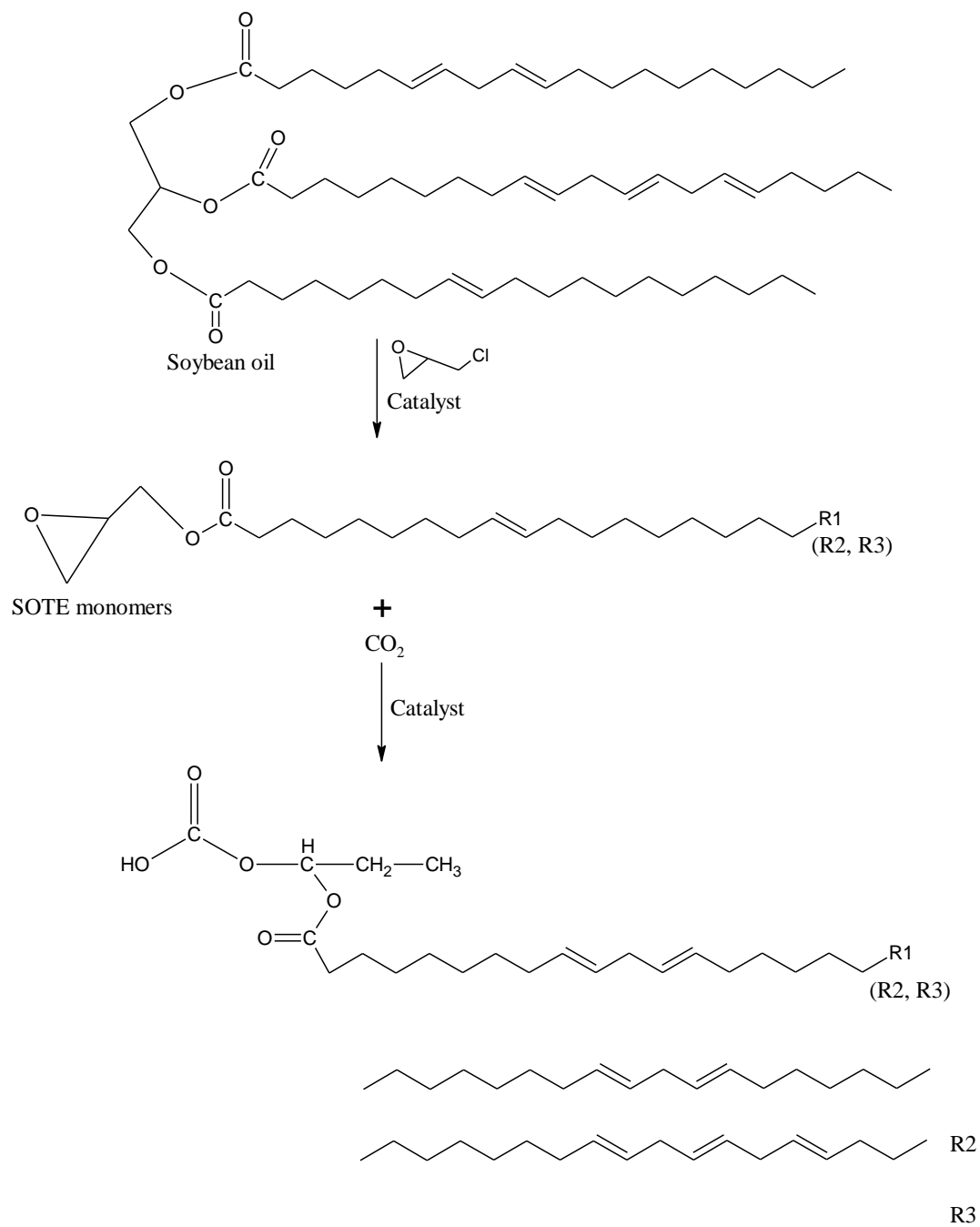


Figure 2.9. Chemical structure of sunflower oil (Michelle, 2020)

2.4.3 Copolymerization of Vegetable Oils-based Epoxides with CO₂

Although the exploration of vegetable oil-based epoxide as a starting material in the copolymerization with CO₂ is not fully extensive, nevertheless some researchers have proven that it is noteworthy to use vegetable oil-based epoxides in the production of polycarbonate. For instance, Chang et al. (2017) have reported on the production of new biodegradable polycarbonates via copolymerization of soybean oil – based terminal epoxide (SOTE) with CO₂. SOTE was produced by reacting soybean oil in the form of soap with epichlorohydrin and cetyltrimethylammonium bromide as a phase transfer catalyst. Copolymerization of SOTE with CO₂ took place in an autoclave with the use of SalenCoCl/PPNCl as the catalyst. The mixture was stirred for 24 hours at room temperature with CO₂ pressure of 4 MPa. Scheme 2.6 illustrates the synthesis of bio-based polycarbonate from soybean oil and CO₂. The formation of polycarbonate was confirmed by means of the FTIR and NMR analysis. From their observation, the intensity of the characteristic absorption peak of the epoxy group at 855 cm⁻¹ and 910 cm⁻¹ decreased, and the characteristic absorption peak of the carbonyl group shifted from 1739 to 1744 cm⁻¹, indicating

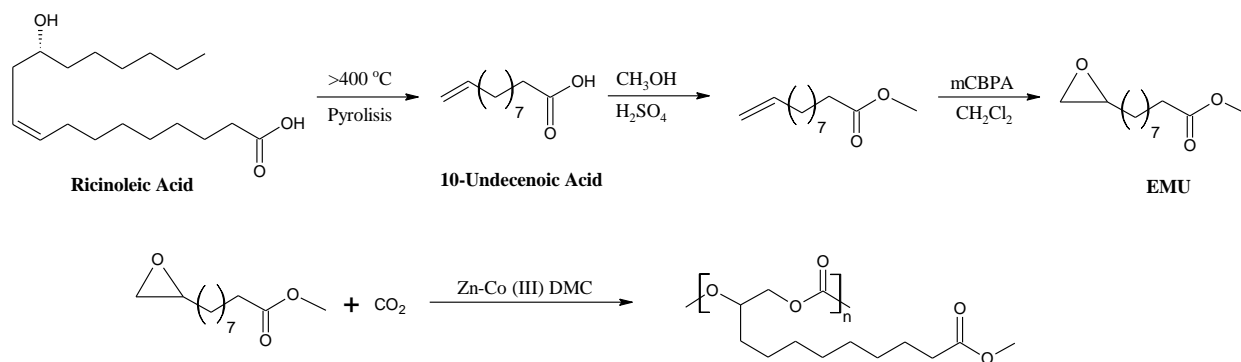
the formation of linear polycarbonate structures. At the same time, the characteristic absorption peak of the C=O stretching vibrations of cyclic carbonate at 1805 cm^{-1} was observed, suggesting the presence of the by-product. Meanwhile at reaction time of 24 hours, both peaks correspond to epoxy group almost vanished implying the conversion of SOTE to polycarbonate and cyclic carbonate. From the NMR spectrum, the peaks around 3.3 – 3.6 ppm which attributed to ether linkages were almost absent, thus the obtained polymer was believed to have a very high alternating structure with carbonate linkages more than 99%. The yield of polycarbonate obtained was reported to be 31.7% while the molecular weight and PDI was about 5100 g/mol and 1.22 respectively.



Scheme 2.5. Synthesis of bio-based polycarbonate from soybean oil and CO_2 (Cui et al., 2019)

Another publication on the copolymerization of vegetable oil-based epoxide with CO₂ was reported by a research group from Canada. In their study, production of polycarbonate was accomplished by utilizing 1,2-epoxydecane an epoxide which was obtained from 1-decene, a canola oil derived monomer. Canola oil which is abundantly available in Canada comprises of approximately 94% unsaturated fatty acids whereby about 60% of the total fatty acids is mainly an oleic acid. In their study, instead of using the conventional heating method, the copolymerization of 1,2-epoxydecane with CO₂ was carried out under microwave conditions with DMC as the catalyst. Under the microwave irradiation condition, the copolymerization become extremely efficient since it can be completed within minutes. On the other hand since microwave assisted copolymerization involve a very rapid reaction and require a lower pressure, consequently the resultant polymer may have a lower carbonate linkage (Jin et al., 2017).

Bio-renewable monomer, epoxy methyl 10-undecenoate (EMU) can be derived from ricinoleic acid which is the major component in castor oil (~90%) via multiple steps process as shown in Scheme 2.7. Zhang et al. (2014) succeeded in producing fully alternating polycarbonate by reacting EMU with CO₂ in the presence of DMC as the catalyst. They have claimed that all resultant copolymers obtained at temperature between 40 to 80°C have carbonate linkages more than 99% since no ether signals were observed in the ¹H NMR spectra. On the other and as the temperature raised to 90 and 100°C polyether signal become more visible as this is typical catalytic behavior for Zn-Co (III) DMCC. The resultant EMU-CO₂ copolymers display low values of *T_gs* ranging from -38 to -44°C which possibly due to the long alkyl side chain with the ester groups.



Scheme 2.6. Synthesis of EMU and its copolymerization with CO_2 (Zhang et al., 2014)

2.5 Degradation of plastics

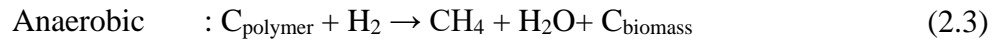
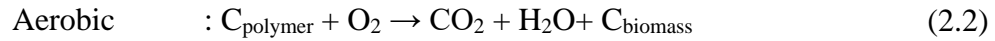
The American Society for Testing and Materials (ASTM) and the International Organization for Standardization (ISO) define degradation as an irreversible process leading to a significant change of the structure of a material, typically characterized by loss of properties (*e.g.*, integrity, molecular weight, structure or mechanical strength) and/or fragmentation. Degradation is affected by environmental conditions and proceeds over a period of time comprising of one or more steps (ASTM International, 2019; International Organization for Standardization, 2013). Likewise, Shah et al. (2008) also refers polymer degradation as any physical or chemical change in polymer as a result of environmental factors, such as light, heat, moisture, chemical conditions or biological activity. Polymer degradation may result in cleavage of bond and chemical alterations which produce shorter oligomers, monomers, and/or other low molecular weight degradation products. In general, degradation can occur via several different mechanisms namely photodegradation, oxidation, thermal degradation, mechanical degradation, chemical degradation and biodegradation. Table 2.12 gives the summary of degradation types and their causes.

Table 2.12. Types and causes of polymer degradation (Kumar et al., 2009)

Types of degradation	Causes/environmental factors
Biodegradation	Micro/macroorganisms, enzymes
Chemical degradation (hydrolysis)	Water
Mechanical degradation	Stress, fatigue (esp. during processing)
Oxidative degradation	Oxygen, ozone
Photodegradation	Light (e.g., ultraviolet and visible light)
Thermal degradation	Heat (esp. during processing)

2.6 Biodegradation

The term biodegradation is often used to refer to degradation which take place in a biological environment. As mentioned by Briassoulis and Dejean (2010) biodegradation is chemical degradation caused by the enzymatic action of microorganisms such as bacteria, fungi, and algae whereby these microorganisms identify the polymeric material as the source of carbon and energy they need for life. Depending on the presence or absence of oxygen, biodegradation is classified as aerobic or anaerobic. In aerobic biodegradation, oxygen is used by the microorganisms to breakdown the polymer chain during the metabolism process which in turn CO_2 gas and water are produced and released to the atmosphere (as shown in equation 2.2). As stated in ASTM D5338-15, this reaction predominates if a high oxygen concentration is available (not less than 6%) (ASTM International, 2015). Conversely, anaerobic biodegradation occurs in an environment without the presence of oxygen. Herein, methane gas (CH_4) and water are generated and released instead of CO_2 . The chemical process can be summarized by equation 2.3. Biodegradation in a compost pile is mainly aerobic whereas examples of anaerobic conditions include those in sewage and in landfills where CH_4 is collected (Kale et al., 2007).



2.6.1 Polymer biodegradation

As mentioned earlier, biodegradation may take place in two different environments namely aerobic and anaerobic condition. These are further divided into aquatic and solid environments whereby the solid environment is mainly soil and compost. As stated by Mittal (2012), microbial degradation of materials may be evaluated by exposing the test material to a huge diversity of environmental microorganisms found in compost, soil, marine, fresh water and activated sludge samples. Another possibility is by selecting pure cultures of bacteria or fungi that are known to have biodegradation potential and they are placed in the environment where biodegradation will take place.

There are several factors that affect biodegradation of polymers as portrays in Figure 2.9. Apart from the type of organism, degradation depends on the polymer characteristics such as its mobility, tacticity, crystallinity, molecular weight, the type of functional groups and substituents present in its structure. Environmental factors also play a prominent role in polymer degradation as they highly influenced the microbial population and their activity. Humidity, temperature, pH, salinity, the presence or absence of oxygen, and the supply of different nutrients are among the parameters which must be taken into consideration when the biodegradability of polymer or plastic materials need to be studied.

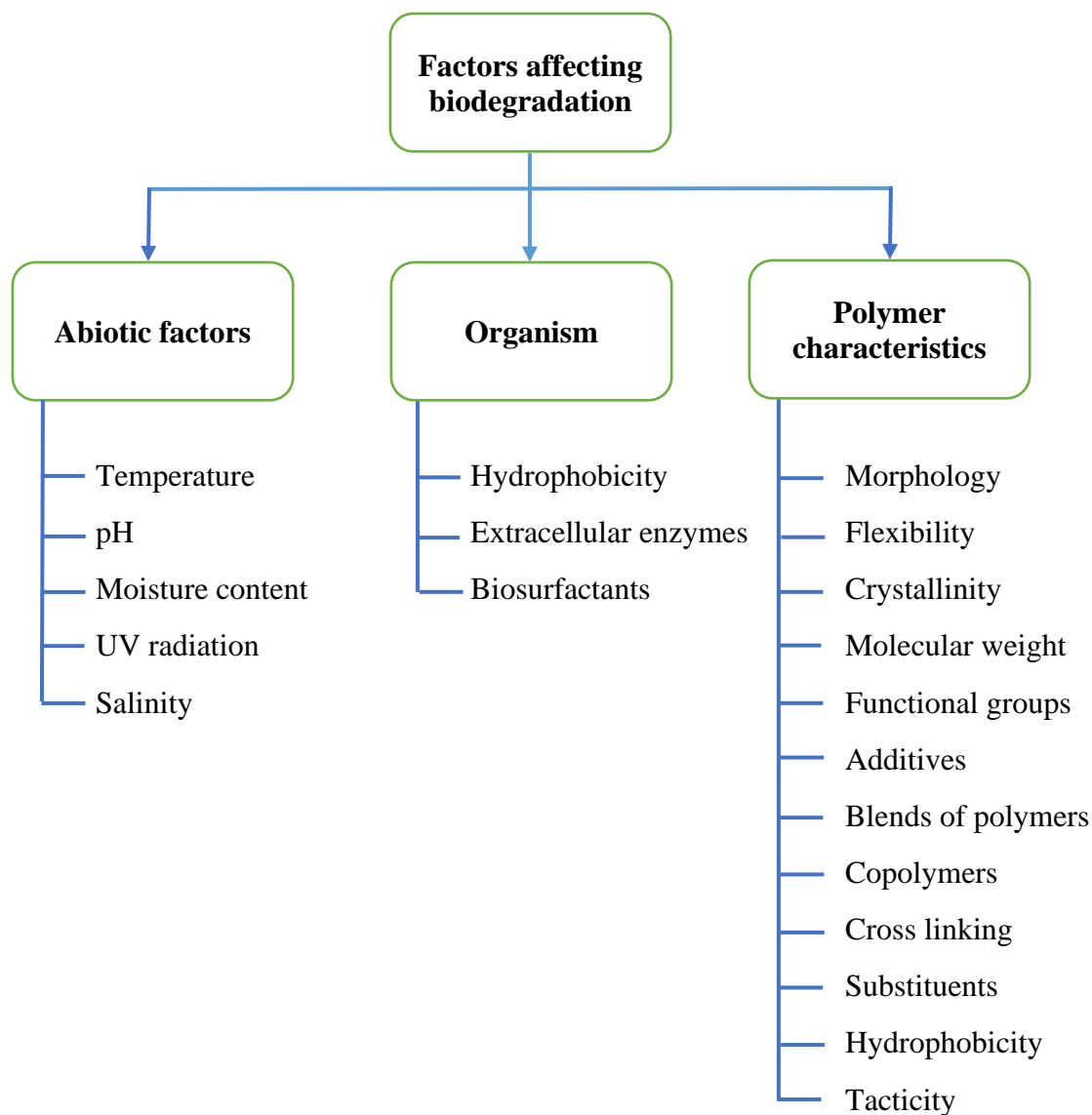


Figure 2.10. Parameters affecting the biodegradation of polymers (Artham and Doble, 2008)

2.6.2. Mechanism of Biodegradation

Biodegradable polymers are generally degraded via two steps: primary degradation and ultimate biodegradation (as shown in Figure 2.10). In primary degradation, disintegration take place due to oxidation or hydrolysis initialized by chemical or biological compounds (microbial enzymes) (Grima et al., 2000; Shah et al., 2008). These processes involve either chain scission or

depolymerization resulting in the formation of low molecular weight chains that can be easily assimilated by the microorganisms. Lastly, ultimate biodegradation eventuates by assimilation of newly formed short polymer chains by microorganisms. This process leads to the formation of biomass, water, carbon dioxide (aerobic) or methane (anaerobic), salts and minerals (Grima et al., 2000; Leejarkpai et al., 2011). This final step is also known as mineralization (Grima et al., 2000; Shah et al., 2008).

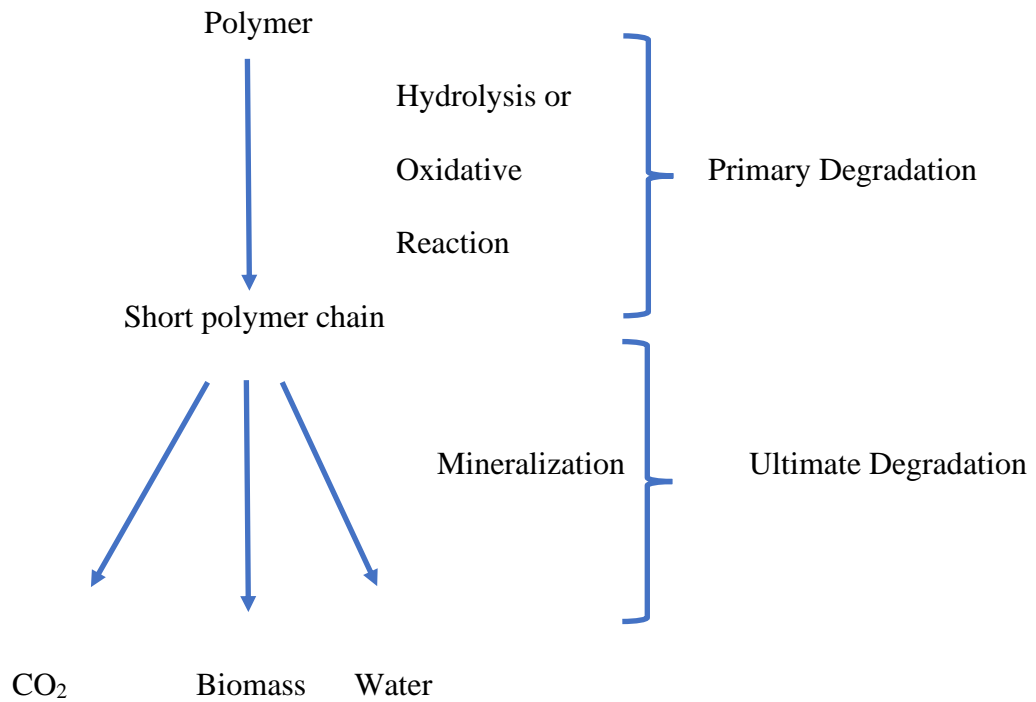


Figure 2.11. Schematic of polymer biodegradation mechanism (Leejarkpai et al., 2011)

2.6.3. Techniques for Evaluation of Biodegradation

Different analytical techniques can be employed to evaluate biodegradation of polymers either in a direct or an indirect approach (Mittal, 2012). The most basic techniques used to assess degradation are by means of visual observations, weight loss measurements, and change in mechanical properties. If the polymer underwent biodegradation, changes on the polymer surface such as formation of holes or cracks, roughening of the surface, de-fragmentation, or changes in colour may be detected through visual observations. Meanwhile, as the name implies weight loss measurements are based on the reduction of polymer weight due to the fragmentation of the polymer. Commonly, polymer samples are weighed before and after biodegradation and the percentage weight loss is determined as follows:

$$\% \text{ Weight loss} = \frac{W_{t_0} - W_{t_s}}{W_{t_0}} \times 100 \quad (2.4)$$

where, W_{t_0} and W_{t_s} refer to the weight of samples at time 0 (before exposure) and at specific sampling time, correspondingly. Materials demonstrating over 90% of weight loss are often assumed to be nearly completely biodegraded. When only minor changes in the mass of the test specimen are observed then changes in mechanical properties will be evaluated. Tensile strength for instance is very sensitive towards changes in the molecular weight of polymers and this often utilized as an indicator of degradation (Erlandsson et al., 1997; Shah et al., 2008).

Despite such physical tests being practical due to their low cost and simplicity, a few issues limit their ability to provide conclusive information on the biodegradability of plastic materials. Visual assessment is qualitative and subject to substantial human error (*e.g.*, due to variation in

experience). Moreover, according to Eubeler et al. (2009) evidence for changes in surface morphology or the degree of microbial attachment are not indicative of biodegradation in their own right. Contrary to with visual assessment, measurements of weight loss are quantitative and typically correlate well with CO₂ evolution. Nevertheless, as measurements of mass loss are performed at specific time intervals (rather than continuously) and are subject to inherent biases, this correlation is relatively poor during the early lag phase. According to the ISO 14855-1 (International Organization for Standardization, 2012), lag phase is define as time, measured in days, from the start of a test until adaptation and/or selection of the degradation microorganisms is achieved and the degree of biodegradation of a chemical compound or organic matter has increased to about 10% of the maximum level of biodegradation.

Even though other laboratory techniques such as infrared (IR) and UV-visible spectroscopy, nuclear magnetic resonance (NMR), gel permeation chromatography (GPC), and scanning electron microscopy (SEM) can be used to assess the biodegradability of polymers, respirometric methods are generally favoured to evaluate biodegradation of polymers in laboratory settings (Shah et al., 2008). Like any chemical reaction, it is possible to monitor biodegradation either by following the consumption of the reagents or the appearance of the products. From a technical viewpoint the best way to monitor and quantify biodegradation is to measure either the reagent (O₂) or the end product (CO₂) of energy metabolism (Equation 2.2).

In general, a respirometer comprises of three major components which are an air supply, an air-tight closed vessel called the bioreactor which contains compost mixture and/or test or reference materials and a measuring device to quantify the amount of O₂ uptake or CO₂ release.

The consumption of oxygen or the evolution of carbon dioxide are directly measured either discretely or continuously by using different techniques. Methods for measuring biodegradation are classified into three whereby these methods are categorized based on the technique used to quantify CO₂ from the exhaust of the bioreactor. The three methods are:

- i. cumulative measurement respirometric system (CMR) (ASTM International, 2015; International Organization for Standardization, 2012),
- ii. direct measurement respirometric system (DMR) and
- iii. gravimetric measurement respirometric system (GMR) (International Organization for Standardization, 2018).

In the CMR, the evolved CO₂ is trapped in a solution, e.g. sodium hydroxide (NaOH) or barium hydroxide (Ba(OH)₂) throughout the test and then the amount of CO₂ is determined by titration (Kijchavengkul and Auras, 2008). Similarly, in gravimetric measurement respirometry (GMR), CO₂ is captured in absorption columns filled with pellets of NaOH, and the amount of CO₂ is quantified by the weight increase in the columns. Meanwhile, when DMR is used the amount of evolved CO₂ is directly measured from the exhaust of the bioreactor using either a gas chromatography (GC) or a non-dispersive infrared (NDIR) gas analyser (Kijchavengkul and Auras, 2008).

2.6.4. International standards related to biodegradation and composting

Study on biodegradation of polymeric materials commonly focused on exposing these materials into different media or environment and measuring the resultant physiochemical changes. As the interest in the field of biodegradable plastics grows it is essential to develop a standard method to accurately assess them. To address this, internationally recognized standardization bodies, such as the International Organization for Standardization (ISO), as well as regional standardization bodies, such as the American Society for Testing and Materials (ASTM) and the European Committee for Standardization (CEN), are actively involved in developing standards related to composting and biodegradation. These standards provide a broad guideline on methodology to assess the biodegradability of polymers in different media such as soil, compost, aqueous and sludge over a specified time. These testing standards attempt to measure the biodegradation in-situ by measuring the carbon dioxide evolved from the medium (Way et al., 2010). Listed in Table 2.13 are some of the ASTM standards related to composting and biodegradation. Subsequently, Table 2.14 gives the list of EN standards related to biodegradation and composting. ISO standards associated with the biodegradation of plastics is also provided in Table 2.15. Among these standards, commonly ASTM D5338 and ISO 14855 are used by researchers around the world to design and developed a respirometric system to assess the aerobic biodegradation of polymers by analysis of evolved carbon under composting conditions.

Table 2.13. ASTM standards related to composting and biodegradation (Rudnik, 2019)

Standard	Title
ASTM D6400-12	Standard specification for labelling of plastics designed to be aerobically composted in municipal or industrial facilities
ASTM D6868-17	Standard specification for labelling of end items that incorporate plastics and polymers as coatings or additives with paper and other substrates designed to be aerobically composted in municipal or industrial facilities
ASTM D 5338-2015	Standard test method for determining aerobic biodegradation of plastic materials under controlled composting conditions. Incorporating thermophilic temperatures.
ASTM D 5929-18	Standard test method for determining biodegradability of materials exposed to source-separated organic municipal solid waste mesophilic composting conditions by respirometry
ASTM D 6954-18	Standard guide for exposing and testing plastics that degrade in the environment by a combination of oxidation and biodegradation

Table 2.14. EN standards related to biodegradation and composting

Standard	Title
EN ISO 14851:2004	Determination of the ultimate aerobic biodegradability of plastic materials in an aqueous medium – Method by measuring the oxygen demand in a closed respirometer
EN ISO 14852:2004	Determination of the ultimate aerobic biodegradability of plastic materials in an aqueous medium – Method by analysis of evolved carbon dioxide
EN ISO 14855-1:2012	Determination of the ultimate aerobic biodegradability of plastic materials under controlled composting conditions – Method by analysis of evolved carbon dioxide-Part 1: General method
EN ISO 14855-2:2009	Determination of the ultimate aerobic biodegradability of plastic materials under controlled composting conditions – Method by analysis of evolved carbon dioxide-Part 2: Gravimetric measurement of carbon dioxide evolved in a laboratory-scale test
EN ISO 20200:2015	Determination of the degree of disintegration of plastic materials under simulated composting conditions in a laboratory-scale test

Table 2.15. ISO standards on biodegradation of plastics (Funabashi et al., 2009)

ISO No.	Title	Content
14851	Determination of the ultimate aerobic biodegradability of plastic materials in an aqueous medium—Method by measuring the oxygen demand in a closed respirometer	aqueous
14852	Determination of the ultimate aerobic biodegradability of plastic materials in an aqueous medium—Method by analysis of evolved carbon dioxide	
14855-1	Determination of the ultimate aerobic biodegradability of plastic materials under controlled composting conditions—Method by analysis of evolved carbon dioxide Part 1: General method	compost
14855-2	Determination of the ultimate aerobic biodegradability of plastic materials under controlled composting conditions—Method by analysis of evolved carbon dioxide Part 2: Gravimetric measurement of carbon dioxide evolved in a laboratory-scale test	
16929	Plastics—Determination of the degree of disintegration of plastic materials under defined composting conditions in a pilot-scale test	disintegration
20200	Plastics—Determination of the degree of disintegration of plastic materials under simulated composting conditions in a laboratory-scale test	
17556	Plastics—Determination of the ultimate aerobic biodegradability in soil by measuring the oxygen demand in a respirometer or the amount of carbon dioxide evolved	soil
14853	Plastics—Determination of the ultimate anaerobic biodegradation of plastic materials in an aqueous system—Method by measurement of biogas production	anaerobic
15985	Plastics—Determination of the ultimate anaerobic biodegradation and disintegration under high-solids anaerobic-digestion conditions—Method by analysis of released biogas	
17088	Specifications for compostable plastics	specification
DIS 10210	Plastics - Preparation of test materials for biodegradation tests	preparation

2.6.4.1 ISO 14855-2 – Determination of the ultimate aerobic biodegradability of plastic materials under controlled composting conditions – Method by analysis of evolved carbon dioxide – Part 2: gravimetric measurement of carbon dioxide evolved in a laboratory-scale test

This standard specifies a procedure for the determination of the ultimate aerobic biodegradability of plastic materials under controlled composting conditions by gravimetric measurement of the amount of carbon dioxide evolved. Via this method, the optimum rate of biodegradation may be achieved by modifying the humidity, aeration and temperature of the composting vessel.

The inoculum used consists of stabilized, mature compost derived, if possible, from composting the organic fraction of solid municipal waste. Alternatively, instead of mature compost, vermiculite (a clay mineral) inoculated with thermophilic microorganisms obtained from compost with a specific activation phase may be used as the inoculum. The used of vermiculite is preferred whenever the determination of the degree of biodegradation is affected by a priming effect induced by the test material. The test material is mixed with the inoculum and introduced into a static composting vessel where it is intensively composted under optimum oxygen, temperature and moisture conditions for a test period not exceeding six months.

During the aerobic biodegradation of the test material, the ultimate biodegradation products from this process are CO₂, water, mineral salts and new microbial cellular constituents (biomass). The amount of CO₂ evolved in test and blank vessels are continuously monitored, or measured at regular intervals, to determine the cumulative carbon dioxide production. The percentage

biodegradation can be calculated by dividing the amount of CO₂ produced from the test material to the maximum theoretical amount of CO₂ that can be produced from the test material. The maximum theoretical amount of CO₂ produced is calculated from the measured total organic carbon (TOC) content.

2.7 Summary of Literature Review

The preceding literature review has described the copolymerization reaction of epoxides with CO₂ to produce polycarbonate. Extensive works utilizing petroleum derivatives epoxides namely PO, CHO, SO with CO₂ together with the development of various homogeneous and heterogeneous catalytic systems were commonly reported in the literatures. Several literature gaps have been identified with regards to the usage of commercial epoxides in copolymerization reaction to synthesize polycarbonate. Although this method is very promising as an alternative to the conventional methods of producing BPA-PC which were harmful, the usage of petroleum-based monomers is becoming a great concern among researchers owing to the dwindling petroleum resources. Therefore, interest to substitute the petroleum derivative epoxides to bio-based epoxide specifically vegetable oil-based epoxide is regarded as practical alternative since it is renewable, abundantly available and reactive functionalities. To date, very few researches on utilization of epoxidized vegetable oil as co-monomer in the copolymerization reaction with CO₂ have been published (Chang et al., 2017; Jin et al., 2017; Zhang et al., 2014). However, information on the biodegradability of these polymeric material was rarely reported. Thus, in this present study, the synthesis of polycarbonate using a mixture of EVO, PO and CO₂ at high pressure with the presence of heterogeneous catalyst were discussed. Additionally, the biodegradation capability of the

produced products will also be assessed via CO₂ evolution according to the standardized ISO 14855 procedures.

CHAPTER 3 : Preparation of Heterogeneous Catalysts and the Selection of Potential Epoxidized Vegetable Oil for Bio-based Polycarbonate Production via Copolymerization Reaction

3.1. Introduction

The growing awareness over environmental issues such as global warming, climate change and improper waste management coupled with the scarcity of non-renewable resources are driving strong demand for potential sustainable and renewable sources. Plant oils are one of the most important classes of renewable sources because of the wide variety of possibilities for chemical transformations, universal availability, inherent biodegradability and relatively low price (Chauhan et al., 2019; Chavan et al., 2012; Farhadian et al., 2017; Montero de Espinosa and Meier, 2011). In the last 20 years, plant oils began to receive a constant and growing attention from the academy and industry as an alternative feedstock to produce chemicals and polymeric materials traditionally prepared from fossil resources. The evident is clearly shown in terms of a literature search for vegetable oil-polymeric materials whereby the number of articles published have grown exponentially since the end of the nineties to present-day (from few articles to hundreds per year) (Abbasi et al., 2019; Laurentino et al., 2018; Lligadas et al., 2013; Miao et al., 2014; Monroe et al., 2019; Zhang et al., 2017) . It is also worth mentioning, in some cases the use of vegetable oils as part of the formulation for polymeric materials have already reached industrial scale.

Both edible and non-edible vegetable oils are composed of triglyceride molecules containing sites (predominantly, double bond and ester groups) that can be chemically reacted in order to introduce new functional groups. Through chemical modification, new functional groups

are incorporated resulting in monomers or resins as a precursor for polymerization reactions, just as polymer precursors derived from the petrochemical industry. Among number of possible reactions of vegetable oils, epoxidation seems to be mostly applied owing to greater possibilities of further application of obtained products. Epoxidation is an oxidation reaction of alkenes in which epoxy group or oxirane oxygen is introduced at the double bonds (Bhalerao et al., 2018). An epoxide is cyclic ether with three ring atoms. This ring approximately defines an equilateral triangle, which makes it highly strained. The strained ring makes epoxides more reactive than other ethers.

Epoxidation of vegetable oils can be performed through several different methods such as ‘traditional’ epoxidation method by Prilezhaev (Dinda et al., 2008), catalytic epoxidation using acidic ion exchange resin (AIER) (Petrović et al., 2002), chemo-enzymatic epoxidation (Rüschgen, Klaas and Warwel, 1999), and metal-catalyzed epoxidation (Gerbase et al., 2002). Among these methods, the most extensively used and cost-effective method for epoxidation is the conventional method based on in situ generation of peracid by reaction between hydrogen peroxide which act as an oxygen donor and a carboxylic acid (e.g., acetic acid or formic acid) as active oxygen carrier as well as a catalyst. Occasionally, to further catalyze the reaction also added is a small amount of inorganic acid (e.g., HCl, H₂SO₄, HNO₃, H₃PO₄) (Dinda et al., 2008; Goud et al., 2006).

The aims of this work were to synthesize the catalyst to be used in the catalytic polymerization reaction between epoxides with CO₂ and to identify potential vegetable oil-based

epoxide as co-monomer for the aforementioned reaction. Prior to copolymerization reaction, these vegetable oils will undergo *in-situ* epoxidation reaction.

Catalysts for the coupling of CO₂ and epoxides include both homogeneous and heterogeneous catalyst. In this work, three well-known heterogeneous catalysts namely Zinc Adipate, Zinc Glutarate and Co-Zn DMC frequently used in the copolymerization of epoxide and CO₂ were selected mainly due to its ease of availability and preparation. Moreover, numerous researchers have reported a promising results of copolymerization reaction involving these catalysts (Liu et al., 2014; Marbach et al., 2017; Meng et al., 2016; Pinilla-de Dios et al., 2017; Sebastian and Darbha, 2015; Tang et al., 2013; Wang et al., 2006).

Several types of vegetable oils have been identified as the potential starting material for the copolymerization reaction. Vegetable oil with high content of unsaturated fatty acid will be an excellent choice to produce epoxidized vegetable oil. In this preliminary study, five different vegetable oils have been selected which are linseed oil (LO), olive oil (OO), palm oil (PaO), soybean oil (SO) and sunflower oil (SFO). These vegetable oils must be converted to epoxidized vegetable oil via epoxidation reaction prior to their use as co-monomer in the catalytic polymerization reaction with CO₂ to manufacture polycarbonate.

Once the suitable candidates of precursor that can meet the need of the project are found, various material characterization techniques were used to understand the newly developed materials.

3.2 Materials and methods

3.2.1 Materials

Adipic acid (AA) (99.0% purity, Merck Chemicals), glutaric acid (GA) (>99% purity, Merck Chemicals) and zinc oxide (ZnO) (99.0% purity, Merck Chemicals) were used without further treatment. Solvents such as acetone, dichloromethane, methanol and toluene were of analytical reagent grade and used without further purification. Materials, such as potassium hexacyanocobaltate (III) ($K_3Co(CN)_6$) (Sigma-Aldrich), zinc chloride ($ZnCl_2$) (Sigma-Aldrich), and tertiary butyl alcohol (tert-butanol) were used without further purification.

Propylene Oxide (PO) ($\geq 99\%$) and Cyclohexene oxide (CHO) (98%) were both purchased from Sigma-Aldrich. Formic acid 98% (analytical grade) and hydrogen peroxide 30% (v/v) was supplied by Labkem. Sulphuric acid 96% and sodium carbonate anhydrous supplied by Panreac and used as received.

The vegetable palm oil (*Elaeis guineensis*) in golden-yellow colour manufactured by FFM Berhad, Malaysia is an edible-oil used mainly for cooking. Olive oil and Sunflower oil are manufactured by Borges International Group and F. Faiges SL respectively. These three vegetable oils were used as received in the epoxidation reaction. The other two vegetable oils were received in the epoxidized form (epoxidized linseed oil and epoxidized soybean oil) from Traquisa (Barbera del Valles, Barcelona Spain).

3.2.2 Methods

3.2.2.1 Catalyst preparation

In preliminary study, three heterogeneous catalysts were synthesized according to the establish method available in the literature. The three catalysts are Zinc Adipate (ZnO/AA), Zinc glutarate (ZnO/GA) and Cobalt-zinc double metal cyanide (Co-Zn DMC) catalyst.

a) Synthesis of Zinc Adipate (ZnO/AA) catalyst

Zinc adipate was prepared from zinc oxide and adipic acid as described by Tang et al. (2013). Herein, 98 mmol of adipic acid and 100 mmol of zinc oxide were dissolved in 150 mL toluene using a round-bottom flask. The mixture was then stirred vigorously at 80 °C for 10 h. Next, the mixture was filtered and washed several times with acetone. Finally, white powdery zinc adipate was obtained and dried under vacuum at 90 °C for 12 h before use.

b) Synthesis of Zinc Glutarate (ZnO/GA) catalyst

Zinc glutarate (ZnO/GA) was prepared as described by Ree et al. (2000). 98 mmol of Glutaric Acid (GA) was dissolved in 150 mL toluene in a round bottom flask (250 mL) equipped with a Dean-Stark trap to separate and remove water by-product and a reflux condenser with a drying tube. Next, 100 mmol of Zinc Oxide in fine powder was added to the GA solution in toluene. Following to the addition, the slurried mixture was stirred vigorously at 55°C for 4 h and immediately being cooled to room temperature. Lastly, the reaction mixture was filtered and washed with acetone several times, giving powdery zinc glutarate.

c) **Synthesis of Co-Zn DMC catalyst**

Co-Zn DMC catalyst was prepared in the presence of tert-butanol as complexing agent. The method of preparation was according to the procedure outlined by Li et al. (2011). Briefly, solution 1 was prepared by dissolving 6.64 g of $K_3Co(CN)_6$ in 100 ml of double distilled water meanwhile solution 2 was made by dissolving 80 g of $ZnCl_2$ in 300 ml of double distilled water and 150 ml of tert-butanol. Solution 1 was added dropwise to solution 2 over a period of one hour and the mixture was kept for aging at $50^\circ C$ for another two hours under vigorous stirring. The resulted white suspension was filtered and centrifuged to segregate the Co-Zn DMC complex. The white precipitate collected was re-dispersed in a solution of tert-butanol and water (1:1 v/v) using high speed stirring. This step was repeated serially by increasing the volume ratio of tert-butanol to water (6:4, 7:3, 8:2, and 9:1, respectively). Finally, the solid was re-dispersed in pure tert-butanol, centrifuged, and vacuum dried until a constant weight was reached (white colour solid, yield = 3.9 g).

3.2.2.2 Epoxidation reaction

In situ epoxidation were carried out in the molar ratio of 0.4:0.1:1.7 (organic acid: double bonds: hydrogen peroxide). A determined amount of formic acid was added to 100 g of palm oil. The reaction flask containing formic acid/palm oil mixture was kept at constant temperature of $70^\circ C$ with continuous stirring. Equivalent quantity of hydrogen peroxide was added dropwise to the mixture and the reaction resumed for 5 h. It is worth mentioning that epoxidation process is exothermic and to prevent overheating reaction mixture suitable precaution was applied. The resulting epoxidized palm oil was cooled down to room temperature and washed with distilled water. Subsequently, the aqueous layer was removed and the produced epoxidized palm oil was

analyzed by FTIR. The same epoxidation procedure was repeated on olive oil and sunflower oil. The samples collected from the epoxidation reaction was analysed by FTIR to verify the formation of epoxide group.

3.2.2.3 Polymerization experiments

a) Epoxides/CO₂ copolymerization with heterogeneous catalysts

The viability of the three heterogeneous catalysts prepared were tested using two commercial epoxides namely CHO and PO. The copolymerization reaction between epoxide and CO₂ was performed in a 100 mL semi batch reactor made of stainless steel (Autoclave Engineers, Erie, PA USA) equipped/furnished with a mechanical stirrer and an automatic temperature controller system. The reactor was dried at 100 °C for at least 12 h and then it was cooled down to room temperature prior to the reaction.

In the preliminary experiments, copolymerization was conducted at fixed CO₂ pressure of 4.0 MPa and reaction time of 6 hours. For copolymerization of CHO and CO₂, 10 mL of CHO was employed, and the reaction took place at the temperature of 70°C meanwhile 20 mL of PO was reacted at reaction temperature of 60°C. All three catalysts namely Co-Zn DMC, Zn/AA and Zn/GA were loaded at fixed quantity of 0.1 g. The obtained copolymer was dissolved in a minimum amount of dichloromethane and precipitated in surplus of methanol. The copolymer was filtered and then dried to a constant weight. Samples obtained were subjected to characterization studies (GPC and ¹H NMR).

b) Copolymerization of EVO, PO and CO₂ with Co – Zn DMC catalyst

The feasibility of using EVO as the monomer in the copolymerization with CO₂ was studied by performing a series of trial experiment. Copolymerization of EVO and CO₂ was carried out in the above-mentioned reactor in the same manner as for CHO/CO₂ and PO/CO₂. Herein, different operating conditions such as reaction temperature, reaction time, pressure of CO₂ and amount of catalyst loading were applied. The product obtained from the copolymerization reaction was dissolved in small amount of dichloromethane and precipitated by excess methanol. If a white precipitate attained from this step, more likely polycarbonate has been synthesized from the copolymerization reaction. Final product was separated by filtration and then dried to a constant weight and send for further characterization.

**Note: The decision to utilize Co-Zn DMC as the catalyst was made based on the preliminary studies conducted in section 3.2.2.3(a) and the results are presented in section 3.3.1 and 3.3.2*

3.2.2.4 Characterizations

a) Copolymerization products

The molecular weight distributions (MWD) of products obtained from copolymerization of CHO/PO and CO₂ using the three catalysts were determined from Gel Permeation Chromatography (GPC) analysis, using an Agilent HPLC model Infinity 1260 GPC system (Agilent Technologies, Santa Clara, CA, USA). This unit is equipped with a separation column (300 x 7.5 mm) of PL hexafluoroisopropanol (HFIP) gel running at room temperature. HFIP is the mobile phase, and it contains 2.72 g·L⁻¹ of sodium trifluoroacetate to avoid polyelectrolyte effect. 100 µL will be injected and the concentration of each sample will be 0.2 w/v%. Calibration was done with polymethyl methacrylate (PMMA) samples.

The formation of polycarbonate was validated via Proton Nuclear Magnetic Resonance (^1H NMR) analysis. The spectra were recorded using a Bruker AMX-300 spectrometer at room temperature operated at 300 MHz and all measurements were made by using CDCl_3 as solvent.

b) Co-Zn DMC

Infrared spectra of $\text{K}_3\text{Co}(\text{CN})_6$ and Co-Zn DMC were recorded using a Fourier Transform Infrared spectrometer (FTIR) (Nicolet iS10) (Thermo Fisher Scientific, Waltham, MA, USA). The FTIR spectra of the samples were obtained at a total of 32 scans using wavenumber interval ranging from 400 to 4000 cm^{-1} at 4 cm^{-1} resolution. The surface morphology of Co-Zn DMC catalyst was examined using a JEOL JSM-5610 Scanning Electron Microscopy (JEOL Ltd., Tokyo, Japan) operating at 12 kV under vacuum. Sample was coated with a thin layer of gold in argon atmosphere prior to testing. To evaluate the thermal stability of Co-Zn DMC, thermogravimetric analyser (TGA) model TGA 2 (SF) (Mettler Toledo, USA) was used. The sample (with an approximate mass of 10 mg) will be heated from environmental temperature to 1000°C in an inert atmosphere of nitrogen.

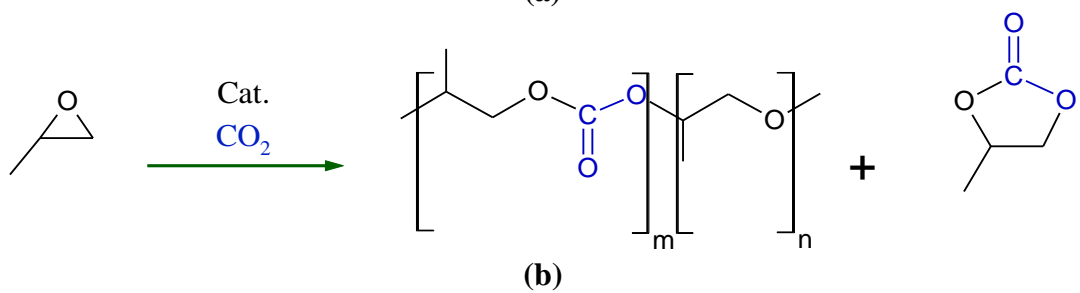
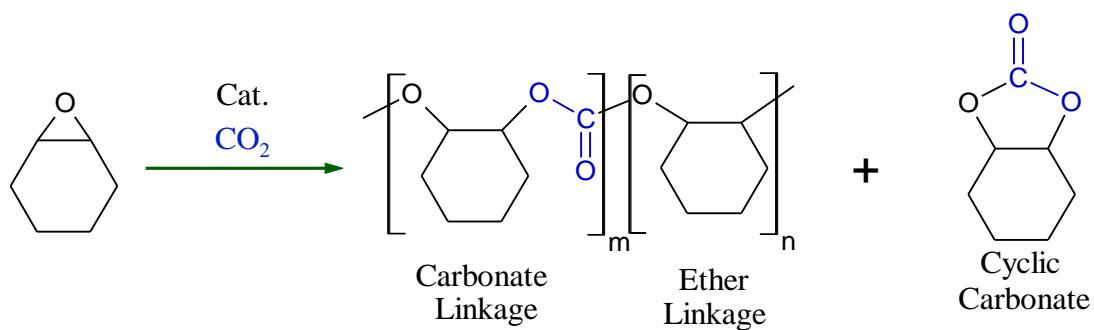
c) VOs and EVOs

FT-IR spectra of VOs and EVOs for the determination of alkene and epoxide group content were recorded using Perkin - Elmer 1000 FTIR spectrometer. The FTIR spectra of the samples were obtained at a total of 32 scans using wavenumber interval ranging from 600 to 4000 cm^{-1} at 4 cm^{-1} resolution.

3.3 Results and discussion

3.3.1 Product analysis and characterization

The first step of this research work was to determine the best heterogeneous catalyst for the copolymerization reaction. In this regards, CHO and PO which are the frequently explored epoxides for copolymerization (Cheng et al., 2018; Fan et al., 2015; Meng et al., 2016; Ni and Kozak, 2018; Sheng et al., 2015; Shi et al., 2018; Trott et al., 2019; Xu et al., 2017) were employed as co-monomer to test the practicality of the prepared catalysts. Hypothetically, copolymerization of CHO/CO₂ may produce poly(cyclohexene carbonate) (PCHC) while PO/CO₂ copolymerization generate poly(propylene carbonate) (PPC) as shown in Scheme 3.1 (a) and (b) respectively. The summary of the copolymerization conditions applied in the screening experiments are presented in Table 3.1. Data collected have shown that under the polymerization conditions applied, the three catalysts used in the preliminary study can give a moderate yield of PCHC and PPC products with the best yield was obtain by Co-Zn DMC.



Scheme 3.1. (a) Copolymerization of CHO and CO₂ and (b) copolymerization of PO and CO₂

(Kothandaraman et al., 2019)

Table 3.1. Preparation conditions of polycarbonate samples by using different types of monomers and catalysts.

Sample	Monomer	Catalyst	Volume Monomer (ml)	Pressure (MPa)	Temp. (°C)	Time (h)	Yield (g)
PCHC1	CHO	Co-Zn DMC	10	4	70	6	3.96
PCHC2	CHO	ZnO/AA	10	4	70	6	2.10
PCHC3	CHO	ZnO/GA	10	4	70	6	2.48
PPC1	PO	Co-Zn DMC	20	4	60	6	5.76
PPC2	PO	ZnO/AA	20	4	60	6	2.40
PPC3	PO	ZnO/GA	20	4	60	6	3.35

3.3.2 GPC Analysis

Number average of molecular weight (M_n), number weight average molecular weight (M_w), Z average molecular weight (M_z) and polydispersity index ratio (PDI) of each polymeric product are summarized in Table 3.2. Both PCHC and PPC samples attained in the trial experiments gave satisfactory M_n values ranging from $3.436 \times 10^3 \text{ g.mol}^{-1}$ to $1.032 \times 10^4 \text{ g.mol}^{-1}$ and $3.700 \times 10^3 \text{ g.mol}^{-1}$ to $1.019 \times 10^4 \text{ g.mol}^{-1}$ respectively. The PDI values of all samples collected are very low and close to unity.

Table 3.2. Molecular weights and PDI of PCHC and PPC samples

Sample	M_n (g/mol)	M_w (g/mol)	M_z (g/mol)	PDI
PCHC1	1.032×10^4	1.049×10^4	1.066×10^4	1.017
PCHC2	3.436×10^3	3.528×10^3	3.614×10^3	1.027
PCHC3	4.004×10^3	5.208×10^3	6.330×10^3	1.301
PPC1	1.019×10^4	1.037×10^4	1.055×10^4	1.018
PPC2	3.700×10^3	3.745×10^3	3.789×10^3	1.012
PPC3	9.935×10^3	1.013×10^4	1.032×10^4	1.020

3.3.3 Characterization of Co-Zn DMC catalyst

Since Co-Zn DMC give the best yield and highest M_n for copolymerization product of both epoxides with CO₂, this catalyst was employed in the subsequent investigation. In brief, DMC is the common heterogeneous catalyst applied in the copolymerization of epoxide with CO₂. Also known as Prussian blue analogues, the synthesis of these compounds is quite straightforward and usually involves fast precipitation reaction, immediately after solution of a water-soluble metal salt (e.g., zinc chloride - ZnCl₂) is mixed with a water-soluble metal cyanide salt (e.g., potassium hexacyanocobaltate - K₃[Co(CN)₆]) (Liu et al., 2003).

DMC catalysts will be less active if prepared in the absence of complexing agents. This is in accordance with the report by Sebastian and Srinivas, which state that coordinated t-BuOH (complexing agent), is essential for inducing activity to the DMCC catalysts. The integration of complexing agents during the synthesis of DMC catalysts help to reduce the crystallinity and crystal symmetry of the catalyst hence improving the catalytic activities of DMCC (Sebastian and Srinivas, 2015). Organic compound such as t-BuOH and low molecular weight functional

polymers (polyethylene glycol, poly(propylene glycol), poly(tetramethylene ether glycol) and etc.) are usually utilized as the complexing agents.

The FTIR spectra of $K_3[Co(CN)_6]$ and Co-Zn DMC catalyst are presented in Figure 3.1. From the spectra, comparing between $\nu(CN)$ of $K_3[Co(CN)_6]$ and stretching vibration of CN^{-1} in Co-Zn DMC catalyst, the peak shifted to higher frequencies, from 2126 cm^{-1} to 2193 cm^{-1} . This implies that CN^{-} acts as σ -donor by donating electrons to the Co^{3+} and as a π -electron donor by chelating to Zn^{2+} ($Co^{3+}-CN-Zn^{2+}$), which is responsible for raising the $\nu(CN)$ value (Dharman et al., 2008). Also prominent from the spectrum of Co-Zn DMC catalyst are the appearance of $-OH$ stretching vibration absorption and C-H stretching vibration absorption at approximate 3482 cm^{-1} and 2985 cm^{-1} respectively, which further validate the presence of complexing agent that is tert-butanol (Guo and Lin, 2014).

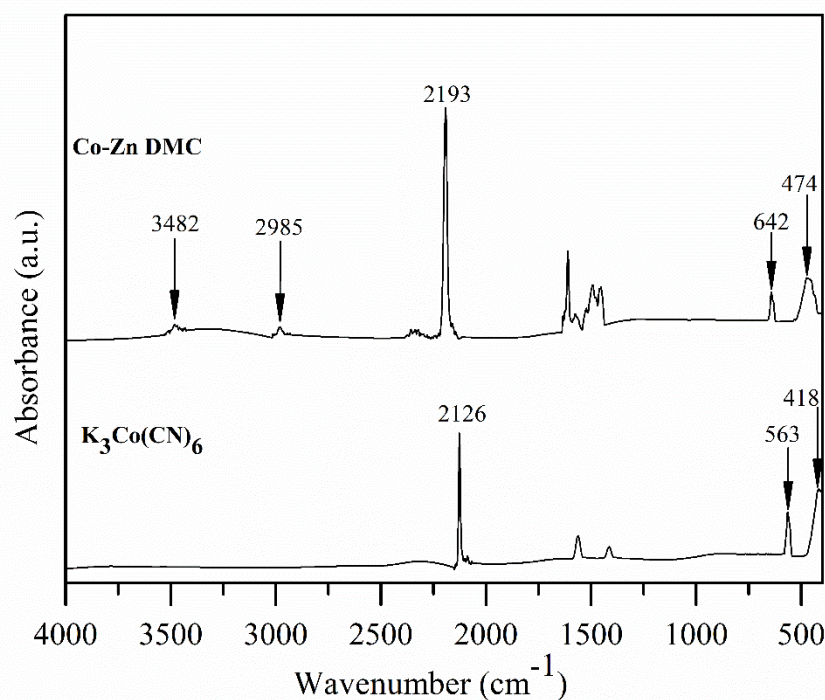
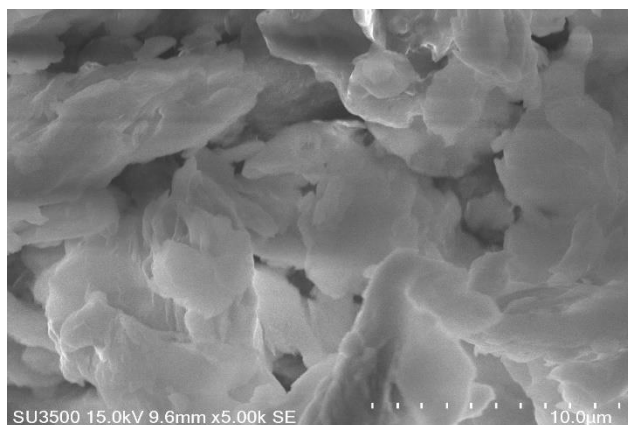
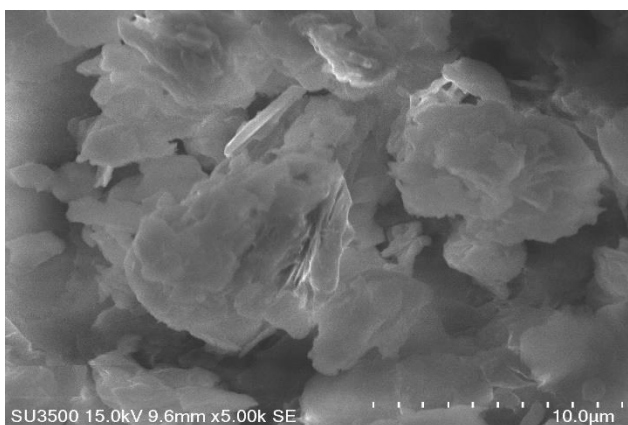


Figure 3.1. IR spectra of $K_3[Co(CN)_6]$ and Co-Zn DMC catalyst

The surface morphology of the Co-Zn DMC catalyst was clearly observed by scanning electron microscopy (SEM) as depicted in Figure 3.2 (a) and 3.2 (b). From the image recorded, the surface of the catalyst prepared in the presence of the complexing agent was relatively dispersive in a flakes shape with a large surface area.



(a)



(b)

Figure 3.2. (a) and (b) SEM images of Co-Zn DMC

The stability and decomposition temperatures of Co–Zn DMC was determined from thermogravimetric (TG) analysis. The result showed the weight loss patterns and decomposition temperatures (Figure 3.3). Three stages of weight losses were observed. Stage-I (25–200°C) was the removal of coordinating water and tert-BuOH molecules in the DMC catalyst. Stage-II (200–610°C) was caused by the decomposition of the cyanide group, followed by the transformation of the double metal cyanide complexes into metal nitrates and carbonates. Stage III (610–850°C) was the complete decomposition of the materials into metal oxide.

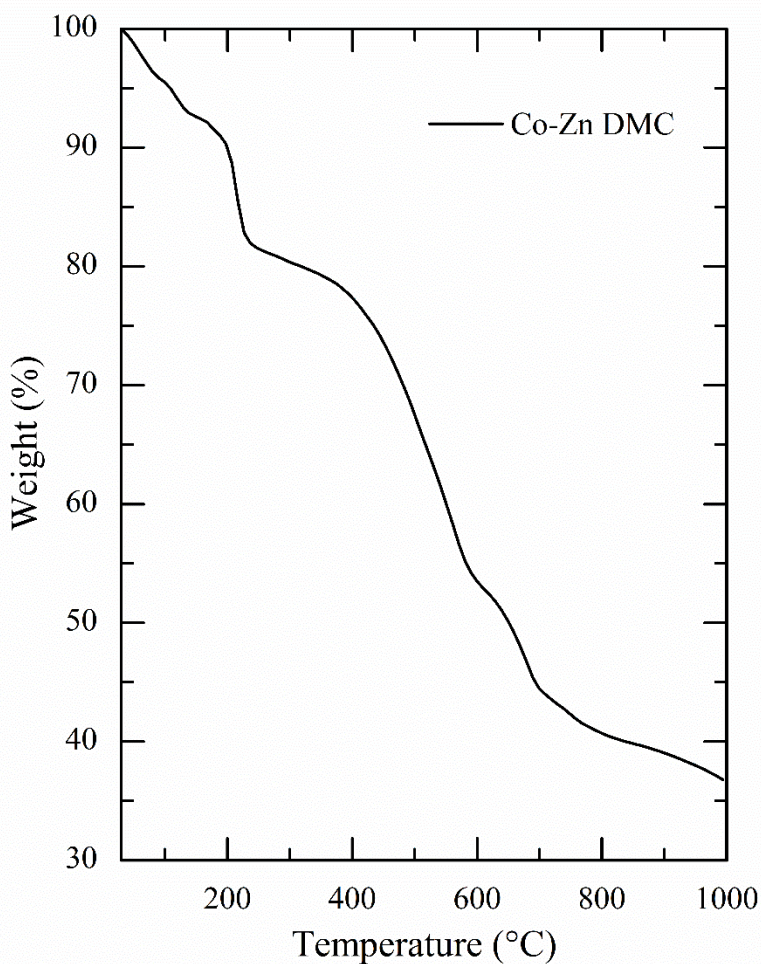


Figure 3.3. Thermogravimetric analysis of Co–Zn DMC complex.

3.3.4 Proton Nuclear Magnetic Resonance (^1H NMR) Analysis

Formation of polymers obtained using Co-Zn DMC was further confirmed by proton nuclear magnetic resonance (^1H NMR) analysis. Figure 3.4 depicts the ^1H NMR spectrum of PCHC1 and the summary of signals assign for PCHC1 is given in Table 3.3.

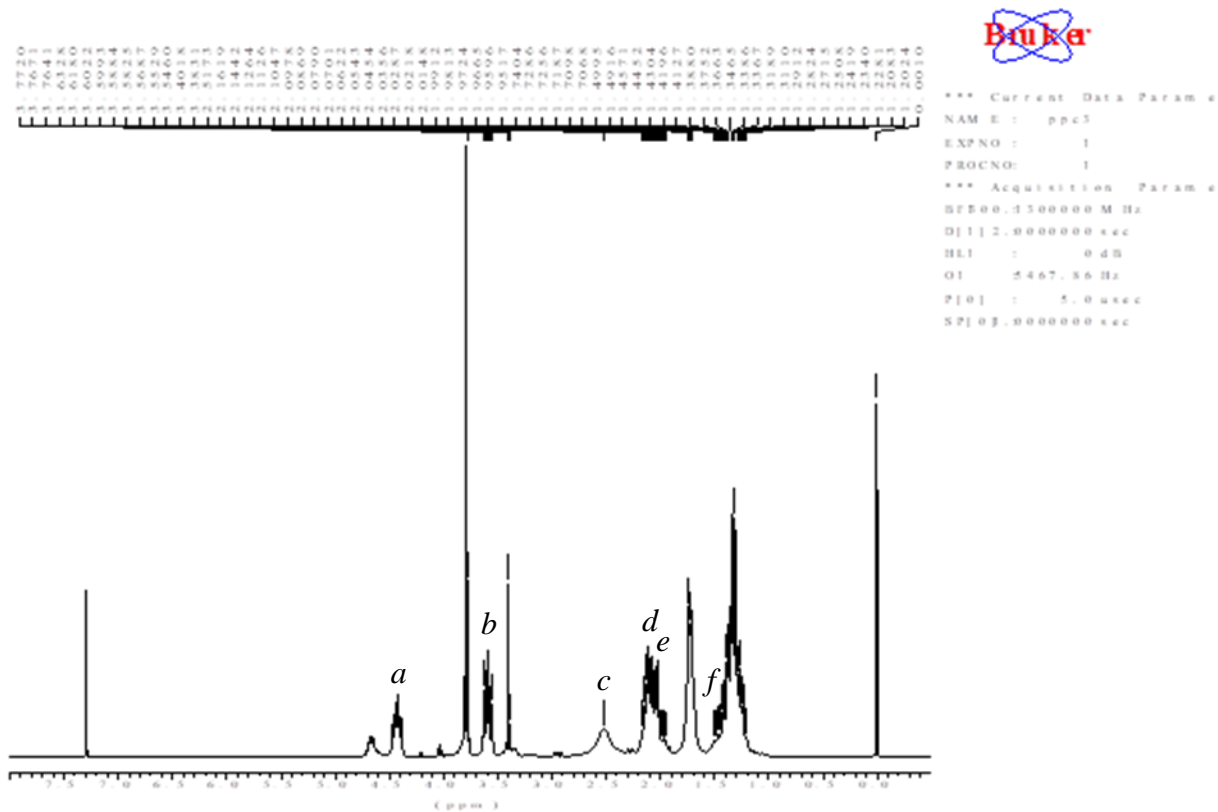
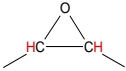


Figure 3. 4. ^1H NMR spectrum of PCHC1

Table 3.3. Summary for ^1H NMR spectrum of PCHC1

Signal	Chemical shift, δ [ppm]	Structure with assignment
<i>a</i>	4.5	–CH–CH–
<i>b</i>	3.5	>CH– at epoxy group 
<i>c</i>	2.5	–CH ₂ –CH ₂ – (β)
<i>d</i>	2.0	–CH ₂ –CH ₂ – (β)
<i>e</i>	1.9	–CH ₂ –CH ₂ –
<i>f</i>	1.6	–CH ₂ –CH ₂ –

The ^1H NMR spectrum of PPC1 and the summary of signals assign for PPC1 is given by Figure 3.5 and Table 3.4 correspondingly.

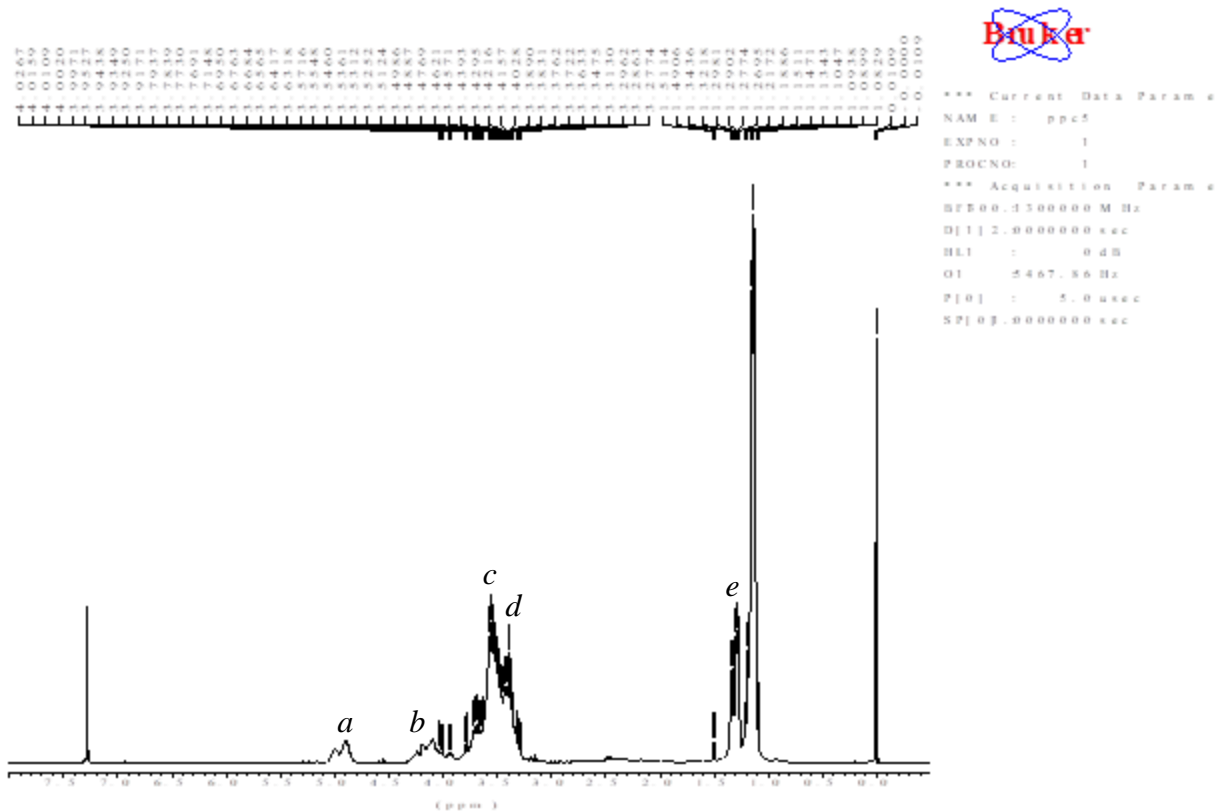


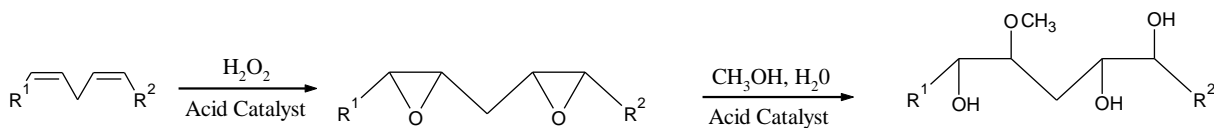
Figure 3.5. ¹H NMR spectrum of PPC1

Table 3.4. Summary for ¹H NMR spectrum of PPC1

Signal	Chemical shift, δ [ppm]	Structure with assignment
<i>a</i>	5.0	–CH–
<i>b</i>	4.3	–CH ₂ –
<i>c</i>	3.5	–CH ₂ – (polyether linkages)
<i>d</i>	3.4	–CH– (polyether linkages)
<i>e</i>	1.3	–CH ₃ –

3.3.5 Epoxidized Vegetable Oil

The oil selection for the epoxidation reaction depends upon the degree of unsaturation of fatty acids. Oils like soybean oil, sunflower oil, linseed oil etc. are rich in oleic, linoleic and linolenic acyl groups, which can be easily used to introduce the epoxide functional group. In this study, epoxidation reaction was performed on three different types of VOs which are OO, PO and SFO. It is well known that in situ epoxidation involves two consecutive reactions which are dependent on hydrogen peroxide concentration (Petrović et al., 2002). The first reaction is the formation of peroxyformic acid (PFA) from formic acid (FA) (reaction 3.1) while the second reaction is the formation of epoxy group (EO) from the double bond (DB) (reaction 3.2).



Scheme 3.2. Conversion of double bond via epoxidation and ring opening (Hazmi et al., 2013)

In epoxidation of VO, conversion of unsaturation to epoxide was confirmed by using FTIR spectrometer. The analyzed infrared spectra contain fundamental and characteristic bands whose frequencies and intensities can clearly determine the relevant functional groups in the investigated oils. Figure 3.6 depicts the FTIR spectra of virgin OO and EOO. Spectrum of virgin OO show the presence of peaks at 3005 and 1642 cm^{-1} which are assigned to double bonds. These peaks

disappeared after epoxidation and a new peak appeared in the spectrum of the reaction product at 837 cm^{-1} indicating a presence of epoxy groups.

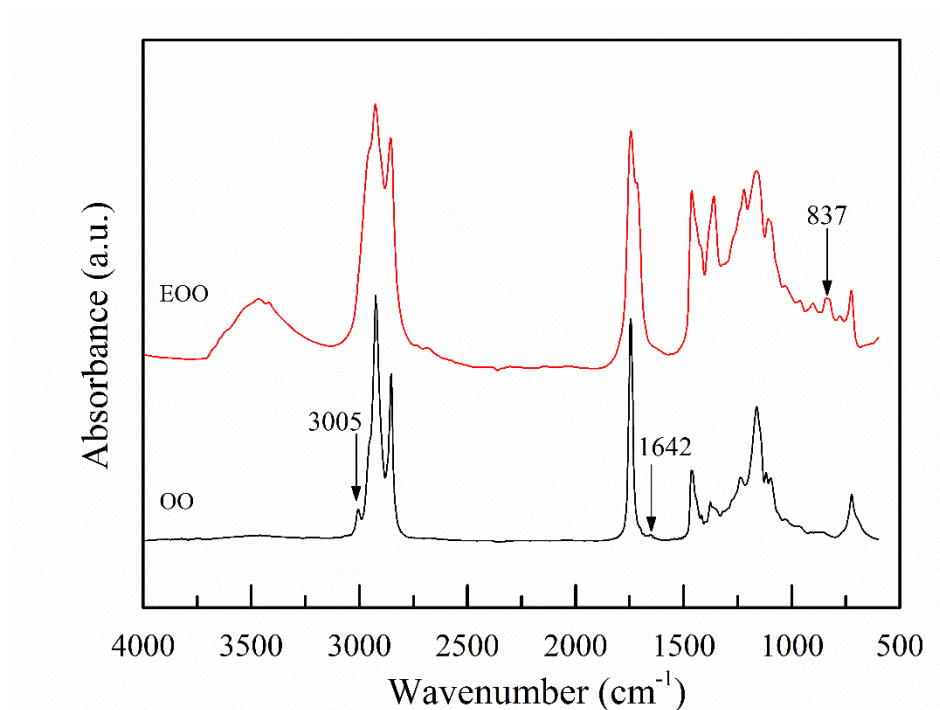


Figure 3.6. FTIR spectra of OO and EOO

Figure 3.7 illustrates the FTIR spectra of virgin PaO and EPaO. Alkene double bonds of PaO at 3004 cm^{-1} disappeared upon epoxidation. Meanwhile formation of epoxy groups in the EPaO is indicated by a band at 826 cm^{-1} . Analogous results are obtained for SFO and the respective product of epoxidation, showing the presence of epoxide group at 834 cm^{-1} . A complete consumption of unsaturation was indicated by the reduction of peak at 3002 cm^{-1} . (Figure 3.8). These results agree with the FTIR obtained reported elsewhere (Bhalerao et al., 2018; Hazmi et al., 2013; Kim et al., 2015; Piccolo et al., 2019; Sienkiewicz and Czub, 2016).

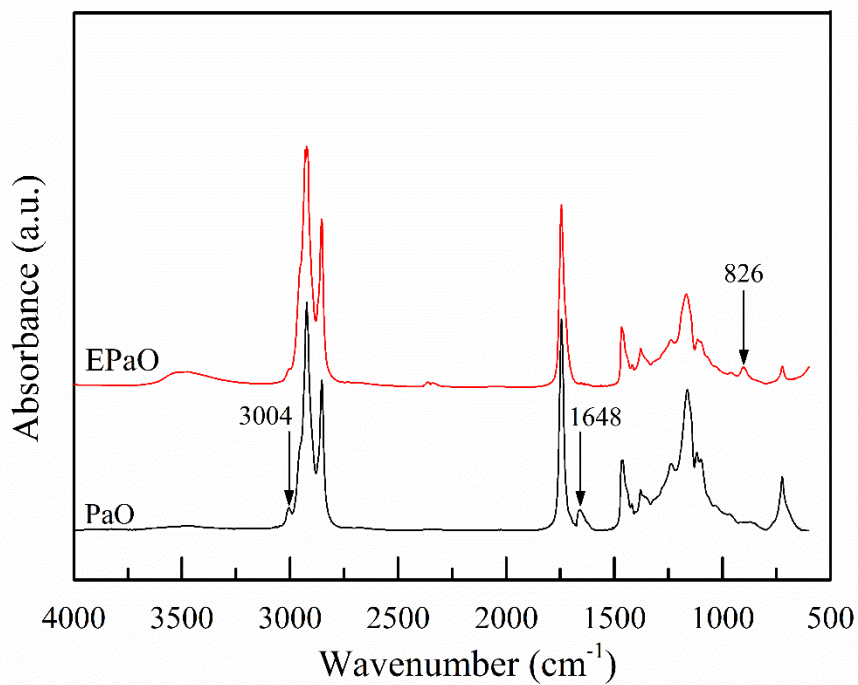


Figure 3.7. FTIR spectra of PaO and EPaO

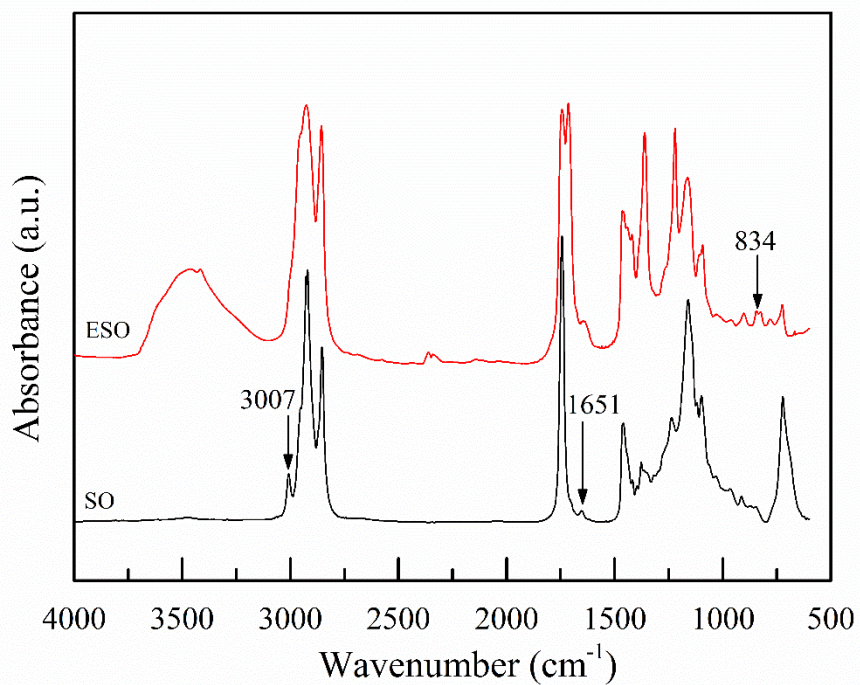


Figure 3.8. FTIR spectra of SFO and ESFO

FTIR spectra for both LO and SO were also analysed and were compared with the epoxide oil obtained from Traquisa (Barbera del Valles, Barcelona Spain). The comparison of the spectrums is illustrated in Figure 3.9 and 3.10. The summary of the band presence on each spectrum are summarized in Table 3.5.

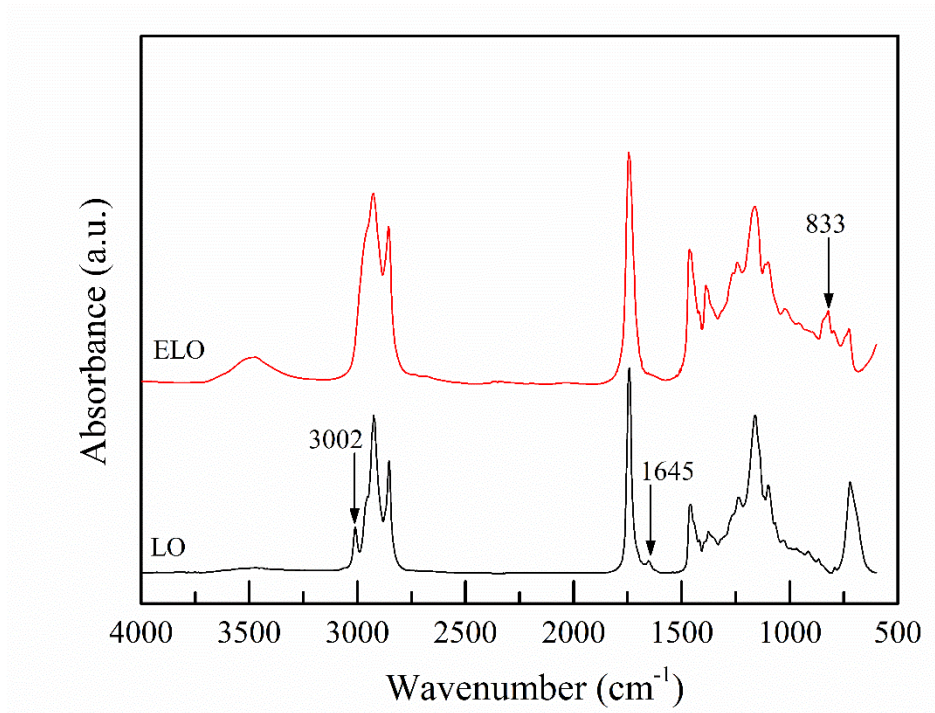


Figure 3.9. FTIR spectra of LO and ELO

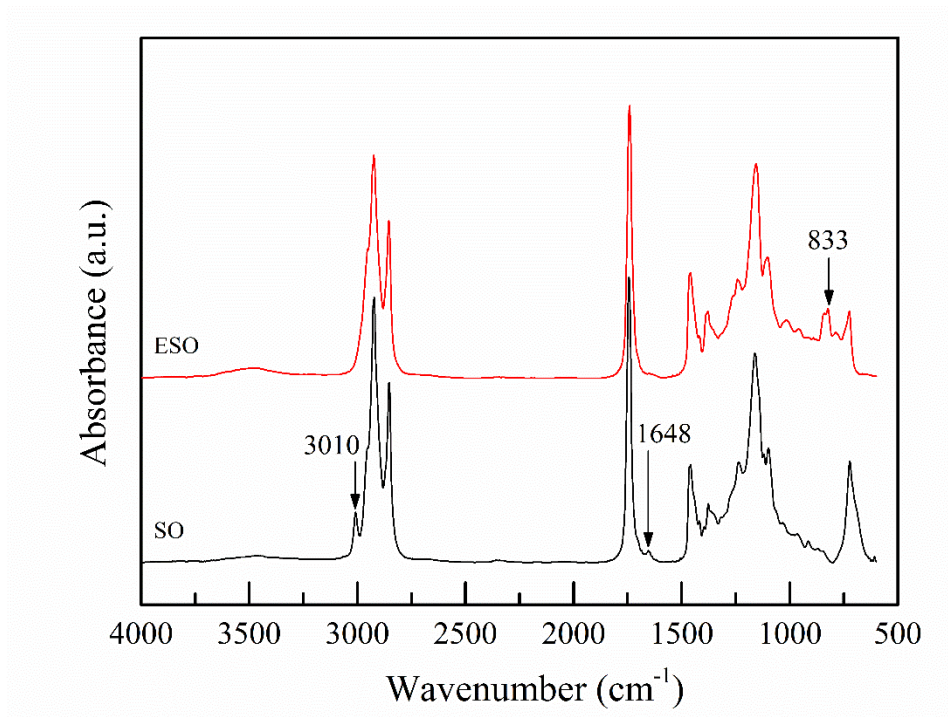


Figure 3.10. FTIR spectra of SO and ESO

Table 3.5. FTIR peaks and their assignment measured for pure oil and epoxidized oil

cm⁻¹										Assignment
LO	ELO	OO	EOO	PaO	EPaO	SFO	ESFO	SO	ESO	
3494	3484	-	3462	-	3494	-	3476	-	3496	C=O ester and OH stretching
3002	-	3005	-	3004	-	3007	-	3010	-	C=C stretching
2928	2928	2927	2927	2925	2925	2925	2925	2925	2925	CH ₃ asymmetric stretching
2854	2854	2854	2854	2854	2854	2854	2854	2854	2854	CH ₂ asymmetric stretching
1737	1737	1740	1740	1741	1741	1743	1743	1741	1741	C=O stretching vibration of triglyceride esters (O=C-O)
1645	-	1642	-	1648	-	1651	1646	1648	-	CH=CH
1457	1457	1461	1461	1463	1463	1463	1463	1463	1463	Scissoring of CH ₂ , asymmetric bending of CH ₃ CH ₂ bending vibration
1384	1384	1372	1365	1375	1375	1374	1363	1375	1375	Symmetric bending of CH ₃ CH ₃ symmetrical bending vibration
1234	1234	1236	1220	1236	1236	1234	1221	1234	1234	C-O-C stretching C-O stretching of ester (C-O-C)
1158	1158	1163	1163	1160	1160	1159	1159	1157	1157	C-O stretching of O=C-O C-O stretching of ester (O=C-O)
1098	1098	1097	1097	1098	1098	1097	1097	1094	1094	C-O stretching of O-CH ₂
-	833	-	837	-	826	-	834	-	833	C-O of epoxides
716	725	723	723	722	722	722	722	722	722	Methylene (CH ₂) rocking vibration

3.3.6 Copolymerization of EVO and CO₂ with Co-Zn DMC

Table 3.6 shows summaries of selected samples prepared during screening experiments for the copolymerization of EVO and CO₂ at different operating conditions. Taking into consideration that all these epoxides never been used as monomer in the copolymerization reaction with CO₂, it has been decided that in the first attempt to manufacture bio-based polycarbonate via copolymerization reaction, a mixture of PO with EVO will be used. From the observation, when the terpolymerization products were dissolved in dichloromethane and excess of methanol no precipitation was found in EOO, EPaO and ESFO. This examination leads to a conclusion that the prepared EVO under the polymerization conditions used in this study are not suitable to produce bio-based polycarbonate. On the other hand, both ESO and ELO obtained from Traquisa (Barbera del Valles, Barcelona Spain) did show formation of white precipitation suggesting that a polymeric product has been synthesized.

Table 3.6. Data of the preliminary experiments

Entry	1st monomer	2nd monomer	P (MPa)	T (C)	T (hr)	W_{cat} (g)	Observation
1	ELO	PO	4	60	6	0.05	No precipitate
2	EOO	PO	4	60	6	0.05	No precipitate
3	EPaO	PO	4	60	6	0.05	No precipitate
4	ESFO	PO	4	60	6	0.05	No precipitate
5	ESO	PO	4	60	6	0.05	No precipitate
6	ELO	PO	4	60	24	0.05	No precipitate
7	EOO	PO	4	60	24	0.05	No precipitate
8	EPaO	PO	4	60	24	0.05	No precipitate
9	ESFO	PO	4	60	24	0.05	No precipitate
10	ESO	PO	4	60	24	0.05	No precipitate
11	ELO	PO	4	60	6	0.1	White precipitate
12	EOO	PO	4	60	6	0.1	No precipitate
13	EPaO	PO	4	60	6	0.1	No precipitate
14	ESFO	PO	4	60	6	0.1	No precipitate
15	ESO	PO	4	60	6	0.1	White precipitate
16	ELO	PO	4	60	24	0.1	White precipitate
17	EOO	PO	4	60	24	0.1	No precipitate
18	EPaO	PO	4	60	24	0.1	No precipitate
19	ESFO	PO	4	60	24	0.1	No precipitate
20	ESO	PO	4	60	24	0.1	White precipitate

3.4 Conclusions

Based on the preliminary experiments conducted, yield and molecular weight of PCHC1 and PPC1 recorded are the highest among other copolymerization products and these implies the viability of using Co-Zn DMC in the copolymerization reaction. Subsequently, in-situ epoxidation

was conducted to transform VO to EVO and to further validate the formation of epoxy group, EVOs samples were analysed using FTIR. Also performed during the primary stage of the experiments were copolymerization reaction between mixture of EVO and PO with CO₂ at different operating conditions. Results obtained signify that two types of epoxides namely ELO and ESO are promising to be used as a co-monomer in the copolymerization reaction most likely due to higher number of epoxide rings available per triglyceride chain of EVO which increases the probability of sites taking part in the reaction.

CHAPTER 4 : Synthesis of Vegetable-Oil based Polymer by Terpolymerization of Epoxidized Soybean Oil, Propylene Oxide and Carbon Dioxide

This part of the work has been published as research article and was presented at the following conference:

1. Shaarani, F.W. and J.J. Bou, Synthesis of vegetable-oil based polymer by terpolymerization of epoxidized soybean oil, propylene oxide and carbon dioxide. *Science of The Total Environment*, 2017. 598: p. 931-936.
2. Shaarani, F.W. and J.J. Bou, Synthesis of vegetable-oil based polymer by terpolymerization of epoxidized soybean oil, propylene oxide and carbon dioxide. Poster presentation at the 10th International Society for Environmental Biotechnology (ISEB) Conference, Barcelona, June 1st to 3rd, 2016.

4.1 Abstract

Although carbon dioxide (CO₂) is well known as one of the major green-house gases, it is also an economical C1 resource. Thus, CO₂ has been regarded as an appealing starting material for the synthesis of polymers, like polycarbonates by the reaction with epoxides. Herein the reaction between natural epoxidized soybean oil (ESO), propylene oxide (PO) and CO₂ under high pressure (4.0 MPa) with the presence of Co-Zn double metal cyanide (Co-Zn DMC) catalyst was studied. Temperature and reaction time were varied accordingly, and the products obtained were characterized by FTIR, GPC and ¹H NMR. The results obtained indicate the formation of polycarbonates in the samples collected with yields vary from 11.2 g to 16.1 g. The number average molecular weight (M_n) of the resultant polymer prepared at reaction temperature of 80°C and reaction time of 6 hours can reach up to 6498 g/mol.

4.2 Introduction

The rising levels of carbon dioxide (CO₂) in the atmosphere are linked to global warming and this phenomenon is becoming a pressing environmental issue. Thus, continuous efforts are being made to mitigate the atmospheric CO₂ concentration via carbon capture and storage. The aforementioned technique is quite popular and received considerable attention among researchers in recent years. This technique requires CO₂ to be removed from the flue gases of large emitters such as power plant by means of membrane separation or an absorbent/adsorbent such as monoethanolamine (MEA) (Coutris et al., 2015). Following to this step, the captured CO₂ then stored in the underground reservoirs. In spite of the fact that this method has great potential in reducing the amount of CO₂ entering the atmosphere, the thought of retaining huge CO₂ reservoirs is not very appealing. In view of that, a more meaningful strategy such as utilization of CO₂ by its

conversion into valuable materials and products is expected to subsidized carbon capture and sequestration processes. Furthermore, the use of CO₂ as a chemical feedstock is ideal since it is abundantly available, inexpensive, non-toxic and non-hazardous (Taşcı and Ulusoy, 2012; Wang et al., 2012).

One of the popular approaches is to use CO₂ as co-monomer in polymerization reactions. In this context, the catalytic copolymerization of epoxides and CO₂ emerges as a promising technology (Sakakura et al., 2007). In the year of 1969, Inoue and co-workers have successfully synthesized poly(propylene carbonate) from propylene oxide (PO) and CO₂ by using ZnEt₂ and water as catalyst (Inoue et al., 1969). To date substantial number of literatures are available revealing different types of outstanding catalyst for the copolymerization process (Ang et al., 2015; Meng et al., 2016; Trott et al., 2016) ever since their discovery. Simultaneously, a number of epoxides and diverse operating conditions for the coupling of CO₂ and epoxides have been reported by devoted researchers (Dai et al., 2016; Darensbourg and Chung, 2014; Oh and Ko, 2013; Sebastian and Srinivas, 2014; Tang et al., 2013). Despite of the countless references available in this field, very few reported on the utilization of renewable bio-resources specifically vegetable oil-based epoxide in copolymerization with CO₂.

The usage of vegetable oil-based epoxide as a starting material can be considered as an interesting strategy to enhance the *green content* of the polymers. Moreover, it may serve as a substitute to the traditional epoxide which is petroleum based. Owing to the heavy dependence of mankind on fossil fuels and its current consumption rates, the worldwide fossil fuel reserves are

depleting rapidly (Ingrao et al., 2015). Hence, it is essential to find an alternative starting material from renewable resources since it can provide both environmental and economic sustainability.

Soybean oil, particularly, is a vegetable oil with interest in polymer since its abundant availability, reactive functionalities and competitive cost (Costa et al., 2016; Miao et al., 2014). This renewable material is composed of triglycerides, which are the major component of plant oil. Triglycerides are formed from three various fatty acid chains joined by a glycerol center. The major composition of fatty acid in soybean oil is linoleic acid with 53% and soybean oil has an average of 4.6 double bonds per molecule (Xia and Larock, 2010).

Polycarbonates are a class of thermoplastic polymers with carbonate linkages in their chemical structure. Commonly, they are categorized as aliphatic or aromatic polycarbonate, depending on the structure of the R groups. The general structure of polycarbonate is shown in Figure 4.1. The conventional method to synthesized polycarbonate is by the reaction between Bisphenol A (BPA) and phosgene (COCl_2) which results an amorphous polymer with high impact strength, toughness, heat resistance and transparency. These exceptional properties made them a versatile material with substantial industrial significance. Although BPA-based polycarbonate produced excellent properties of products, on the other hand it also has some drawbacks such as the usage of highly poisonous phosgene and chlorinated solvents. Utilization of BPA itself as a monomer caused a great anxiety regarding negative health effects due to leaching out of the polymer when in contact with food (US Food and Drug Administration, 2014) . Additionally, both monomers used are fossil-based compounds.

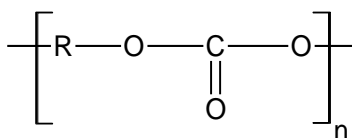


Figure 4.1. General structure of polycarbonate

From the environmental point of view, copolymerization of natural epoxides with CO₂ may lead to significant environmental impacts since they contribute to reduce the atmospheric emissions of CO₂, circumvent the use of very toxic and hazardous phosgene in the traditional route of polycarbonate production and involve the use of renewable bio-resources like vegetable oils which will lessen the dependency on the petroleum-based routes of synthesis.

Therefore, in the present work, an attempt was made to terpolymerize ESO, PO and CO₂ in the presence of heterogeneous catalyst namely Co-Zn Double Metal Cyanide (Co-Zn DMC). The reaction takes place at fixed CO₂ pressure of 4.0 MPa with equal volume of ESO and PO. The reaction temperature and reaction time were varied in the range of 60-100°C and 6-72h and respectively. Under the conditions studied, the resultant products yield a mixture of polycarbonate, cyclic carbonate and polyether.

4.3 Experimental

4.3.1 Material

ESO with approximately 4.5 oxirane rings per triglyceride (Figure 4.2) obtained from Traquisa (Barbera del Valles, Barcelona Spain) was used in this research work whereas PO (>99%) was supplied by Sigma Aldrich. Materials, such as potassium hexacyanocobaltate (III) (K₃Co(CN)₆), zinc chloride (ZnCl₂), and tertiary butyl alcohol (tert-butanol) were used without

further purification. CO₂ with a purity of 99.99% was used as received. Other solvents such as chloroform, dimethyl sulfoxide (DMSO), hexafluoroisopropanol (HFIP), methylene chloride, methanol and toluene were of analytical reagent grade and used without further purification.

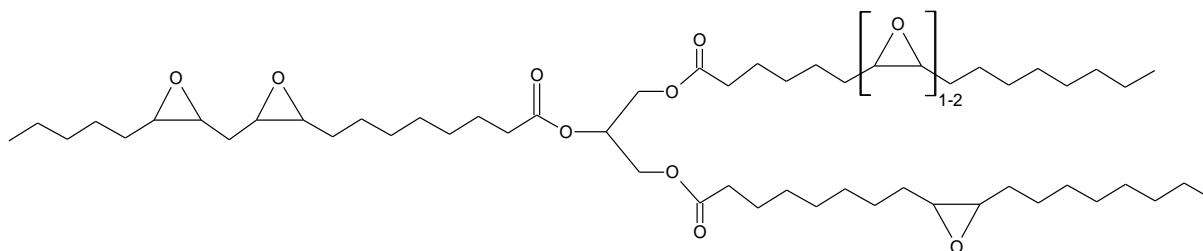


Figure 4.2. Structure of ESO

4.3.2 Preparation of the Catalyst

Co-Zn DMC catalyst was prepared in the presence of tert-butanol as complexing agent. The method of preparation was according to the procedure outlined by Li et al. (2011). Briefly, solution 1 was prepared by dissolving 6.64 g of K₃Co(CN)₆ in 100 ml of double distilled water meanwhile solution 2 was made by dissolving 80 g of ZnCl₂ in 300 ml of double distilled water and 150 ml of tert-butanol. Solution 1 was added dropwise to solution 2 over a period of one hour and the mixture was kept for aging at 50°C for another two hours under vigorous stirring. The resulted white suspension was filtered and centrifuged in order to segregate the Co-Zn DMC complex. The white precipitate collected was redispersed in a solution of tert-butanol and water (1:1 v/v) using high-speed stirring. This step was repeated serially by increasing the volume ratio of tert-butanol to water (6:4, 7:3, 8:2, and 9:1, respectively). Finally, the solid was redispersed in

pure tert-butanol, centrifuged, and vacuum dried until a constant weight was reached (white colour solid, yield = 3.9 g).

4.3.3 Polymerization of ESO, PO and CO₂

Terpolymerization was carried out in a 100 mL stainless steel reactor (Autoclave Engineers, Erie, PA USA) autoclave equipped with a mechanical stirrer and an automatic temperature controller system. The autoclave was first dried at 100°C for at least 12 hours then it was cooled down to 25°C. Subsequently, the reactor was charged with 10 mL of ESO, 10 mL of PO and 0.1 g of dried Co-Zn DMC catalyst. Initially, the reactor was purged twice with CO₂ and next slowly pressurized to 4.0 MPa. The reaction temperature was then raised and maintained between 60 to 100°C with a stirring speed of 500 rpm to initiate the polymerization reaction. Meanwhile the reaction time was ranging between 6h to 72h. Once the reaction ends, the autoclave was cooled down to room temperature, slowly depressurized and opened. The products obtained were purified by dissolving in dichloromethane, precipitated by excess methanol and then dried at room temperature to a constant weight.

4.3.4 Characterizations

The functionalization of K₃Co(CN)₆ and Co-Zn DMC catalyst were examined using IR spectroscopy. Absorption spectra were recorded on a Nicolet iS10 FTIR spectrometer (Thermo Fisher Scientific, Waltham, MA, USA) in attenuated total reflectance (ATR) mode meanwhile spectra of ESO and terpolymerization products were recorded on a Perkin–Elmer 1000 FTIR spectrometer in the wavenumber region of 400 to 4000 cm⁻¹. ¹H NMR spectroscopic analysis of ESO and final products was recorded using a Bruker AMX-300 spectrometer at 25°C. The

equipment operated at 300 MHz and all measurements were made by using CDCl_3 as solvent. In Gel Permeation Chromatography (GPC) test, the number average molecular weight (M_n) and the polydispersity index (PDI) were determined using a Agilent HPLC equipped with a separation column of PLHFIP gel running at room temperature. Mobile phase is HFIP containing $2.72 \text{ g}\cdot\text{L}^{-1}$ of sodium trifluoroacetate to prevent polyelectrolyte effect. $100 \mu\text{L}$ will be injected and the concentration of each sample will be 0.2 w/v%. Calibration was performed with polymethyl methacrylate (PMMA) samples.

4.3.5 Solubility Test

A simple test was conducted to check on the solubility of the insoluble polymers. 20 mg of the samples were mixed in 2 mL of solvent which are chloroform, DMSO, HFIP and toluene at room temperature. The dissolution of the samples in solvent was observed every one-hour interval for the first 6 hours and later monitored once a day up to seven days.

4.4 Results and Discussion

4.4.1 IR of Co-Zn DMC Catalyst

In this study, the DMC catalyst composed of zinc hexacyanometalate was prepared by means of precipitation reaction in a traditional method between $\text{K}_3\text{Co}(\text{CN})_6$ and metal salt namely ZnCl_2 along with tert-butanol as complexing agent. The incorporation of tert-butanol during the preparation of DMC catalyst was claimed could help to heighten the activity of the catalyst (Tharun et al., 2012; Zhang et al., 2011). Shown in Figure 4.3 is the IR spectrums of $\text{K}_3\text{Co}(\text{CN})_6$ and Zn-Co DMC catalyst. It was observed that the $\nu(\text{CN})$ of $\text{K}_3\text{Co}(\text{CN})_6$ shifted to higher wave number approximately 2193 cm^{-1} in Co-Zn DMC catalyst. The $\nu(\text{CN})$ shift to higher frequency is in a good

agreement with report by Dharman et al. (2008) which suggest that CN^- acts as σ - donor by donating electrons to the Co^{3+} and as a π electron donor by chelating to Zn^{2+} , which is responsible for raising the (CN) value (Dharman et al., 2008). The presence of complexing agent tert-butanol, was verified by the $-\text{OH}$ stretching vibration absorption and C-H stretching vibration absorption at approximate 3482 cm^{-1} and 2985 cm^{-1} respectively (Guo and Lin, 2014).

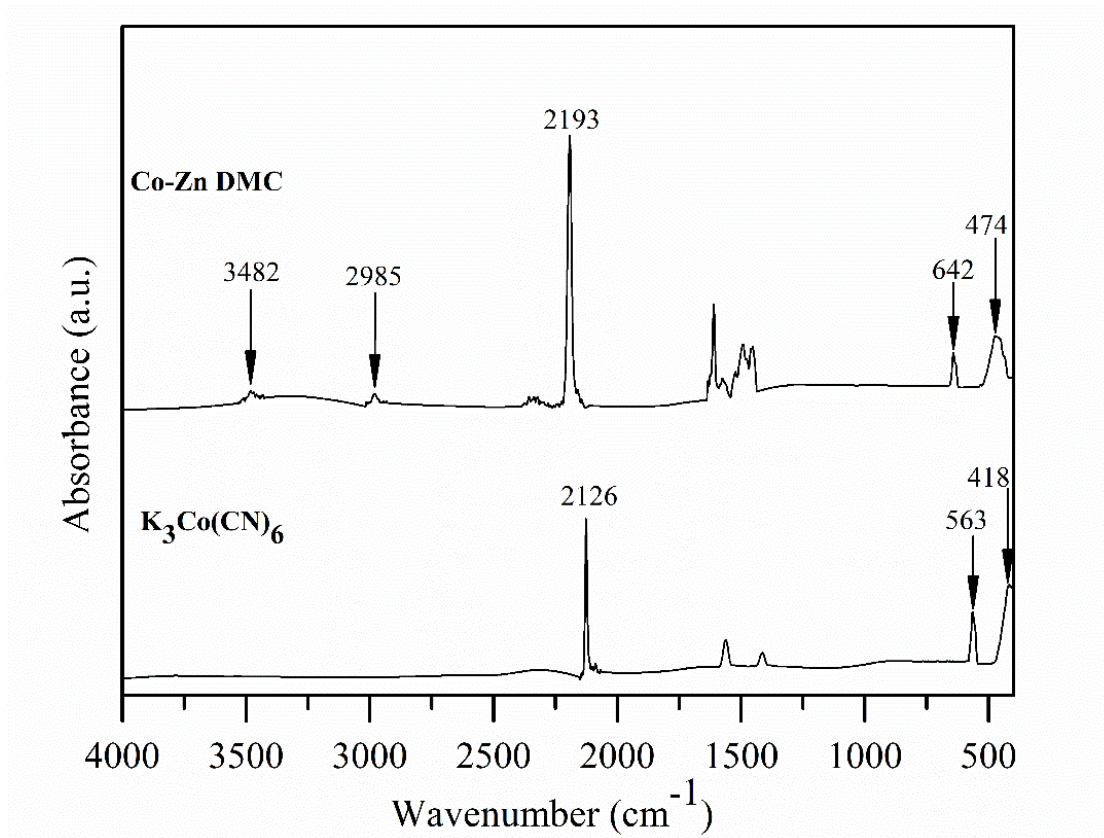


Figure 4.3. IR spectra of $\text{K}_3\text{Co}(\text{CN})_6$ and Co-Zn DMC catalyst

4.4.2 Properties and Characterization of Terpolymerization Products

The properties of individual products obtained from terpolymerization reaction are tabulated in Table 4.1. As shown in Table 4.1, at reaction temperature of 60°C and 80°C the yield of polymerization products are 11.2 g and 14.2 g respectively and reach plateau at 90°C with a maximum yield of 15.4 g meanwhile the productivity was observed to increase from 112 g product/g catalyst to 154 g product/ g catalyst as the temperature raised from 60°C to 90°C. However, at 100°C the productivity decreased slightly to 151 g product/ g catalyst. Meanwhile for the effect of reaction time, in general the longer the reaction time, the higher the yield and productivity. When the reaction time varied from 6h to 72h, the yield recorded ranging between 12.9 g to 16.1 g whereas productivity was in-between 129 to 161 g product/ g catalyst.

Analysis of the products by GPC revealed the M_n for all samples prepared ranges between 1983 g/mol to 6498 g/mol. These values are comparable with the M_n reported elsewhere (Dai et al., 2016; Guo and Lin, 2014; Wei et al., 2013). Considering the starting material used for this reaction comprises of a mixture of natural ESO and commercial PO, thus this has shown a good indication of the viability of natural ESO as a precursor for the synthesis of vegetable oil-based polymer. However, two samples prepared at 90 and 100°C were unable to be characterized by GPC perhaps due to the formation of a cross-linked material.

Table 4.1. Data on the terpolymerization of ESO, PO and CO₂ under Co-Zn DMC catalyst

Entry	Reaction Temp. (°C)	Time (h)	Yield (g)	Productivity (g Product/g Catalyst)	$M_n/M_w/PDI$
1	60	24	11.2	112	2323/4251/1.8
2	80	24	14.2	142	3834/4962/1.3
3	90	24	15.4	154	Crosslinked material
4	100	24	15.1	151	Crosslinked material
5	80	6	13.0	130	6498/8462/1.3
6	80	48	16.1	161	1983/5696/2.9
7	80	72	12.9	129	3541/4246/1.2

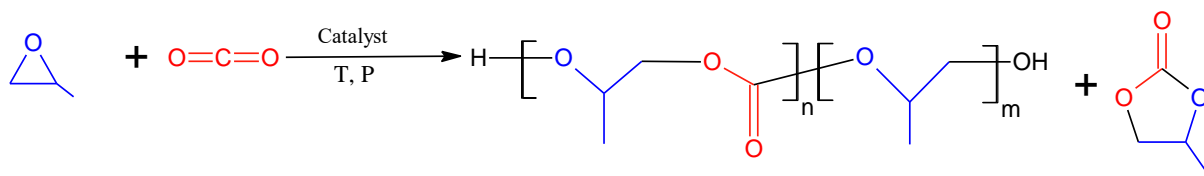
Reaction conditions: Volume of ESO = 10 mL, Volume of PO = 10 mL, Co-Zn DMC amount = 0.1 g, Pressure of CO₂ = 4.0 MPa

To further validate the possibility of the formation of a cross-linked material, a simple solubility test was conducted. From the observation, the two samples prepared at higher temperature were insoluble in all solvent (chloroform, DMSO, HFIP and toluene). These results confirm the probability of the two samples obtained at higher temperature are both cross-linked materials.

4.4.3 Analysis of Products

Polycarbonates and cyclic carbonates are the two types of products generally produced from the reaction of CO₂ with epoxide (Scheme 4.1). In an ideal copolymerization reaction, an alternating insertion of CO₂ and epoxide will take place in the growing polymer chain. However, the consecutive insertion of two epoxides may also happen and leads to the formation of ether bonds in the copolymer which typically is undesired. The consecutive insertion of two CO₂

molecules has never been observed as this is strongly disfavored from a thermodynamic perspective (Coates and Moore, 2004a).



Scheme 4.1. Copolymerization of CO₂ and epoxide

In this work, the vegetable oil based polymer synthesized from the terpolymerization reaction of ESO, PO and CO₂ with the presence of Co-Zn DMC catalyst is a polycarbonate, specifically a poly(propylene carbonate). At the same time, cyclic carbonate and polyether linkages were also detected. The extent of carbonate and ether backbone could be easily traced by IR and ¹H NMR spectroscopies of the resultant polymers. Figure 4.4 shows the FTIR spectrum of terpolymerization product prepared at reaction temperature and reaction time of 80°C and 6h respectively. It was pronounced from the spectrum the intense C=O asymmetric vibration absorption peak at approximately 1745 cm⁻¹. Together with this, the presence of absorption peak around 1256 cm⁻¹, which correspond to C-O stretching vibration absorption, provides confirmation for the presence of both carbonate and ether backbone in the resultant terpolymer. Besides, the characteristic absorption peak of the C=O stretching vibrations of cyclic carbonate was detected at 1810 cm⁻¹. The FTIR spectrums of the remaining samples prepared illustrate the same characteristic peaks and given in Appendix C4.1 and C4.2.

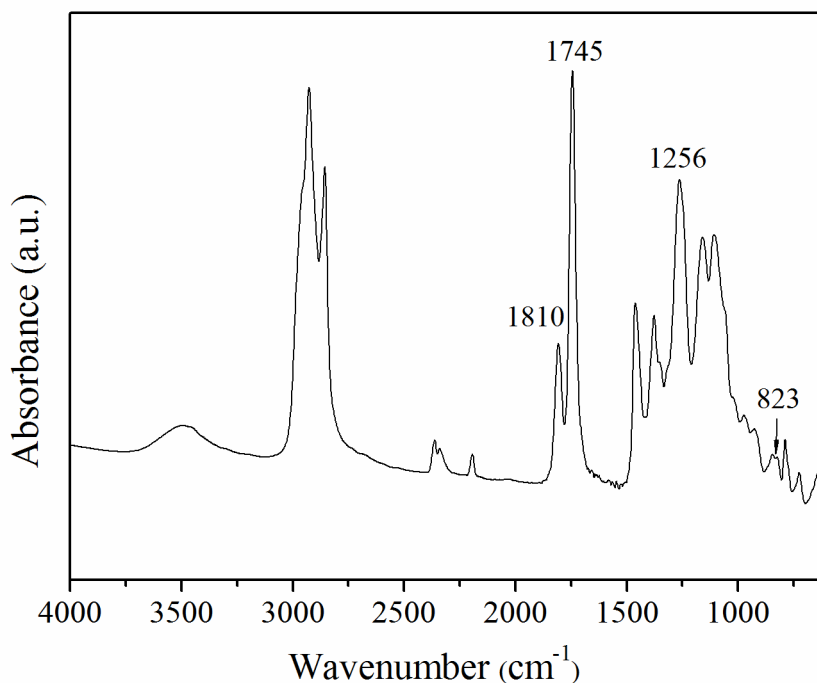


Figure 4.4. FTIR spectrum for sample prepared at $T = 80^{\circ}\text{C}$ and $t = 6\text{h}$ (entry no. 5 in Table 4.1)

All polymers were subjected to ^1H NMR analysis in CDCl_3 , and a representative spectrum of the polymer produced by Co-Zn DMC catalyst at 80°C and 6h is shown in Figure 4.5, together with that of ESO monomer for the comparison. In general, based on the ^1H NMR analysis it was confirmed that the resultant products from the terpolymerization of ESO, PO and CO_2 consist of chain of poly(propylene carbonate) bonded to the triglyceride. At the same time the presence of polyether linkages and cyclic carbonate are also detected in the products. As mentioned by Zhang et al. (2014) the formation of the ether units is usually thermodynamically favorable during Co-Zn (III) DMCC catalysis. The peaks at δ 2.8-3.2 ppm region related to epoxy proton are apparent in both spectra of ESO and the polymer product. The signal of epoxy proton in the resultant polymer signify that a fraction of epoxide was unreacted during the polymerization reaction probably due to the steric hindrance owing to the long chain structure of triglyceride. Also notable

are the methine proton $-\text{CH}_2-\text{CH}-\text{CH}_2-$ of the glycerol backbone at δ 5.1-5.3 ppm and methylene protons $-\text{CH}_2-\text{CH}-\text{CH}_2-$ of the glycerol backbone at δ 4.1-4.3 ppm which revealed triglyceride structure of ESO is not disturbed (Liu et al., 2013).

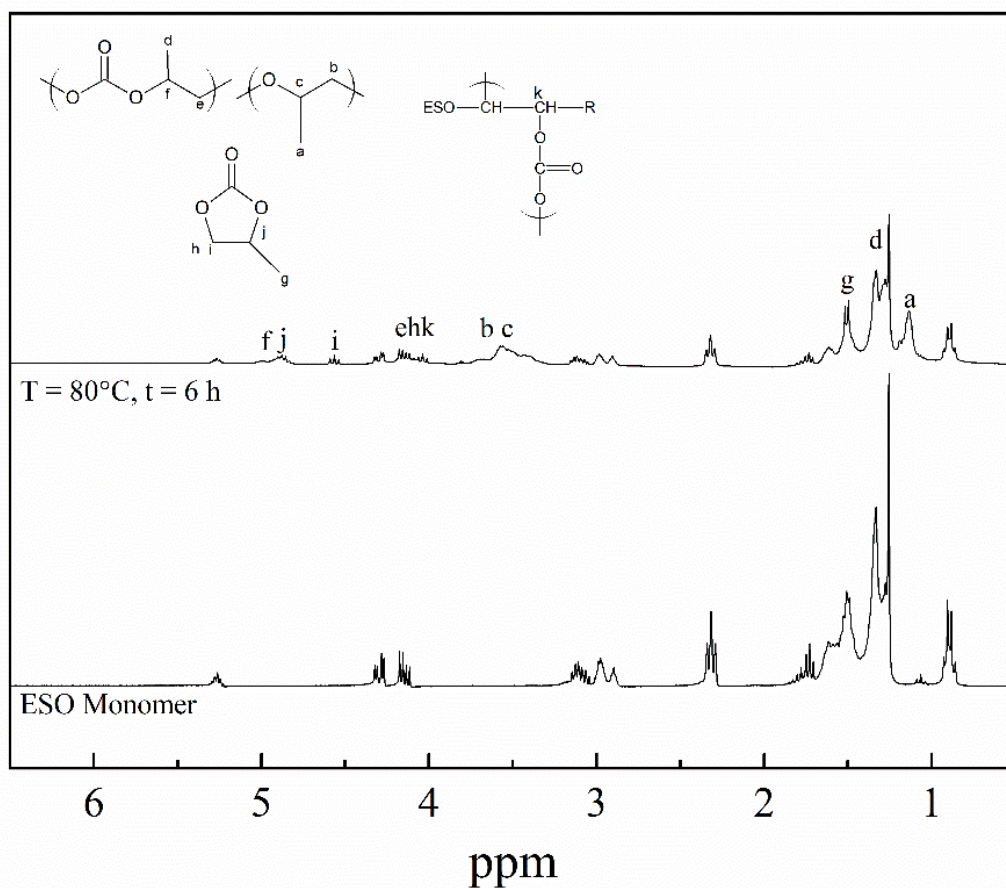


Figure 4.5. ^1H NMR spectra for sample prepared at $T = 80^\circ\text{C}$ and $t = 6\text{ h}$ (entry no. 5 in Table 4.1)

The percentage incorporation of ESO in the polymer was calculated from the integrated peak areas taking the terminal methyl signals as an internal reference standard. Equation 4.1 was used in the calculation as per following:

$$F_{ESO} = \frac{A_{reacted\ epoxy}}{A_{reacted\ epoxy} + A_{polycarbonate} + A_{ether\ unit}} \times 100 \quad \text{Equation 4.1}$$

where, $A_{reacted\ epoxy}$ is the integrated area of the methine epoxy proton at δ 4.07 - 4.16 ppm (Salih et al., 2015) meanwhile the $A_{polycarbonate}$ and $A_{ether\ unit}$ are the integrated peak area of the methine proton of polycarbonate unit (δ 5.10 ppm) and ether unit (δ 3.5 ppm) respectively. Note that the peak of reacted epoxy overlapped with the peaks of cyclic carbonate and methylene protons of the glycerol backbone, thus these peaks areas were subtracted in the calculation. The percentage incorporation of ESO in the polymer is only 7.8% at the shortest reaction time and in general the amount is found to be decreasing with the elevation of reaction temperature and prolonged reaction time (Table 4.2). The amount of ESO incorporated in the polymer obtained is quite low as ESO is less reactive than PO. Even so, considering that this is the first attempt utilizing ESO as one of the starting materials in the polymerization reaction with CO₂, thus the results gave a good sign of utilizing renewable bio-resources for this particular reaction in the future.

Table 4.2. Percentage incorporation of ESO and amount of cyclic carbonate in the terpolymerization products

Entry	Reaction Temp. (°C)	Time (h)	F_{ESO}^a (%)	W_{CC}^b (wt%)
1	60	24	6.7	20.6
2	80	24	6.0	18.8
3	90	24	0.8	10.4
4	100	24	0.0	9.5
5	80	6	7.8	14.1
6	80	48	3.2	9.1
7	80	72	6.2	12.6

Reaction conditions: Volume of ESO = 10 mL, Volume of PO = 10 mL, Co-Zn DMC amount = 0.1 g, Pressure of CO₂ = 4.0 MPa

^a F_{ESO} (%) indicates the molar fraction of ESO incorporated in the polymer product

^b W_{CC} (wt%) indicates the weight percentage of cyclic carbonate in the total product

The weight percentage of cyclic carbonate, (W_{CC}) can be determined using the formula as below:

$$W_{CC} = \frac{Mass_{cyclic\ carbonate} \times A_{cyclic\ carbonate}}{Mass_{ether\ unit} \times A_{ether\ unit} + Mass_{cyclic\ carbonate} \times (A_{cyclic\ carbonate} + A_{polycarbonate}) + Mass_{ESO} \times A_{ESO}} \times 100 \quad Eq. 4.2$$

where, $A_{cyclic\ carbonate}$, $A_{ether\ unit}$ and $A_{polycarbonate}$ are the integrated areas of –CH₃ protons of cyclic carbonate (δ 1.50 ppm), polyether (δ 1.14 ppm) and polycarbonate (δ 1.33 ppm) accordingly meanwhile A_{ESO} represents by the area of terminal methyl protons of ESO (δ 0.89 ppm). The calculated results are tabulated in Table 4.2. Surprisingly in this study, the weight percentage of the cyclic carbonate in the product was found to decrease with increasing reaction temperature. This is in contrast with the report mentioned elsewhere where stated that the formation of thermodynamically stable cyclic carbonate is highly favored at higher reaction temperature (Li and

Niu, 2011). Another important finding was that the signal of ether unit becomes more significance at higher reaction temperature (Appendix C4.3). A possible explanation for this might be that the homopolymerization of epoxides are more dominant during the terpolymerization reaction considering that the concentration of CO₂ supplied was fewer as the temperature raised from 60°C to 100°C (Henry's law) whilst the amount of both epoxides were kept constant (Tang et al., 2013).

4.5 Conclusions and outlook

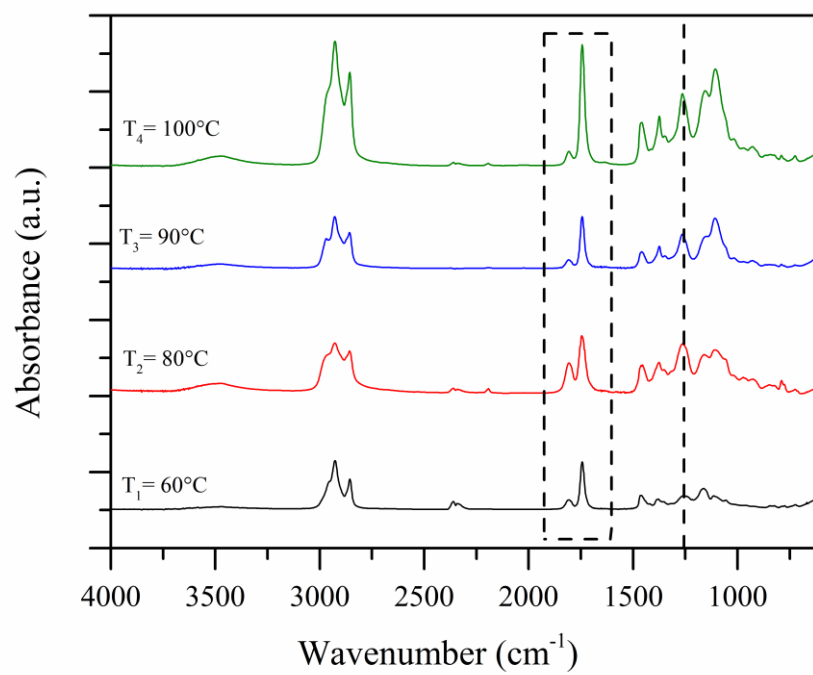
The results of this study demonstrated that under the reaction conditions studied, the resultant terpolymerization products comprise of a mixture of poly(propylene carbonate), cyclic carbonate and polyether unit. The constituent of the resultant products have been verified by the FTIR and ¹H NMR analysis. Polymeric product with yield of 13.0 g and M_n of 6498 g/mol was recorded at reaction temperature of 80°C and reaction time of 6 hours. The resultant polymer obtained through this research work has proven the viability of utilizing natural epoxide, namely ESO for the production of bio-based polymer.

In order to incorporate the *green* material in the formulation, initially the use of natural epoxide was presented as partial replacement of petroleum-based epoxide. However, with persistent and extensive research effort, natural epoxide may compete well with their petroleum-based counterparts in terms of properties, performance and applications. The prospect of using ESO as a substitute to the petroleum-based epoxide may as well provide solutions to increasing environmental and energy concern. Nevertheless, countless challenges must be overcome to develop better vegetable oil-based polymers.

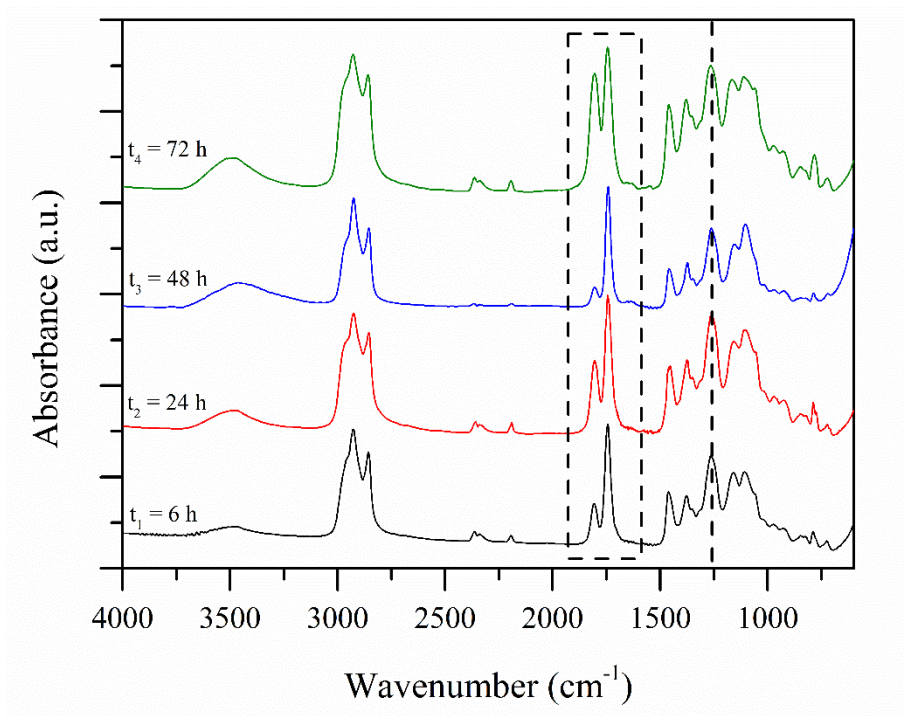
Acknowledgment

The authors would like to thank Spanish Ministry of Economy and Competitiveness (Program RETOS, Grant No. MAT2016-80045-R) for the financial support of this work. Majlis Amanah Rakyat and Universiti Kuala Lumpur, Malaysia are both acknowledged for funding a fellowship to make this study possible.

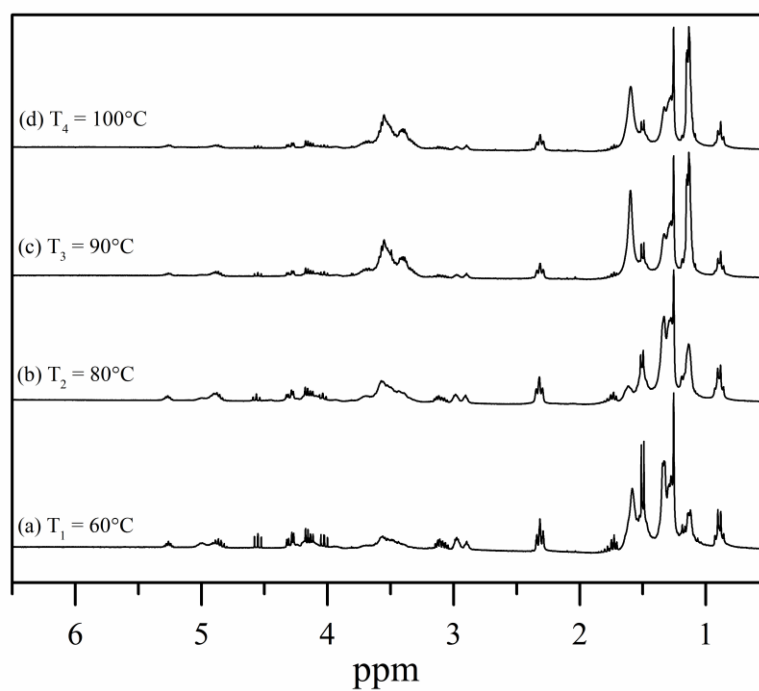
Appendix C4: Supplementary material



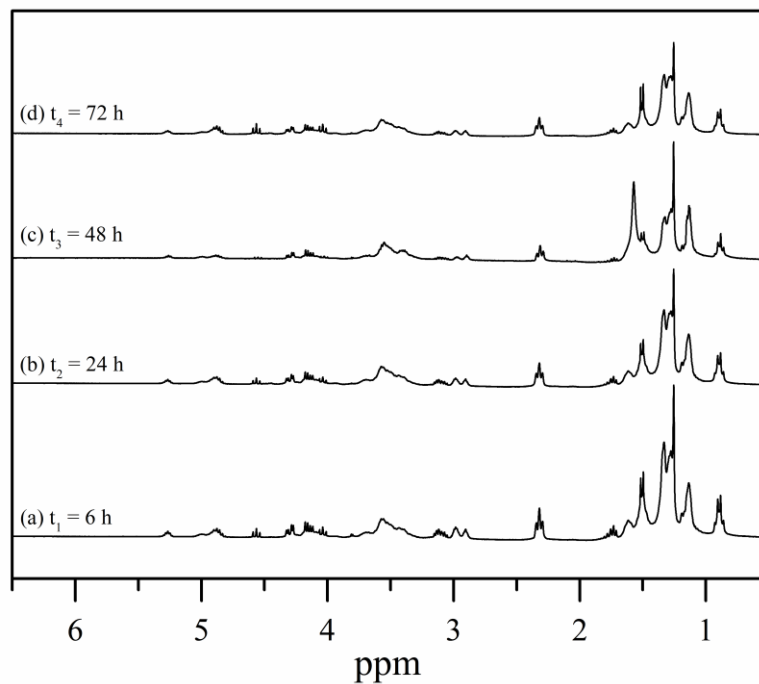
Appendix C4.1. FTIR spectrums of resultant polymers prepared at different reaction temperature



Appendix C4.2. FTIR spectra of resultant polymers prepared at different reaction time



Appendix C4.3. ^1H NMR spectra of terpolymerization products in CDCl_3 over the range of reaction temperature



Appendix C4.4. ^1H NMR spectra of terpolymerization products in CDCl_3 over the range of reaction time

CHAPTER 5 : Synthesis of Bio-based Poly(carbonate-co-ether) by means of Catalytic Polymerization of Epoxidized Linseed Oil, Propylene Oxide and Carbon Dioxide

This part of the work has been published as research article and was presented at the following conference:

1. Shaarani, F.W., J.J. Bou, and R.N. Hakim, Production of Poly(carbonate-co-ether) via Catalytic Polymerization of Epoxidized Linseed Oil, Propylene Oxide and Carbon Dioxide. IOP Conference Series: Materials Science and Engineering, 2019. 548: p. 012019.
2. Shaarani, F.W. and J.J. Bou, Synthesis of Bio-based Poly(carbonate-co-ether) with Epoxidized Linseed Oil. Poster presentation at the 68th Canadian Chemical Engineering Conference (CSCHE2018), Oct 28th to 31st, 2018.

5.1 Abstract

The aim of this research work is to utilize epoxidized linseed oil (ELO) – a product from sustainable resource for the production of polycarbonate via copolymerization of epoxide with carbon dioxide (CO₂). Herein, terpolymerization took place between natural ELO, propylene oxide (PO) and CO₂ with the presence of heterogeneous catalyst namely Co-Zn double metal cyanide (Co-Zn DMC). CO₂ pressure was maintained at 5.0 MPa while the reaction temperature, reaction time and catalyst loading were varied accordingly. The resultant polymeric products as being verified by Fourier transform infrared spectroscopy (FTIR) and proton nuclear magnetic resonance (¹H NMR) showed a formation of polycarbonate-co-ether bonded to the triglyceride chain of the ELO. The average molecular weight of the polymeric products recorded by gel permeation chromatography (GPC) were between 4.09 x10⁵ g/mol to 6.21 x 10⁵ g/mol.

5.2 Introduction

The fact that the modern society relies heavily on polymeric materials is undeniable. Polymers, being versatile materials, are used in almost every sector of manufacturing, from the materials used to make clothing, building materials for transportation and infrastructure (Correia Diogo, 2015; Lamnatou et al., 2018; Patil et al., 2017), high-tech devices for communication and information processing (Tomlinson et al., 2014) to sophisticated medical devices that improve quality of life (Rokaya et al., 2018; Teo et al., 2016). Currently, almost all commercially available polymers are derived from non-sustainable petroleum resources. Petroleum resources are finite and non-renewable. In due course, they will be scarce and costly. These factors have prompted the development of innovative technologies for novel polymeric materials from renewable feedstocks. The renewable materials can partially or in some rare cases even totally replace the petroleum-based polymers.

The most extensively used renewable feedstocks are vegetable oils, polysaccharides (starch and sugars), wood (lignocellulose), and proteins (Belgacem and Gandini, 2008; Brodin et al., 2017; Laurichesse and Avérous, 2014; Miao et al., 2014; Zia et al., 2015). Of these materials, vegetable oils are receiving overwhelming attention worldwide due to their ability to form pre-polymers, a surplus of availability, inexpensive, renewable and biodegradable compounds with low toxicity to the environment (Albarrán-Preza et al., 2016; Das et al., 2016). These vegetable oils consist of triglycerides in which the main components are saturated and unsaturated fatty acids of varying compositions depending on the plants or crops. These triglycerides contain several reactive sites such as hydroxyls and epoxies which can undergo various chemical reactions and synthetic transformations (Miao et al., 2014).

Linseed oil which also known as flaxseed oil is a natural oil derived from the *Linum usitatissimum* plant. This plant generally regarded as a dual-purpose crop plant due to its main products, the fiber and seed. The use of flax fibers dates back tens of thousands of years, whereby the fiber has been converted to yarn, which served as a major source to manufacture textiles such as tablecloth, bed sheet and clothing, whereas seeds have been pressed to extract oil (Zuk et al., 2015). The phenotype and physiology of *Linum usitatissimum* plant may vary depending on whether the plant is cultivated for its fiber or seed. Fibrous plant grows up to 80 – 120 cm and is less branched and on the other hand linseed flax grows up to 40 – 60 cm tall with highly branched stem. The leaves, alternating on the stalk, are small and lance-shaped besides it has five pale blue colored petals on each flower. A distinctive feature of this plant are the capsules/pods which grow on the stalks. These measure around 10 mm in diameter and are home to the flaxseeds which are brown or golden in color. It is from these seeds that the flaxseed oil is extracted (Figure 5.1). Specifically, linseed oil is viewed as an ideal candidate for the synthesis of polymeric materials because of its distinctive structure which has a high

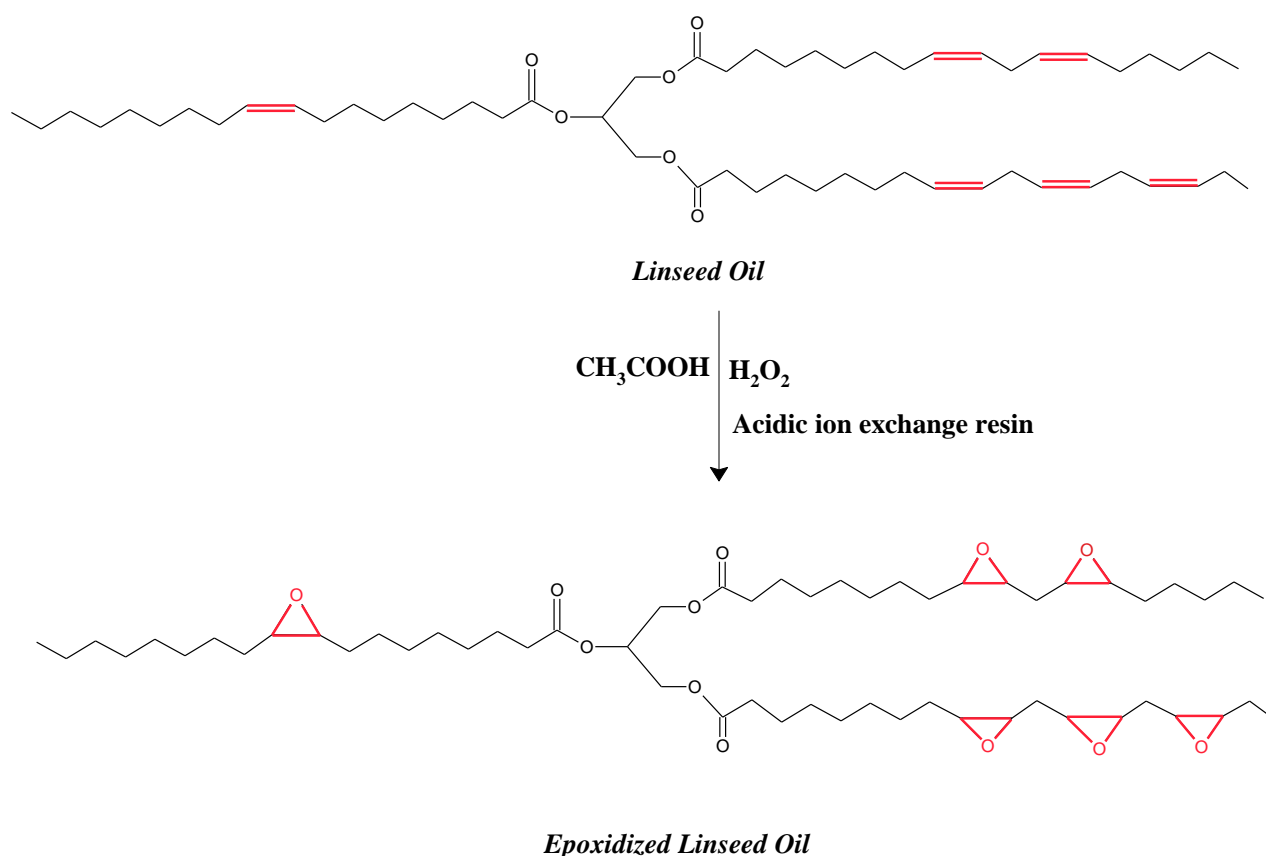
degree of unsaturation or reactive sites (approximately 6.6 double bonds per triglyceride chain) (Albarrán-Preza et al., 2016; Khandelwal et al., 2018; Sahoo Sushanta et al., 2017). The fatty acid composition of linseed oil is dominated by C18 fatty acids, with 52 % of linolenic acid (C18:3) and 16 % of linoleic acid (C18:2) (Zhang et al., 2017). These unsaturated fatty acids may be used to introduce functional groups like epoxides by means of epoxidation reactions, which add an oxygen atom to a carbon–carbon double bond (olefin) (Chavan and Gogate, 2015).



Figure 5.1. Illustration of flaxseed plant (*Linum usitatissimum*) (Schneider, 2014)

Epoxidation of vegetable oils can be accomplished through several methods with the conventional method (Prilezhaev epoxidation) being the most commonly used and more cost-effective. In the aforementioned technique, a short chain peroxy acid, preferably peracetic acid is prepared by an in-situ reaction of acetic acid with hydrogen peroxide (H_2O_2) and is used as

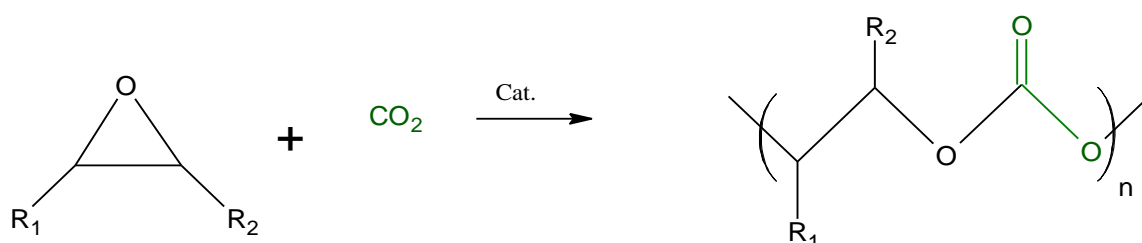
a catalyst (Scheme 5.1). Epoxides which also known as oxiranes, are cyclic ethers with a three-member ring and they are more reactive in comparison to other ethers owing to the highly strained ring in the molecule (Chavan et al., 2012). Due to the high reactivity of epoxides, they are used as precursor in the synthesis of a variety of chemicals, such as alcohols, glycols, alkanolamines, carbonyl compounds, olefinic compounds, and polymers like polyesters, polyurethanes (Dinda et al., 2008), and polycarbonate (Jin et al., 2017; Poland and Darensbourg, 2017).



Scheme 5.1. Epoxidation procedure for linseed oil (Khandelwal et al., 2018)

Polycarbonate is a class of thermoplastic polymer and traditionally it is being synthesized via condensation reaction between bisphenol-A (BPA) and phosgene resulting in

products with excellent properties such as outstanding toughness, high impact strength, good heat resistance and transparency (Hauenstein et al., 2016). Despite of the exceptional properties of the BPA-based polycarbonate, this conventional route has some drawbacks as the choice of monomer such as phosgene being a highly toxic volatile compound and it may also dissociate into two other poisonous gases including carbon monoxide and chlorine at elevated temperature (Jin et al., 2017). Moreover, utilization of BPA as the monomer sparked anxiety among the consumers as it has the tendency to leach out from the polymer when in contact with food resulting in detrimental health (US Food and Drug Administration, 2014). Since both monomers used in the conventional production of polycarbonate are petroleum-based compounds and with the current trend in the field, efforts have been made to replace them, at least partially with bio-based feedstock. In the past decades industries have been developing more environmentally benign synthesis process, by which carbon dioxide is use as alternatives to substitute poisonous phosgene. Copolymerization of natural epoxide, i.e. vegetable oil-based epoxide with carbon dioxide (CO₂) is perceived as a good strategy to produce polycarbonate (Scheme 5.2) since both monomers are renewable and this helps to minimize the reliance on petroleum-based feedstock. Additionally, the utilization of renewable raw materials meets the 7th principle of 12 Principles of Green Chemistry that contributes to sustainability in chemistry (Anastas and Eghbali, 2010).



Scheme 5.2. General mechanism of Polycarbonates production

In this present study, we report on the first approach of utilizing natural epoxide namely epoxidized linseed oil (ELO) as a starting material in the production of bio-based polycarbonate. ELO was used alongside with the commercial epoxide namely propylene oxide (PO) in the catalytic polymerization with CO₂. Co-Zn double metal cyanide (Co-Zn DMC) catalyst was chosen as the catalyst and the reaction took place at fixed CO₂ pressure of 5.0 MPa with equal volume of ELO and PO. Effect of operating conditions such as catalyst loading (0.05 – 0.3 g), reaction temperature (50 – 90 °C) and reaction time (4 – 24 h) were studied. Under the conditions studied, the resultant products yield poly(carbonate-co-ether) bonded to the triglyceride chain of the ELO.

5.3. Experimental section

5.3.1. Materials

In this study, chemicals required were purchased from various manufacturers. Reagents needed for the preparation of the catalyst such as potassium hexacyanocobaltate (III) (K₃Co(CN)₆), zinc chloride (ZnCl₂), and tertiary butyl alcohol (tert-butanol) were used as received. As for the polymerization reaction, CO₂ of 99.99% purity was used without further purification. ELO with approximately 6 oxirane rings per triglyceride (Scheme 5.1) was obtained from Traquisa (Barbera del Valles, Barcelona Spain) whereas liquid PO (>99%) was supplied by Sigma Aldrich. Methanol (99.9%) and methylene chloride (CH₂Cl₂) of analytical reagent grade were supplied by Scharlau and Panreac respectively and directly applied in the experiments.

5.3.2. Preparation of the catalyst

A heterogeneous catalyst namely Co-Zn DMC catalyst was used in the terpolymerization reaction between ELO, PO and CO₂. The catalyst was prepared using the

same method as being described in chapter four whereby tert-butanol was used as the complexing agent. In brief, solution 1 was made by dissolving $K_3Co(CN)_6$ in double distilled water meanwhile solution 2 was prepared by dissolving $ZnCl_2$ in double distilled water and tert-butanol. Slowly solution 1 was added to solution 2 over a period of one hour and the mixture then was stirred vigorously for another two hours at 50 °C. Subsequently, the white suspension resulting from the reaction was filtered and centrifuged to isolate the Co-Zn DMC complex. The white precipitate collected was re-dispersed in a solution of tert-butanol and water (1:1 v/v) using high-speed stirring. This procedure was conducted repetitively with increasing volume ratio of tert-butanol to water (6:4, 7:3, 8:2, and 9:1, correspondingly). Finally, the solid was re-dispersed in pure tert-butanol, centrifuged and vacuum dried until a constant weight was reached.

5.3.3. Polymerization of ELO, PO and CO₂

All reactions were performed in a 100 mL semi batch reactor made of stainless steel (Autoclave Engineers, Erie, PA USA) equipped with a mechanical stirrer and an automatic temperature controller system (Figure 5.2). First, the reactor was dried at 100 °C for at least 12 h and then it was cooled down to 25 °C. Later the reactor was loaded with dried Co-Zn DMC catalyst (between 0.05 g to 0.30 g), 10 mL of ELO and 10 mL of PO. Subsequently followed by purging with CO₂ twice and then slowly pressurized to 5.0 MPa. The reaction temperature was then raised and maintained between 50 and 90 °C with a stirring speed of 500 rpm to initiate the polymerization reaction. Meanwhile the reaction time was ranging between 4 h to 24 h. Upon completion of the reaction, the reactor was cooled to room temperature and the CO₂ released. A small aliquot of the reaction mixture was removed from the reactor for proton nuclear magnetic resonance (¹H NMR) analysis. A viscous reaction mixture was then dissolved

in small amount of dichloromethane and precipitated by excess methanol. Final product was separated by filtration and then dried to a constant weight.

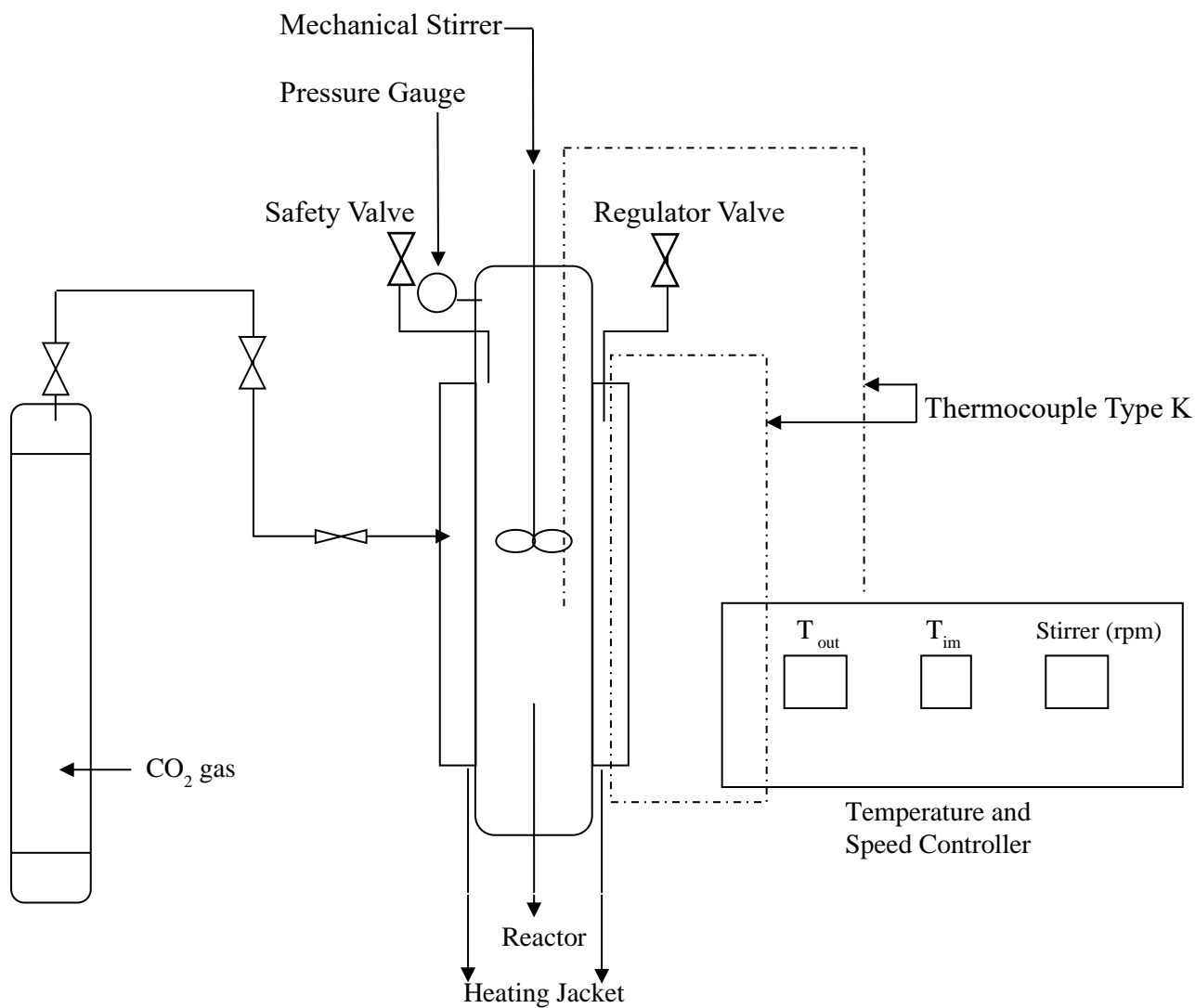


Figure 5.2. Schematic diagram of the experimental setup for polymerization of ELO, PO and CO₂

5.3.4. Characterizations

The IR spectroscopy was used to examine the functionalization of $\text{K}_3\text{Co}(\text{CN})_6$ and Co-Zn DMC catalyst. Absorption spectra for both substances were recorded on a Nicolet iS10 FTIR spectrometer (Thermo Fisher Scientific, Waltham, MA, USA) in attenuated total reflectance (ATR) mode. On the other hand, spectra of ELO and terpolymerization products were recorded on a Perkin–Elmer 1000 FTIR spectrometer in the wavenumber region of 600 to 4000 cm^{-1} . ^1H NMR spectra of ELO and final products were recorded at room temperature on a Bruker AMX-300 spectrometer. The equipment operated at 300 MHz and all measurements were made by using deuterated chloroform (CDCl_3) as solvent. The molecular weights (both M_n and M_w) and polydispersity index (PDI) of the resultant polymer products were characterized by gel permeation chromatography (GPC) system (Agilent HPLC) equipped with a separation column of PL HFIP gel running at room temperature. Mobile phase is hexafluoroisopropanol (HFIP) containing $2.72\text{ g}\cdot\text{L}^{-1}$ of sodium trifluoroacetate to prevent polyelectrolyte effect. $100\text{ }\mu\text{L}$ will be injected and the concentration of each sample will be 0.2 w/vol%. Calibration was performed with polymethyl methacrylate (PMMA) samples.

5.4 Results and discussion

5.4.1 Co-Zn DMC catalyst

Double-metal cyanides (DMC) are inorganic coordination polymers, structurally and molecularly analogues to Prussian blues. Being a heterogeneous catalyst, it is commonly used in the copolymerization of epoxide and CO_2 . DMC catalysts are typically prepared via a precipitation process between a metal salt such as zinc chloride (ZnCl_2) and an alkali metal hexacyanometallate such as potassium hexacyanocobaltate ($\text{K}_3[\text{Co}(\text{CN})_6]$) in aqueous form. The zinc hexacyanocobaltate precipitated as a white suspension as given in Eq. 5.1:



In practice, generally organic complexing agents (CAs) such as alcohols are introduced into the catalyst matrix to increase their catalytic activity, and the structures are usually hydrated. The accurate structural formula of an active DMC is therefore more complex and can formally be written as follows: $\text{M}^{\text{II}}_u[\text{M}(\text{CN})_n]_v \cdot x\text{M}^{\text{II}}\text{X}_w \cdot y\text{L} \cdot z\text{H}_2\text{O}$ ($\text{M}^{\text{II}} = \text{Zn}^{2+}, \text{Fe}^{2+}, \text{Ni}^{2+}, \text{Co}^{2+}$ etc.; $\text{M} = \text{Co}^{2+}, \text{Co}^{3+}, \text{Fe}^{2+}, \text{Fe}^{3+}$, etc.; $\text{X} = \text{Cl}^-, \text{Br}^-, \text{I}^-$ and OAc^- , etc.; L is an electron-donating complexing agent). Figure 5.3 depicts schematically a plausible structure of Co-Zn DMC with $\text{M}^{\text{II}} = \text{Zn}^{2+}$, $\text{M} = \text{Co}^{3+}$, $\text{CA} = \text{tert-butanol}$. As portrayed by Figure 5.3, one Co^{3+} is coordinated by six CN^- s, meanwhile CN^- become the bridge between Zn^{2+} and Co^{3+} . According to Zhang et al. (2015c) and Sun et al. (2012), the structure of Co-Zn DMC meets the electroneutrality principle and it keeps the tetrahedral coordination structure since it contains one or two CN^- , one OH^- (or Cl^-) and complexing agent (or H_2O). Lewis acid, Zn^{2+} is deemed as the local active site for the copolymerization.

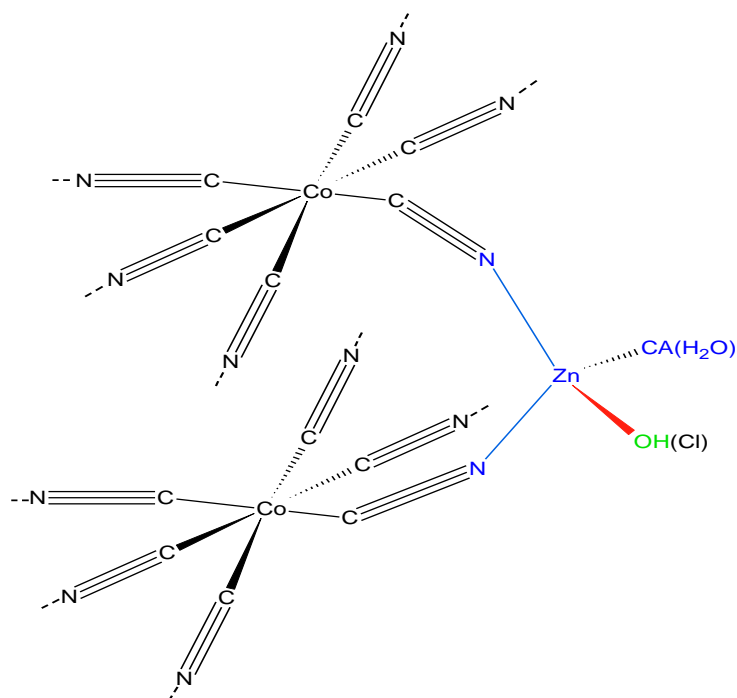


Figure 5.3. Plausible structure of Co-Zn DMC catalyst (Liu et al., 2020)

In this study, both $\text{K}_3\text{Co}(\text{CN})_6$ and Co-Zn DMC catalyst were characterized by FTIR and the spectrums are presented in Figure 5.4. It was revealed that the $\nu(\text{CN})$ of $\text{K}_3\text{Co}(\text{CN})_6$ shifted to higher wave number approximately 2193 cm^{-1} in Co-Zn DMC catalyst. The $\nu(\text{CN})$ shift to higher frequency is coincides with report by Dharman et al. (Dharman et al., 2008) which suggests that CN^- acts as σ -donor by donating electrons to the Co^{3+} and as a π -electron donor by chelating to Zn^{2+} , which is responsible for raising the (CN) value. The presence of complexing agent namely tert-butanol, was verified by the $-\text{OH}$ stretching vibration absorption at approximate 3482 cm^{-1} and C–H stretching vibration absorption peak appeared at 2985 cm^{-1} (Guo and Lin, 2014). In addition to $\nu(\text{CN})$, at the lower frequency region both spectrums exhibit $\nu(\text{Co-C})$ and $\delta(\text{Co-CN})$ bands. The $\nu(\text{Co-C})$ band in $\text{K}_3\text{Co}(\text{CN})_6$ shifted from 563 to 642 cm^{-1} for the Co-Zn DMC catalyst. Another peak which corresponds to $\delta(\text{Co-CN})$ band shifted from 418 cm^{-1} ($\text{K}_3\text{Co}(\text{CN})_6$) to 474 cm^{-1} (Co-Zn DMC catalyst) resulted due to the formation of $\text{Zn}^{2+}-\text{CN}-\text{Co}^{3+}$ complex. These findings are consistent with data obtained by Lee et al. (2009) which showed that these two peaks shifted on the IR spectrums of the catalysts prepared using various complexing agents.

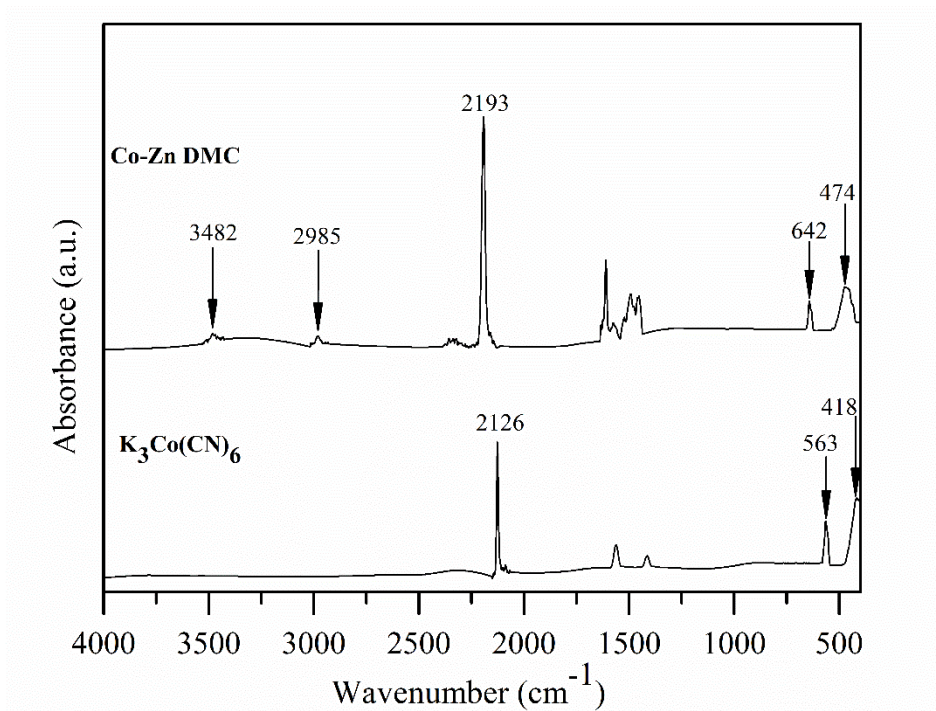


Figure 5.4. IR spectra of $\text{K}_3\text{Co}(\text{CN})_6$ and Co-Zn DMC catalyst

5.4.2. Characterization of ELO

The IR spectrum of ELO is portrayed in Figure 5.5. The characteristic band of the epoxide ring is detected at 833 cm^{-1} and the carbonyl group stretching from the ester functionality in the triglycerides is spotted at 1737 cm^{-1} . The other characteristic bands of ELO are summarized in Table 5.1.

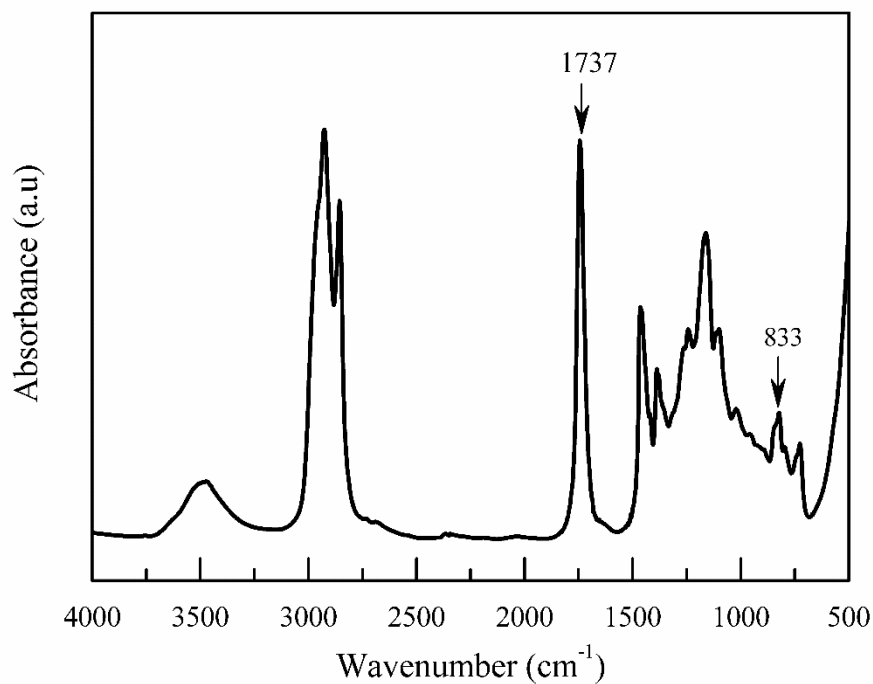


Figure 5.5. FTIR Spectrum of ELO

Table 5.1. FTIR assignment of ELO (Salih et al., 2015)

Absorption band (cm^{-1})	Assignment of the functional group
3484	OH stretching
2928	C-H stretching (CH_3)
2856	C-H stretching (CH_2)
1737	C=O stretching vibration of triglyceride esters
1456	Scissoring of CH_2 , asymmetric bending of CH_3
1384	Symmetric bending of CH_3
1241	C-O-C stretching
1158	C-O stretching of $\text{O}=\text{C}-\text{O}$
1098	C-O stretching of $\text{O}-\text{CH}_2$
833	C-O of epoxides
725	Methylene (CH_2) rocking vibration

The structure of ELO was investigated by ^1H NMR spectrometry. For this, the epoxide was dissolved in deuterated chloroform (CDCl_3) and ^1H NMR spectrum was recorded. Figure 5.6 represents the ^1H NMR of ELO and the summary of signals assign for ELO is given in Table 5.2.

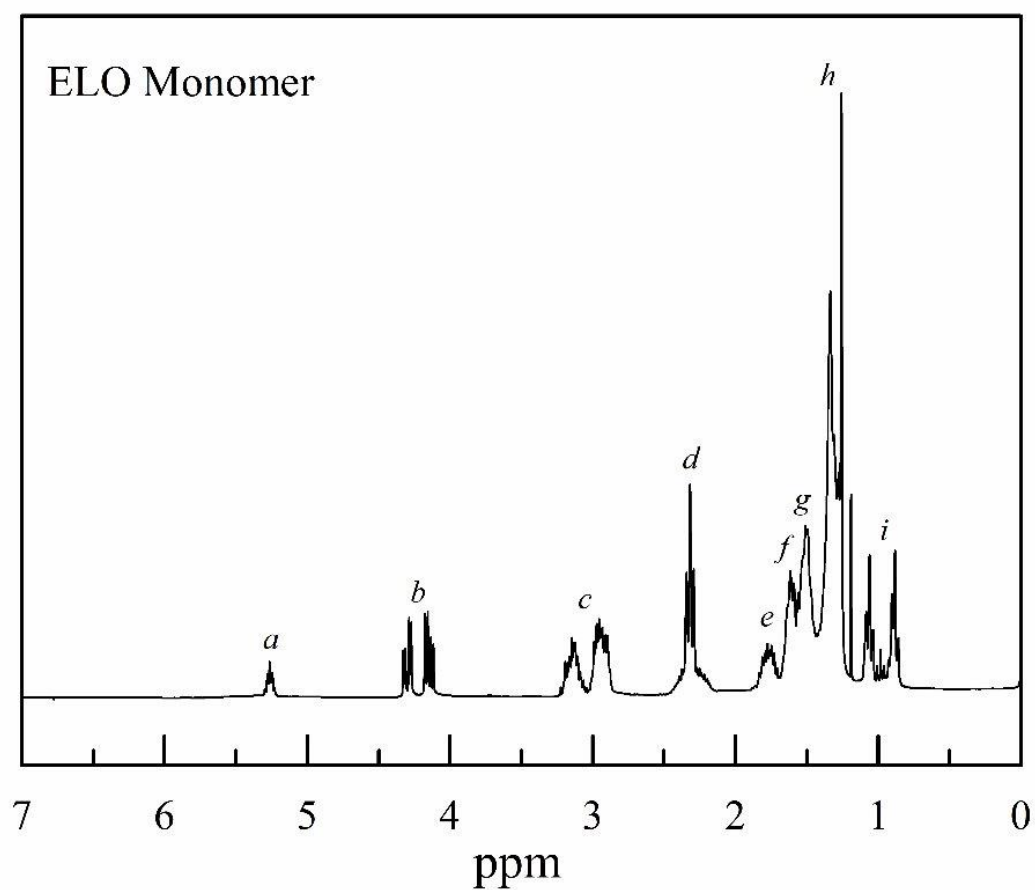
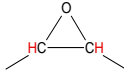
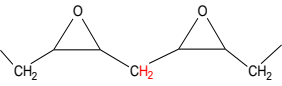
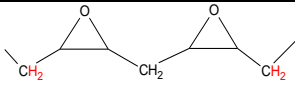


Figure 5.6. ^1H NMR Spectrum of ELO

Table 5.2. Assignment of signals of ^1H NMR spectra for the ELO (Jebrane et al., 2017)

Signal	Chemical shift, δ [ppm]	Structure with assignment
<i>a</i>	5.20 - 5.30	$-\text{CH}_2-\text{CH}-\text{CH}_2-$ of the glycerol backbone
<i>b</i>	4.10 - 4.30	$-\text{CH}_2-\text{CH}-\text{CH}_2-$ of the glycerol backbone
<i>c</i>	2.80 - 3.20	$>\text{CH}-$ at epoxy group 
<i>d</i>	2.20 - 2.35	$\alpha-\text{CH}_2$ to the carbonyl group $-\text{OCO}-\text{CH}_2-$
<i>e</i>	1.60 - 1.80	$\alpha-\text{CH}_2-$ adjacent to two epoxy groups 
<i>f</i>	1.50 - 1.70	$\beta-\text{CH}_2$ to the carbonyl group $-\text{OCO}-\text{CH}_2-\text{CH}_2-$
<i>g</i>	1.35 - 1.50	$\alpha-\text{CH}_2-$ to epoxy group 
<i>h</i>	1.20 - 1.40	saturated methylene group $-(\text{CH}_2)_n-$ in acyl chain
<i>i</i>	0.84–1.09	terminal $-\text{CH}_3$

5.4.3. Polymerization of ELO, PO and CO_2

Ideally in the copolymerization reaction, an alternating insertion of CO_2 and epoxide will take place in the growing polymer chain. Having said that, depending on the conditions, substrate and catalyst selected, side reactions may as well take place within this process. In copolymerization reaction, cyclic carbonate by-product may be synthesized via back-biting pathway. Simultaneously, the formation of ether linkages in the polymer chain can take place when epoxides are consecutively inserted into the growing polymer chain instead of CO_2 insertion. Such linkages alter the polymer properties, which may be beneficial depending on the application, but nevertheless reduce the CO_2 sequestered in the polymer backbone (Trott et al., 2016). On the other hand, the consecutive insertion of two CO_2 molecules has never been

observed as this is strongly disfavored from a thermodynamic perspective (Coates and Moore, 2004b).

To identify the identity of the synthesized polymers, they were characterized by spectroscopic techniques. Presented in Figure 5.7 is the FTIR spectrum of the terpolymerization product obtained at reaction temperature of 60 °C and reaction time of 24 h (ELO 60). As can be seen from Figure 5.7, the polymer exhibits a peak at 1740 cm⁻¹ which corresponds to the characteristic absorption of the carbonate group, confirming the formation of polycarbonate. However, besides carbonate absorption, a peak at 1231 cm⁻¹ confirms the presence of the ether linkage $\nu(\text{C-O-C})$, suggesting that the homopolymer part of the epoxide also exists in addition to the polycarbonate. In general, the FTIR spectra of the remaining polymers (Figure not shown) obtained in this study illustrate the same characteristic peaks. These results were further confirmed by ¹H NMR analysis. Figure 5.8 gives the comparison between ¹H NMR spectra of ELO monomer with crude ELO 60. It was pronounced that the polymer synthesized via terpolymerization of ELO, PO and CO₂ was mainly polycarbonate bonded to the triglyceride chain. Simultaneously, the existence of polyether linkages and cyclic carbonate are also detected in the product. As stated by Zhang et al. (2011) during Zn-Co (III) DMCC catalysis, the formation of the ether units is usually thermodynamically favorable. As can be seen from Figure 5.8, the peaks at δ 2.8–3.2 ppm region associated to epoxy proton are apparent in both spectra of ELO and the polymer product. A possible explanation for this might be that a fraction of epoxide was unreacted during the polymerization reaction probably due to the steric hindrance owing to the long chain structure of the triglyceride chain. As a result, signal of epoxy proton still can be observed in the resultant polymer. Also notable are the methine proton $-\text{CH}_2-\text{CH}-\text{CH}_2-$ of the glycerol backbone at δ 5.1–5.3 ppm and methylene protons $-\text{CH}_2-\text{CH}-\text{CH}_2-$ of the glycerol backbone at δ 4.1–4.3 ppm which revealed triglyceride structure of ESO is not disturbed (Liu et al., 2013). From the analyses, it can be

concluded that the bio-based polymer obtain from this work is a poly(carbonate-co-ether) bonded to the triglyceride chain of the ELO.

It is noteworthy to highlight that this result does not apply to all polymers synthesized in this study. For instance, the ^1H NMR spectrum of sample collected at reaction temperature of 50 °C is similar to the spectrum of ELO. Therefore, it can be concluded that no reaction has taken place at the lowest reaction temperature. On the other hand, polymer obtained at the highest temperature was mainly polyether bonded to the triglyceride chain and cyclic carbonate. This behavior is expected as homopolymerization of epoxide generally takes place during the polymerization of epoxide and CO_2 at relatively higher temperature, thus resulting in higher polyether content. Cyclic carbonate formation during terpolymerization reaction takes place through the backbiting reaction from both dead polymer chain and growing polymer chain. Comparison of the ^1H NMR for all products are given in Appendix C5.1, C5.2 and C5.3.

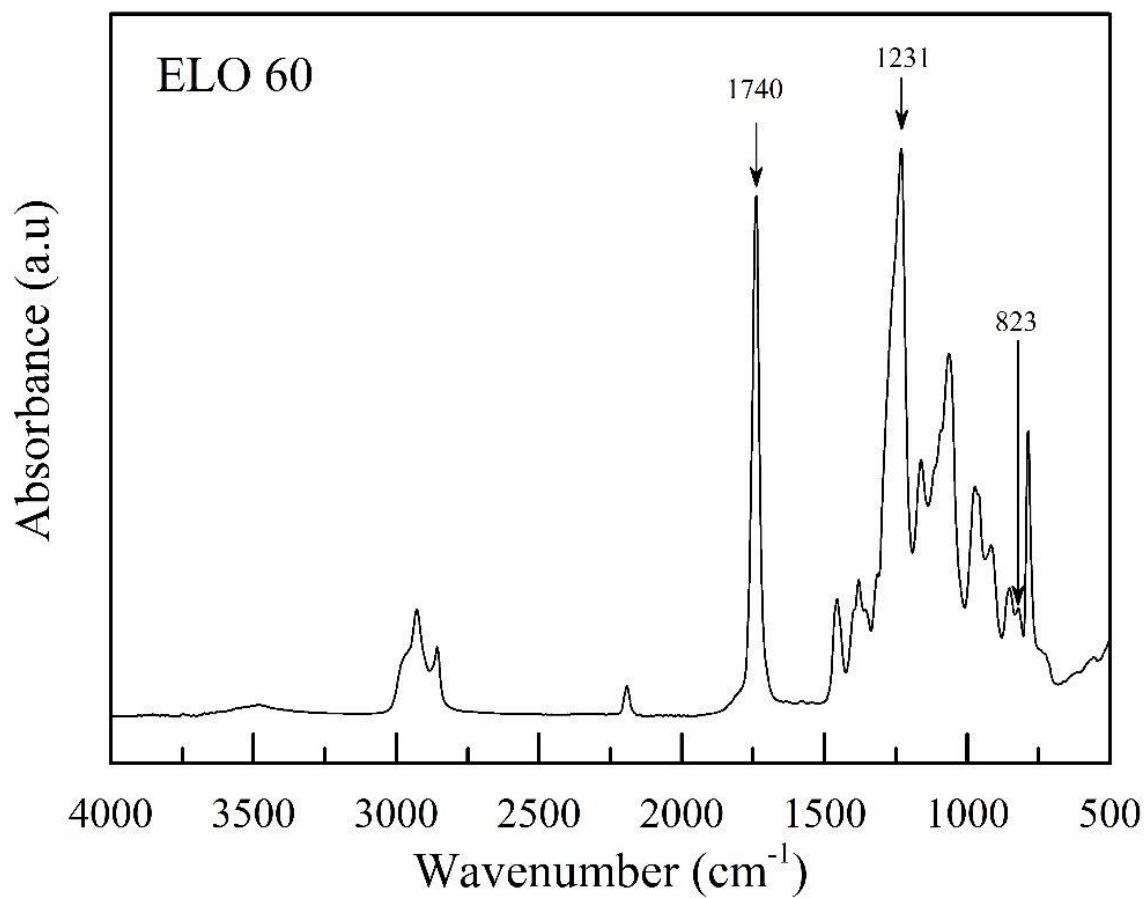


Figure 5.7. FTIR spectrum of purified ELO 60 (prepared at $T = 60\text{ }^{\circ}\text{C}$ and $t = 24\text{ h}$ and catalyst loading = 0.20 g)

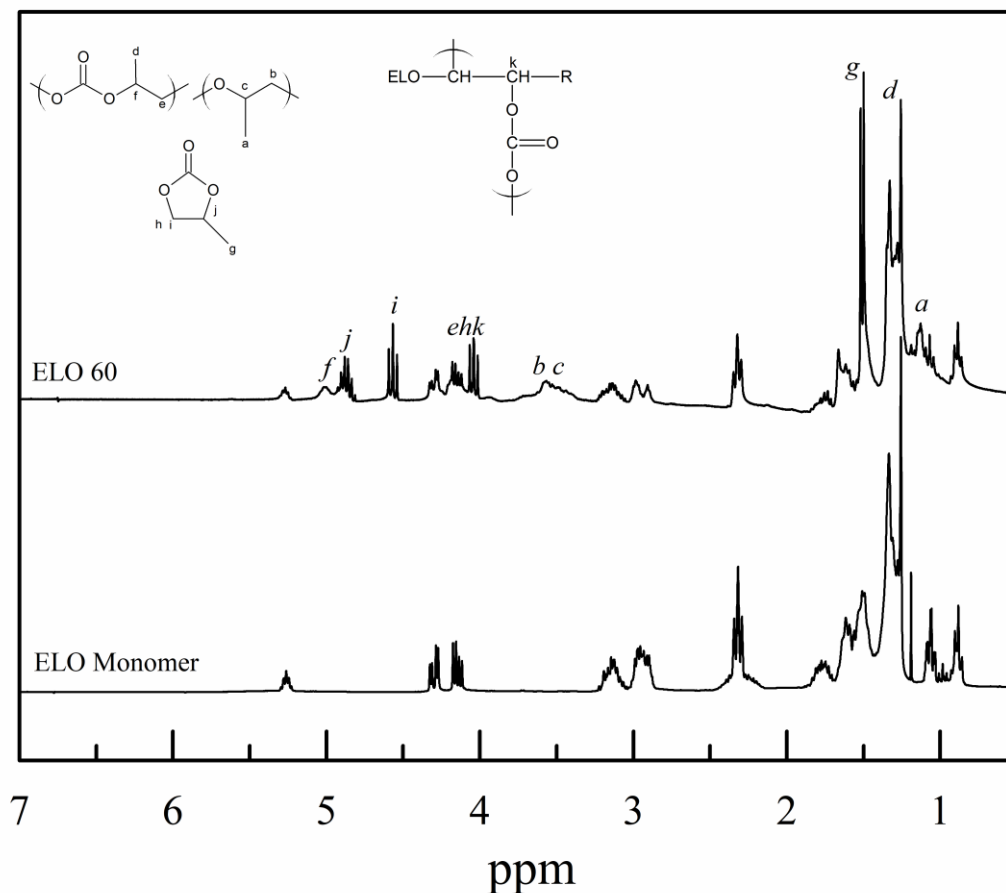


Figure 5.8. Comparison of ^1H NMR spectra for ELO monomer and crude ELO 60

The percentage of ELO (F_{ELO}) incorporated in the resultant polymer can be calculated according to Eq. (5.2). Here the integrated peak areas of the respective unit were determined by taking the terminal methyl signals as an internal reference standard.

$$F_{ELO} = \frac{A_{reacted\ epoxy}}{A_{reacted\ epoxy} + A_{polycarbonate} + A_{ether\ unit}} \times 100 \quad (5.2)$$

where, $A_{reacted\ epoxy}$ is the integrated area of the methine epoxy proton at δ 4.07 - 4.16 ppm (Salih et al., 2015) meanwhile the $A_{polycarbonate}$ and $A_{ether\ unit}$ are the integrated peak area of the methine proton of polycarbonate unit (δ 5.10 ppm) and ether unit (δ 3.5 ppm) respectively. Note that the peak of reacted epoxy overlapped with the peaks of cyclic carbonate and methylene protons

of the glycerol backbone, thus these peaks areas were subtracted in the calculation. The calculated values of ELO incorporated in the resultant polymers are summarized in Table 5.3. For samples prepared at reaction temperature of 4 h (ELO 4) and 6 h (ELO 6), even no formation of polycarbonate was observed the calculated values of F_{ELO} were slightly high in comparison to other resultant polymers. This is due to only side reactions took place at shorter reaction time instead of terpolymerization reaction between epoxides and CO₂.

Table 5.3. Percentage incorporation of ELO and amount of cyclic carbonate in the polymeric products

Sample	Reaction Temp. (°C)	Time (h)	Catalyst loading (g)	F_{ELO}^a (%)	W_{cc}^b (wt%)
ELO 0.05	60	24	0.05	/	/
ELO 0.10	60	24	0.1	8.61	27.82
ELO 0.20	60	24	0.2	8.10	26.03
ELO 0.30	60	24	0.3	7.54	23.71
ELO 4	60	4	0.2	13.89	25.70
ELO 6	60	6	0.2	25.93	26.21
ELO 16	60	16	0.2	8.20	26.21
ELO 24	60	24	0.2	8.10	26.03
ELO 50	50	24	0.2	/	/
ELO 60	60	24	0.2	8.10	26.03
ELO 70	70	24	0.2	7.75	26.52
ELO 80	80	24	0.2	3.56	25.49
ELO 90	90	24	0.2	4.46	19.13

Reaction conditions: Volume of ELO = 10 mL, Volume of PO = 10 mL, Pressure of CO₂ = 5.0 MPa

^a F_{ELO} (%) indicates the molar fraction of ELO incorporated in the polymer product

^b W_{cc} (wt%) indicates the weight percentage of cyclic carbonate in the total product

Eq. (5.3) gives the formula used to calculate the weight percentage of cyclic carbonate,

(W_{CC}):

$$W_{CC} = \frac{Mass_{cyclic\ carbonate} \times A_{cyclic\ carbonate}}{Mass_{ether\ unit} \times A_{ether\ unit} + Mass_{cyclic\ carbonate} \times (A_{cyclic\ carbonate} + A_{polycarbonate}) + Mass_{ELO} \times A_{ELO}} \times 100 \quad (5.3)$$

where, $A_{cyclic\ carbonate}$, $A_{ether\ unit}$ and $A_{polycarbonate}$ are the integrated areas of $-CH_3$ protons of cyclic carbonate (δ 1.50 ppm), polyether (δ 1.14 ppm) and polycarbonate (δ 1.33 ppm) accordingly meanwhile A_{ELO} represents by the area of terminal methyl signals of ELO (δ 0.89 ppm). The calculated results are tabulated in Table 5.3.

5.4.4. Effect of Operating Conditions

The properties of the product are highly dependent on the operating conditions applied during the polymerization reaction. Herein, different parameters had been investigated such as reaction temperature, reaction time and the catalyst loading.

5.4.4.1. Effect of Catalyst Loading

The effect of catalyst loading is shown in Table 5.4. Varying the catalyst loading will greatly affect the yield and molecular weight of the resultant copolymer. Theoretically, smaller catalyst loading will lead to lower yield of copolymer since the amount of catalyst in the reaction system is lower. On the other hand, higher catalyst loading may result in more viscous polymerization system that impedes the diffusion of living polymer end and then reduces the yield of copolymer (Wang et al., 2006). In this work, formation of poly(carbonate-co-ether) was not detected when 0.05 g of Co-Zn DMC was used in the system, perhaps too little to initiate the reaction. The results also showed that yield of resultant polymer increased as the catalyst loading was increased whereas on the contrary opposite behaviour was demonstrated by the catalyst activity.

Table 5.4. Study of reaction parameters in semi-batch reactor

Sample	Reaction temp. (°C)	Time (h)	Catalyst loading (g)	Yield ^a (g)	Productivity g product/g catalyst	M _n /M _w ^{b,*} x10 ⁵	PDI ^{b,*}
ELO 0.05	60	24	0.05	/	/	/	/
ELO 0.10	60	24	0.1	2.045	20.45	4.09/5.43	1.30
ELO 0.20	60	24	0.2	3.720	18.60	6.21/6.54	1.05
ELO 0.30	60	24	0.3	3.885	12.95	4.75/5.89	1.23
ELO 4	60	4	0.2	1.562	7.81	5.02/5.89	1.17
ELO 6	60	6	0.2	1.906	9.53	5.04/5.93	1.18
ELO 16	60	16	0.2	2.411	12.06	5.08/5.93	1.17
ELO 24	60	24	0.2	3.720	18.60	6.21/6.54	1.05
ELO 50	50	24	0.2	/	/	/	/
ELO 60	60	24	0.2	3.720	18.60	6.21/6.54	1.05
ELO 70	70	24	0.2	4.388	21.94	6.08/6.51	1.07
ELO 80	80	24	0.2	4.955	24.76	4.36/5.13	1.18
ELO 90	90	24	0.2	3.808	19.04	4.59/5.16	1.13

Reaction conditions: volume of ELO = 10 mL, volume of PO = 10 mL, pressure of CO₂ = 5.0 MPa.

^a Weight of the polymer obtained

^b Determined by gel permeation chromatography (GPC)

*Two peaks were observed in the GPC spectrums of the resultant polymers, representing the highest molecular weight of the polymer (quasi-crosslinked sample) also the oligomeric mixtures containing polyether and the unreacted ELO. The molecular weight reported here was from the quasi-crosslinked sample. Sample of the GPC spectrum is given in the supplementary document.

5.4.4.2. Effect of Reaction Time

The effect of polymerization time on ELO, PO and CO₂ terpolymerization was studied by varying the reaction temperature between 4 to 24 h whilst the other parameters were kept constant. Generally, both yield and productivity of Co-Zn DMC catalyst increased as the reaction time prolonged from 4 – 24 h. The M_n and PDI recorded were in the ranges of 5.02 -

6.21×10^5 and 1.05 to 1.18 respectively. The small PDI values signify the polymer chains have a narrow molecular weight distribution.

5.4.4.3. Effect of Reaction Temperature

As shown in Table 5.4, no polymer was collected when the reaction temperature was lowered to 50 °C most probably due to at this temperature the DMC catalyst was not activated at all. However, as the reaction temperature was increased more meaningful activity was detected. It was observed that reaction temperature had a pronounced positive effect on the coupling reaction when the reaction temperature was raised from 60 to 90 °C. The productivity of Co-Zn DMC catalyst increased from 18.60 to 24.76 g polymer/g catalyst when the reaction temperature was elevated from 60 °C to 80 °C. However, further increase in reaction temperature led to a decrease in catalyst activity. This is mainly due to the molar equivalents of CO₂ in solution was gradually diminished as temperature rose, and this would lead to a decrease in yield and the catalytic activity. As for the M_n, the highest value recorded for poly(carbonate-co-ether) was at reaction temperature of 60 °C with 6.21×10^5 g/mol at reaction temperature of 60°C with PDI of 1.05. Results attained from this study demonstrated that the properties of the resultant polymer may vary depending on the polymerization temperature.

5.5 Conclusions

In this study, bio-based poly(carbonate-co-ether) was successfully synthesized via catalytic polymerization of ELO, PO and CO₂. Analyses from both FTIR and ¹H NMR confirmed the formation of poly(carbonate-co-ether) bonded to the triglyceride chain of the ELO. The effects of polymerization parameters on the physical properties of the resultant polymers were also analyzed and reported. The polymerization parameters under investigation were the reaction temperature, reaction time and catalyst loading. In this study, the resultant

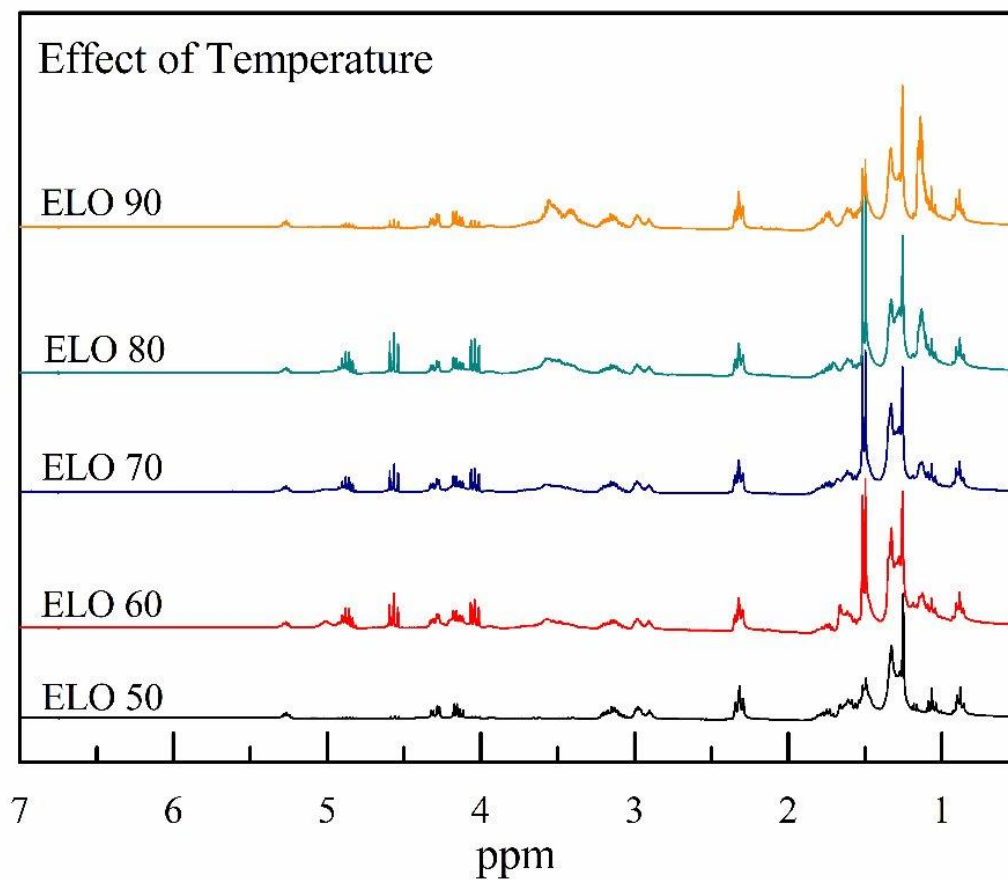
polymer with maximum M_n was prepared using 0.2 g of Co-Zn DMC catalyst at reaction temperature and reaction time of 60 °C and 24 h respectively.

In summary, ELO is a promising precursor for production of polycarbonate via catalytic polymerization with CO₂. The feasibility of utilizing renewable epoxide as a replacement to the petroleum-based epoxide is viewed as a positive solution to increasing environmental and energy concern. Nevertheless, since the discovery is still at the infancy stage, a thorough research need be conducted to improve the properties of the bio-based polymers so that it is at par with the petroleum-based counterpart.

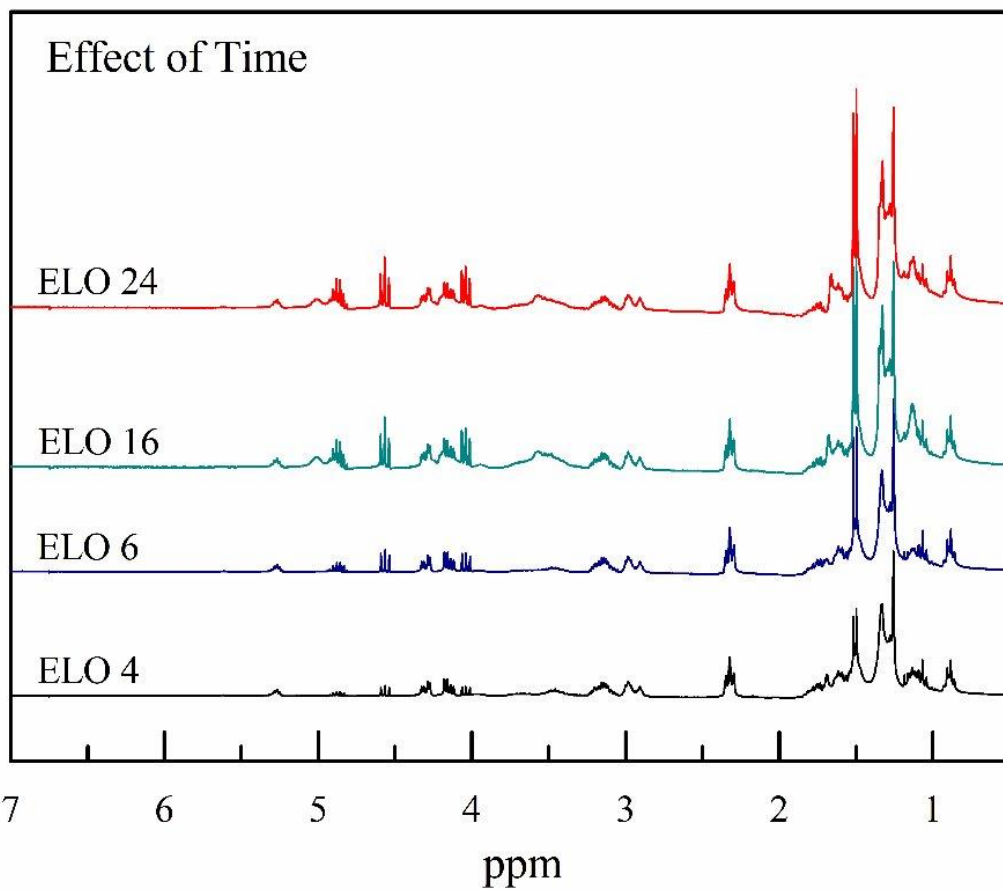
Acknowledgments

This work is supported by the Spanish Ministry of Economy and Competitiveness (Program RETOS, Grant No. PID2019-106518RB-I00). The authors would also like to acknowledge both Majlis Amanah Rakyat and Universiti Kuala Lumpur, for funding a fellowship to make this study possible (MARA No.: 330406768645).

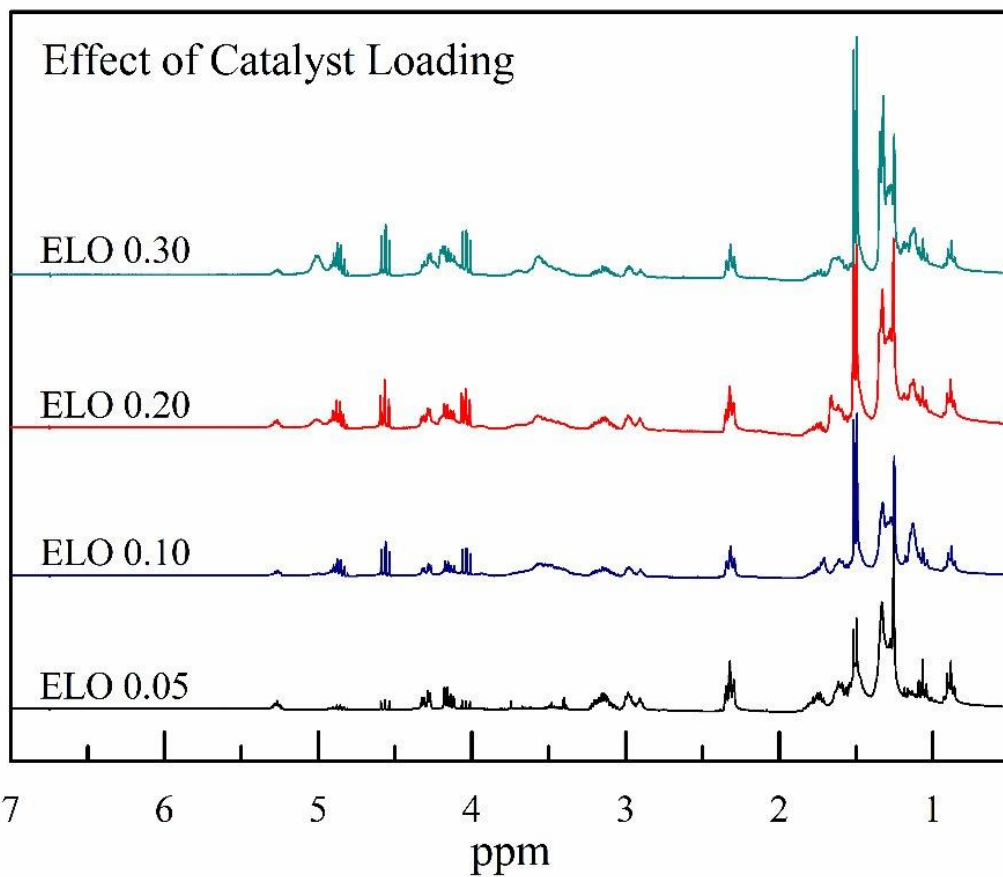
Appendix C5: Supplementary material



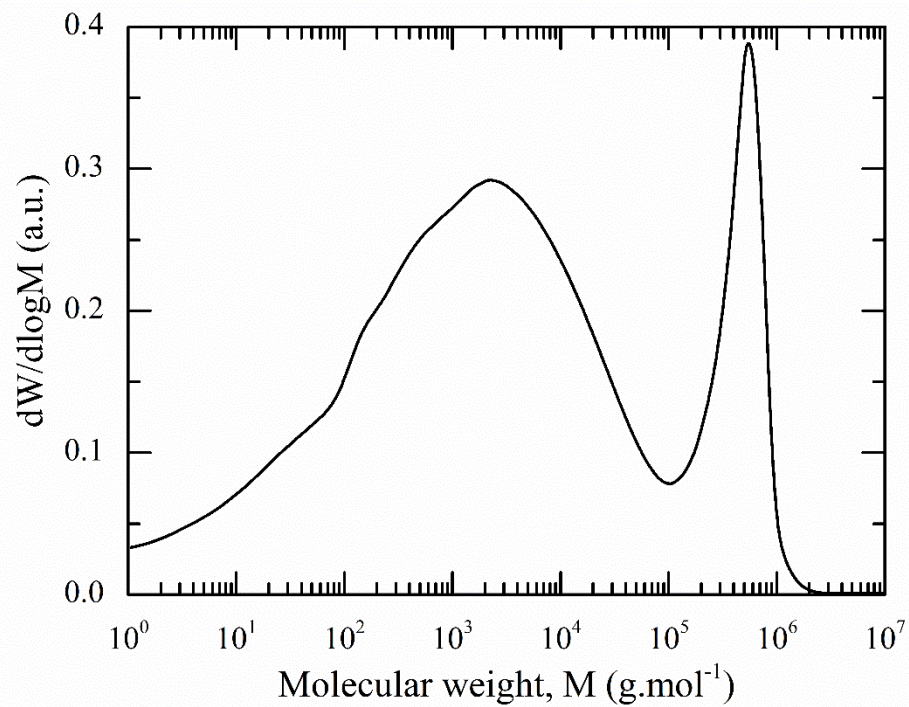
Appendix C5.1. ¹H NMR spectra of terpolymerization products in CDCl₃ over the range of reaction temperature



Appendix C5.2. ^1H NMR spectra of terpolymerization products in CDCl_3 over the range of reaction time



Appendix C5.3. ^1H NMR spectra of terpolymerization products in CDCl_3 over the range of catalyst loading



Appendix C5.4. GPC spectrum of ELO 80

CHAPTER 6 : Aerobic Biodegradation of Bio-based Poly(carbonate)-co- ether

This part of the work has been presented at the following conference:

1. Farra Wahida Saarani, Laura de Sousa Serrano, Jordi J Bou, 2020. Aerobic Biodegradation of Polycarbonates based on vegetable oils. 14th Mediterranean Congress of Chemical Engineering, Barcelona, November 16th to 20th, 2020. doi.org/10.48158/MeCCE-14.DG.09.01

6.1 Abstract

A medium scale direct measurement respirometric (DMR) system was designed to evaluate the aerobic biodegradation of bio-based poly(carbonate)-co-ether and its precursor. The bio-based poly(carbonate)-co-ether were synthesized via catalytic copolymerization of epoxidized vegetable oil (EVO), propylene oxide (PO) and carbon dioxide (CO₂). Herein, two types of EVO were used specifically epoxidized linseed oil (ELO) and epoxidized soybean oil (ESO) which produced ELO based poly(carbonate)-co-ether (PC-ELO) and ESO based poly(carbonate)-co-ether (PC-ESO) respectively. Under a controlled composting condition, the biodegradation rate of two vegetable oils, two EVOs and the two bio-based poly(carbonate)-co-ether was measured. Activated vermiculite was used as inoculum instead of mature compost. CO₂ emissions were recorded by a non-dispersive infrared gas analyser (NDIR). Findings from this study showed that after 50 days, cellulose reached 75% biodegradation whereas both bio-based poly(carbonate)-co-ether could reach up to 44.6 to 51.8% biodegradation.

6.2 Introduction

Conventional polymers which are petroleum derived are manufactured specifically for their mechanical, thermal stability and durability. Their uses are greatly acknowledged as lifelong polymers, but they do not degrade at all owing to their chemical framework. It was reported that in the year of 2016, Europe generated approximately 27.1 million tonnes of plastic waste. Out of this number, 41.6% was recovered via energy recuperation process followed by recycling process with 31.1% and the remaining ended up in landfills (PlasticsEurope, 2018). However, the three methods commonly used to manage the plastic waste specified earlier have some drawbacks and this often cause difficulty in managing sites where polymer waste is deposited. Incineration of polymeric products such as plastic for instance, may enhance the net

carbon dioxide (CO₂) emissions. In addition, substantial amount of ash and slag containing hazardous and toxic compounds may be released into the atmosphere in the process. This later may result in other serious environmental problems.

Despite the huge number of plastics which can be recycled, and the materials recovered can be given a second life, this method is not fully employed. The reason being is due to troubles with the accumulation and sorting of plastic waste. In addition, factors such as the low demand of recycled plastics, low commodity prices and ambiguities about market outlets has impeded the growth of European Union (EU) plastic recycling sector (Milios et al., 2018). The poor waste management facilities in both developing and developed countries often results in plastic and other waste being recklessly disposed into rivers and waterbodies. Although some members of the EU have banned landfilling applications, in Spain alone approximately 46.4% of plastic wastes generated in the country in the year of 2016 are still being disposed in landfills (PlasticsEurope, 2018). This activity results in generation of toxic leachate owing to the interactivity of plastics with groundwater and moisture-rich substances present in the dump, which is of hazardous nature (Moharir and Kumar, 2019). Taking into consideration that these approaches all has downsides and limitations, thus the best alternative is by substituting the traditional polymeric material with biodegradable polymers.

The term “biodegradability” however has been used by many researchers and authors negligently or inaccurately in their publication (for instances in the abstracts or in the titles). Even without conducting the biodegradation experiments, many researchers have claimed that the polymeric materials synthesized are biodegradable. It is noteworthy to highlight that bio-based materials are not necessarily biodegradable thus it is very important to use the right definition. To reiterate, bio-based polymers are materials which are produced from renewable

resources. Bio-based polymers can be biodegradable such as polylactic acid (PLA) or nondegradable such as bio-derived polyethylene (Bio-PE), also known as biopolyethylene. Similarly, although lots of bio-based polymers are biodegradable for instance starch and Polyhydroxyalkanoate (PHAs), there are several biodegradable polymers that are not bio-based such as Poly(ϵ -caprolactone) (PCL) (Ashter, 2016).

Biodegradation is the process by which organic substances are broken down by the enzymes produced by living organisms. Two biodegradation conditions, namely aerobic and anaerobic, are categorized by the presence or absence of oxygen (O_2), respectively. In aerobic environments, microorganisms break the polymer chains down using oxygen during the metabolism process. As a result, CO_2 gas and water are produced and released to the atmosphere. On the other hand, anaerobic biodegradation happens in an oxygen-absent environment. Instead of CO_2 , methane gas (CH_4) and water are generated and released. Evaluation on the biodegradability of polymers in aerobic condition can be done precisely via respirometric technique, in which the consumption of O_2 and/or the evolution of CO_2 is/are measured. Commonly, respirometric system are made of three major components namely (1) an air supply; (2) an air-tight closed vessel called the 'bioreactor', which contains compost mixture and/or test or reference materials; and (3) a measuring device, to quantify the amount of O_2 uptake or CO_2 release. Depending on the technique used to quantify CO_2 from the exhaust of the bioreactor, they are classified into three categories which are (1) cumulative measurement respirometric system (CMR) (ASTM International, 2015; International Organization for Standardization, 2012), (2) direct measurement respirometric system (DMR) (ASTM International, 2015; International Organization for Standardization, 2012) and (3) gravimetric measurement respirometric system (GMR) (International Organization for Standardization, 2006). In the CMR, basic solution such as sodium hydroxide (NaOH) or

barium hydroxide ($\text{Ba}(\text{OH})_2$) are used to trapped the CO_2 evolved and later the solution is titrated to quantify the amount of CO_2 released by the test material. Likewise, in GMR, CO_2 is captured in absorption columns filled with pellets of NaOH , and the amount of CO_2 is measured by the weight increase in the columns. Meanwhile, when DMR is applied, the concentration of CO_2 is measured directly from the exhaust of the bioreactor using gas chromatography (GC), or a non-dispersive infrared (NDIR) gas analyser sensor (Kijchavengkul and Auras, 2008).

In this study, two partially bio-based polycarbonate-co-ether were synthesized via copolymerization of epoxidized vegetable oil (EVO), propylene oxide (PO) and CO_2 . Two EVOs were used namely epoxidized linseed oil (ELO) and epoxidized soybean oil (ESO). The polymeric products are denoted as PC-ELO and PC-ESO to indicate the use of ELO and EPO as the precursor in the copolymerization reaction. The main objective of this study was to evaluate the biodegradability of both polymeric products under aerobic conditions using standard respirometric test. Vermiculite was used as inoculum instead of mature compost and the trials was conducted for 50 days. The biodegradability of both polymers were then compared with the pristine vegetable and epoxidized oil.

6.3. Experimental

6.3.1 Preparation of poly(carbonate)-co-ether

6.3.1.1 Materials

Both EVOs specifically ELO and ESO were obtained from Traquisa (Barbera del Valles, Barcelona Spain) whereas PO (>99%) was supplied by Sigma Aldrich. Materials, such as potassium hexacyanocobaltate (III) ($\text{K}_3\text{Co}(\text{CN})_6$), zinc chloride (ZnCl_2), and tertiary butyl alcohol (tert-butanol) were used without further purification. CO_2 with a purity of 99.99% was

used as received. Methylene chloride (CH_2Cl_2) and methanol (CH_3OH) were of analytical reagent grade and used without further purification.

6.3.1.2 Polymerization of EVO, PO and CO_2

Poly(carbonate)-co-ether was synthesized via catalytic polymerization of EVO, PO and CO_2 . Preparation of catalyst was according to the method described by Li et al. (2011). The polymerization reaction took place in a semi batch reactor made of stainless steel (Autoclave Engineers, Erie, PA USA) equipped with a mechanical stirrer and an automatic temperature controller system. Prior to the reaction, the reactor needs to be dried first at 100°C for a minimum of 12 h. Subsequently, the reactor has to be cooled down and this was followed by loading the catalyst (Co-Zn double metal cyanide) and equal volume of EVO and PO into the reactor. The EVO employed are ELO and ESO which produced ELO based poly(carbonate)-co-ether and ESO based poly(carbonate)-co-ether (hereafter referred to as PC-ELO and PC-ESO respectively).

Next, CO_2 was purged twice and then slowly pressurized to the desired pressure. Only then the reaction temperature was elevated and kept constant throughout the reaction. Stirrer with a stirring speed 500 rpm was turn on to initiate the polymerization reaction. Table 6.1 gives the summary of the parameters/operating conditions applied during the copolymerization reaction. Once the reaction ends, the reactor was cooled down to room temperature, slowly depressurized and opened. The products obtained were purified by dissolving in dichloromethane, precipitated by excess methanol and then dried at room temperature to a constant weight.

Table 6.1. Parameters/Operating conditions for polymerization reaction

Parameters	PC-ELO	PC-ESO
Monomers	ELO and PO	ESO and PO
Catalyst dosage (g)	0.2	0.1
Pressure (MPa)	5	4
Temperature (°C)	60	80
Time (h)	24	24

6.3.1.3 Characterizations

¹H NMR spectroscopic analysis of EVOs, PC-ELO and PC-ESO was/were recorded using a Bruker AMX-300 spectrometer at 25°C. The equipment operated at 300 MHz and all measurements were made by using CDCl₃ as solvent. The ¹H NMR spectra of both products are presented in Appendix C6.1 and C6.2.

In gel permeation chromatography (GPC) test, the number average molecular weight (M_n), weight average molecular weight (M_w) and the polydispersity index (PDI) were determined using a Agilent HPLC equipped with a separation column of PLHFIP gel running at room temperature. Mobile phase is HFIP containing 2.72 g·L⁻¹ of sodium trifluoroacetate to prevent polyelectrolyte effect. 100 μL will be injected and the concentration of each sample will be 0.2 w/v%. Calibration was performed with polymethyl methacrylate (PMMA) samples.

The volatile solid and ash content of the synthesized polymers was determined by thermogravimetric analyser (TGA) model TGA 2 (SF) (METTLER TOLEDO, USA). Differential scanning calorimetry (DSC) analysis was conducted in a DSC 2000 equipment (TA Instruments, New Castle, DE, USA) that is cooled using an Intracooler TA Instruments TC100 Chiller system (TA Instruments, New Castle, DE, USA) under dried N₂ atmosphere. 3

to 4 mg of each sample were encapsulated in aluminium T_{zero} pan. Initially, experiments were conducted at a heating/cooling rate of $10\text{ }^{\circ}\text{C}\cdot\text{min}^{-1}$ using the following protocol:

- **First heating scan (H1)** from $30\text{ }^{\circ}\text{C}$ to $200\text{ }^{\circ}\text{C}$ and isothermally held at $200\text{ }^{\circ}\text{C}$ for $t_{eq} = 2\text{ min}$ in order to reveal the thermal transitions and to erase the previous thermal history, respectively.
- **Cooling scan (C)** from $200\text{ }^{\circ}\text{C}$ to $30\text{ }^{\circ}\text{C}$ in order to induce a controlled or “standard” thermal history and isothermally held at $30\text{ }^{\circ}\text{C}$ for $t_{eq} = 1\text{ min}$.
- **Second heating scan (H2)** from $30\text{ }^{\circ}\text{C}$ to $200\text{ }^{\circ}\text{C}$ in order to determine the thermal properties.

In order to improve accuracy and to minimize the errors brought by baseline fluctuations and calibrations, this procedure was repeated three times using fresh samples taken from different zones of the manufactured sheets.

The following calorimetric parameters were determined from the above steps:

- (1) **The midpoint glass transition temperature ($T_{g,m}$)**. It is defined as the temperature at half-height of the heat capacity surge ($1/2\Delta C_p$) or alternatively called as the “temperature of half-unfreezing”. T_g can also be taken as the “inflection” point, which is slightly different and corresponds to the peak in the derivative of the heat flow or heat capacity versus temperature. However, the mid-point method T_g has been generally considered to be more reliable than the method using the “inflection” temperature (Menczel et al., 2008).

- (2) The melting transition was described using three parameters: The **melting peak temperature** (T_{mp}) was determined as the point when the endotherm peak was reached and the **end melting temperature** (T_{me}) as the temperature at the end peak of the melting endotherm (*i.e.* the temperature when melting is complete). The **melting enthalpy** (ΔH_m) was determined by integration of corresponding area underneath the dominant endothermic melting peak.

6.3.2 Biodegradation study

The aerobic biodegradation of the test materials was determined under controlled composting conditions by analysis of evolved CO₂ using an in-house built DMR system. The details information of the materials, equipment and the calculation method are given in the following sections.

6.3.2.1 Materials

Vermiculite of premium grade (3–6 mm in diameter) and organic compost were obtained from the local plant nursery. All laboratory grade chemicals or reagents used to prepare the inoculum solution were procured either from Merck–Schuchardt, Germany or Sigma Aldrich, Malaysia and used as such without further purification. Microcrystalline cellulose powder (20 mm, Sigma-Aldrich) was used as a positive reference. Both vegetable oils namely linseed oil (LO) and soybean oil (SO) were purchased from local market (Barcelona, Spain) meanwhile ELO and ESO were supplied by Traquisa (Barbera del Valles, Barcelona Spain). Samples of bio-based poly(carbonate)-co-ether were synthesized via catalytic polymerization of EVO, PO and CO₂ as detailed in section 6.3.1.2

6.3.2.2 Apparatus

A typical test set-up is shown in Figure 6.1. Basically, the set-up is made of three basic parts:

- (1) An air-feed control system (including a flow-rate controller and a humidifier) to ensure accurate control of the aeration of the test mixture.
- (2) A composting vessel containing the mixture of reference material or test material and inoculum, located in a closed chamber.
- (3) An infrared gas analyser (IRGA) for measuring the concentration of CO₂ evolved from the bioreactors.

Herein, compressed air is used to stimulate aerobic biodegradation of the test materials. The test materials are kept in air-tight closed vessels (bioreactors) and exposed to inoculated vermiculite. Vermiculite activated with inoculum solution and compost extract contain nutrients and living microorganisms and this will help to promote the biodegradation of the samples which can be justified by the formation of CO₂. The measurements of CO₂ in parts per million (ppm) are performed directly on the exhausted air of each bioreactor by means of the appropriate IRGA sensor (Model K30 from Senseair, Sweden). Analog sensor signals are then converted and recorded in every two seconds by means of a Data Acquisition Software (DAS). The software is structured with a front panel that monitors the trial and shows the results in real time.

The bioreactors are placed inside a closed chamber (Mettler, Germany) outfitted with a temperature controller and equipped with a suitable passage for the air-tight tubes. In order to humidify the inlet air, each bioreactor is connected with another vessel containing distilled

water. A tube was used to drive the air exhausted from each vessel towards the measuring line where the IRGA sensor is located.

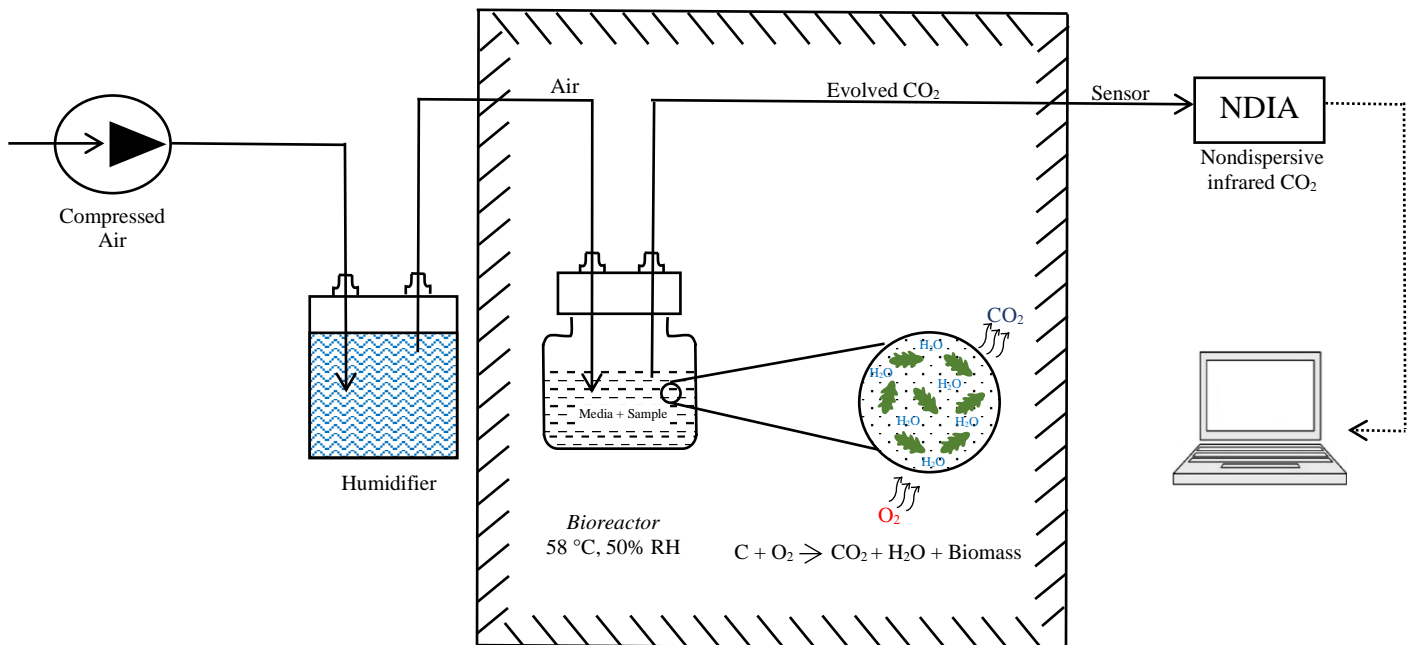


Figure 6.1. Schematic diagram of the experimental apparatus

6.3.2.3 Preparation of inoculum solution

In this present work, vermiculite is used as the solid media instead of mature compost. Vermiculite is a clay mineral with excellent water holding capacity and act as a good support for microbial growth and activity (Tosin et al., 1998). To circumvent the priming effect, usage of vermiculite as the solid media in biodegradation tests is highly recommended (Bellia et al., 2000).

Vermiculite needs to be activated beforehand by inoculating it with mineral solution (containing both organic and inorganic nutrients) and compost extract at ratio 1:1. Composition of mineral solution is listed in Table 6.2. Preparation of compost extract was done by blending dry compost with deionized water (20% wt./vol.), stirring and letting sit for 30 min followed by filtration through a sieve with 1 mm mesh. Vermiculite and inoculum solution were mixed accordingly and subsequently were incubated at $50^{\circ}\text{C} \pm 2^{\circ}\text{C}$ for three days.

Table 6.2. Detailed composition of 1 L of mineral solution

1 L of Mineral solution	
KH ₂ PO ₄ , g	1
MgSO ₄ , g	0.5
CaCl ₂ (10% sol), mL	1
NaCl (10% sol), mL	1
Trace-element solution, mg	1
1 L of trace-element solution, mg	
H ₃ BO ₃	500
KI	100
FeCl ₃	200
MnSO ₄	400
(NH ₄) ₆ Mo ₇ O ₂₄	200
FeSO ₄	400

6.3.2.4 Experimental Conditions

In keeping with several methodologies reported in the literature (Pagga, 1997), our trials were conducted in triplicate: 3 vessels contained the inoculum, 3 vessels contained inoculum plus a reference biodegradable material (namely cellulose, Sigma-Aldrich), and 18 vessels contained inoculum plus test materials. Ideally ratio between the dry mass of vermiculite and the dry mass of the test material should preferably be about 6:1. In this study 90 g of dry vermiculite and 15 g of reference material or test material are added to the bioreactor.

To ensure the test materials underwent a homogeneous degradation process, throughout the trials the samples were shook manually once per week. At the beginning of the trials, the moisture content of the inoculum was adjusted to about 50% (w/w) and held constant by means of inlet air humidification. Nonetheless, distilled water was added from time to time to maintain the humidity inside the bioreactors.

6.3.3. Data Analysis

6.3.3.1 Theoretical amount of carbon dioxide (Th_{CO_2}) evolved by test material

According to ISO 14855 (International Organization for Standardization, 2012) , the theoretical amount of CO_2 (Th_{CO_2}) evolved by the test material in a test vessel is given, in grams by Eq. (6.1):

$$Th_{CO_2} = m \times w_c \times \frac{44}{12} \quad (6.1)$$

where m (g) is the mass of test material introduced into the test vessel, w_c is the carbon content of the test material, determined from the chemical formula or from elemental analysis, expressed as a mass fraction whereas 44 and 12 are the molecular and atomic masses of CO_2 and carbon respectively. The same calculation was applied for the theoretical amount of CO_2 evolved by the reference material in each vessel.

6.3.3.2 Cumulative CO_2

The amount of CO_2 evolved between successive data points in each of the bioreactors was calculate using the data collected from the gas sensors. Eq. (6.2) gives the cumulative

$$Mass\ CO_2 = [CO_2] \times \Delta t \times Q \quad (6.2)$$

where $[CO_2]$ is the concentration of CO_2 evolved in ppm (corrected for the background CO_2 concentration of the inlet CO_2 -free air), Δt is the period of measurement cycle and Q refers to the flowrate of compressed air in $L.hr^{-1}$.

6.3.3.3 Percentage biodegradation

A biodegradation curve was obtained by plotting released CO_2 (%) versus exposure time. Biodegradation was calculated as the percentage of test material carbon mineralized as CO_2 according to the following expression:

$$D_T = \frac{(CO_2)_T - (CO_2)_B}{Th_{CO_2}} \times 100 \quad (6.3)$$

where:

$(CO_2)_T$ is the cumulative amount of CO_2 evolved in each composting vessel containing test material, in grams per vessel;

$(CO_2)_B$ is the mean cumulative amount of CO_2 evolved in the blank vessels, in grams per vessel;

Th_{CO_2} is the theoretical amount of CO_2 which can be produced by test material, in grams per vessel

The same equation is used to calculate the degree of biodegradation of the test material.

6.4. Results and Discussion

6.4.1. Biodegradation environment

The aerobic biodegradation test was performed for a period of 50 days using an in-house built DMR system (Figure 6.1). Apart from the CO_2 concentration which was measured on daily basis, other parameters affecting biodegradation (environment-related factors) such as

temperature, pH, moisture content and air flow rate were also recorded at designated time interval (Figure 6.2).

During this study, the ambient temperature inside the closed chamber was recorded everyday meanwhile the pH of the inoculum inside the blank reactor was measured once a week. In general, both temperature and pH were stable at 58°C and 7, respectively. Normally, temperatures between 54 - 60°C are deemed ideal for composting since this favour the thermophilic compost microorganism. If the composting temperature exceeds 60°C, this might destroy diverse microbial species and results in drying out the compost rapidly thus limits the biodegradation rate (Grima et al., 2000; Stoffella and Kahn, 2001).

Meanwhile, as being suggested by ISO 14855 standard, the best pH for composting are within the range 7–9. According to Grima et al. (2000) a neutral pH is more suitable to guarantee the survival and full activity of the microorganisms. In addition, Lauber et al. (2009) mentioned that the microbial community diversity activity was highest in soils with neutral pH. pH beyond the ideal range may results inhibition (acidic pH) or odour related problem (alkaline pH) (Stoffella and Kahn, 2001). Since the source of the microorganism used in this biodegradation study comes from the compost extract, hence it is appropriate to maintain the pH at 7 during the trial period.

Water act as a distribution channel for microorganism and nutrients. Both microbial growth and metabolic activity are highly dependence on the amount of water added in the inoculum. Water deficiency may drop/plunge the metabolism and the microorganism development rates. On the contrary, a moisture excess causes substrate packing down and anaerobiosis. In this study, moisture content was measured periodically in a control bioreactor

to regulate the amount of water needed for adjustment. From time to time, water is added to each bioreactor to avoid excessive drying in the inoculum. The quantity of water needs to be added was determined by weighing each bioreactor followed by adding adequate water to restore the initial weight. At the same time, the inlet air is humidified by passing through a vessel containing distilled water and this vessel is connected in-line with the bioreactor. At the same time, each bioreactor is also connected in-line with another vessel containing distilled water used to humidify the inlet air. Despite the importance of water in composting process, too much water may lessen the airspace within the inoculum leading to oxygen deficiency and anaerobiosis. In this circumstance, usage of vermiculite is beneficial since it can improve the porosity and helps to preserve the aerobic conditions (International Organization for Standardization, 2012). Besides, as being recommended by Way et al. (2010) after water was replenished, the bioreactor should be shaken to homogenize the contents as well as avoiding the vermiculite from sticking together and clogging. Furthermore, if water addition into bioreactor was done without mixing, most likely moisture irregularity throughout the inoculum would result in regions with insufficient water for the biodegradation process (Castro-Aguirre et al., 2017). During this study, the moisture content recorded in the blank bioreactor was between 48 – 56%.

To ensure that the biodegradation performed in this work was under aerobic condition, a continuous flow of air was supplied into the bioreactors. The biodegradation rate relies on the amount of oxygen supply. If the air flow rate is too low, the biodegradation process might be slowing down. Contrariwise, high air flow rate may as well decelerate the biodegradation process due to rapid drying and cooling of the compost which result from decreasing of water availability and temperature correspondingly (Sundberg and Jönsson, 2008). The flow rate of air passing in each bioreactor was adjusted to 1 L.hr⁻¹ throughout the trial period.

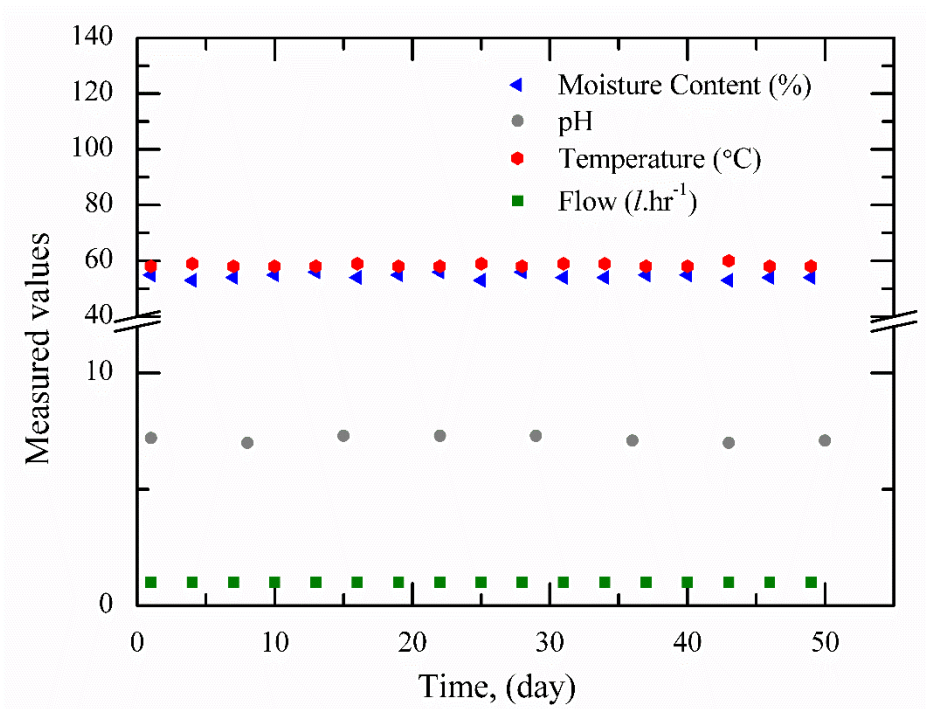


Figure 6.2. Biodegradation test parameters as a function of time.

6.4.2. Physical characterizations

Determination of ash content, dry solids, and volatile solids (Table 6.3) of the inoculated vermiculate, reference material and test materials was performed using a thermogravimetric analyzer model TGA 2 (SF) (METTLER TOLEDO, USA). The heating rate was set at $10^{\circ}\text{C}\cdot\text{min}^{-1}$, and the samples were run from room temperature to 600°C . As stated in the ISO 14855 Standard, the total dry solids are acquired after drying the sample to about 105°C , while the volatile solids are obtained by subtracting the residues after incineration at about 550°C from the total dry solids of the same sample (International Organization for Standardization, 2005). Volatile solids refer to the presence of organic matter in a substance. Taking into consideration that other non-organic compounds such as carbonates and water possibly lost after ignition at 550°C , the quantity of organic carbon is normally considered to be around 50-58% of the volatile solids (Stoffella and Kahn, 2001; Woods End Laboratories Incorporated, 2005). Referring to the aforementioned statement, therefore the percentage of

carbon presence in inoculum and both PC-ELO and PC-ESO can be estimated using the data extracted from the TGA results. As predicted, the amount of volatile solids recorded for inoculum is very low owing to the nature of vermiculite which is made of clay mineral.

Table 6.3. Characteristics of the samples used in the trials of the experimental apparatus

	Inoculum	Ref Material	SO	ESO	PC- ESO	LO	ELO	PC- ELO
Dry solid (%)	96.0	94.6	99.7	99.6	98.3	99.8	99.6	98.7
Volatile Solid (%)	2.0	83.0	99.0	98.0	89.5	99.6	98.7	92.0
Carbon (%)	1.2 ^b	44.4 ^a	78.0 ^a	72.0 ^a	52.0 ^b	78.0 ^a	70.0 ^a	53.0 ^b
<i>Th</i> _{CO₂} (g)	3.96	24.2	42.9	39.6	28.6	42.9	38.5	29.2

CO₂ was calculated based on chemical structure^a or TGA (percentage by weight)^b

ThCO₂ was calculated using Eq. (6.1)

6.4.3. Aerobic Biodegradation of test materials

The biodegradation of the refence material and test materials was evaluated in inoculated vermiculite. Vermiculite is a clay mineral (Mg,Fe,Al)₃(Al,Si)₄O₁₀(OH)₂.4H₂O, used in flakes and expanded shape. Vermiculite must be inoculated by a suitable microbial population, through a pre-fermentation process before it used in the biodegradation studies.

Since vermiculite does not contain substantially available organic carbon, it generates less CO₂ than the mature compost. Therefore, in respirometric studies the background production of CO₂ should be considerably lower than the expected CO₂ production of the test material, otherwise the sensitivity of the measurement can be very low.

During the trial period, normal air was fed into bioreactors instead of CO₂ free air. Therefore, measurement of the CO₂ concentration were recorded at both the inlet and outlet of each test vessel. The inlet concentration was subtracted from the outlet concentration for correction. Inoculum with no sample was used as the blank to determine the respiration activity of the inoculum. The amount of CO₂ evolved from the blank bioreactors represents the background. Thus, in order to determine the actual amount of CO₂ evolved by the reference and test materials in each bioreactor, the average of background value is subtracted from the amount of CO₂ produced by the reference and test materials as shown in Eq. (6.2).

As predicted, the quantity of CO₂ released in blank bioreactors was very low but stable throughout the trial period. After 10 days of the trial period, the inoculum showed a cumulated emission of 0.26 g CO₂ per vessel, which equivalent to 147 mg CO₂ per gram of volatile solids (Figure 6.3). This is in accordance with the range recommended by ISO 14855-1:2012 which stated that the inoculum in the blank bioreactor should produce more than 50 mg but less than 150 mg of carbon dioxide per gram of volatile solids (mean values) after 10 days of incubation (International Organization for Standardization, 2012). This suggest that the inoculated vermiculite used in this study was adequately rich in microorganism that drive the biodegradation of the specimens tested. By the end of the trial period, a total of 2.19 g of CO₂ was released in the blank bioreactor. Additionally, usage of vermiculite is extremely favourable due to its ability to avoids any priming effect, which can be found in controlled compost.

Priming effect refers to an event whereby humified portion of soil or compost begins to degrade at an accelerated rate after substrate addition (Tuomela et al., 2002).

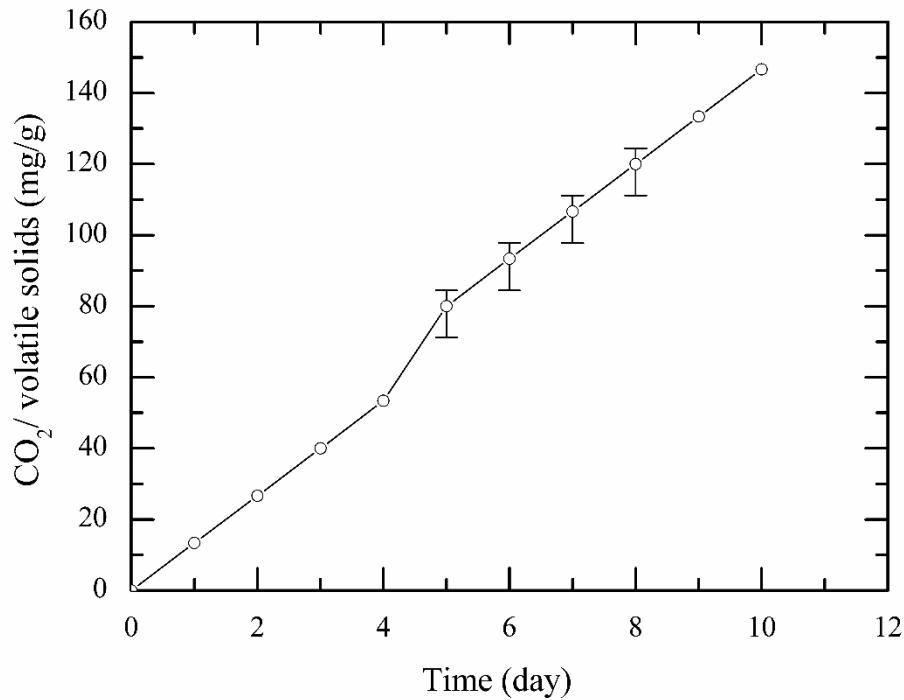


Figure 6.3. Production of CO₂ per g of volatile solids in inoculum bioreactor

The cumulative amount of CO₂ released by cellulose at the end of trial period was 21.1g CO₂ per vessel (Figure 6.4) which corresponds to 78.2 % biodegradation (Figure 6.5). At 45 days, the degradation of cellulose has exceeded 70 % and this was in agreement with the ISO 14855-1:2012 (International Organization for Standardization, 2012) which confirm the validity of the trial conducted.

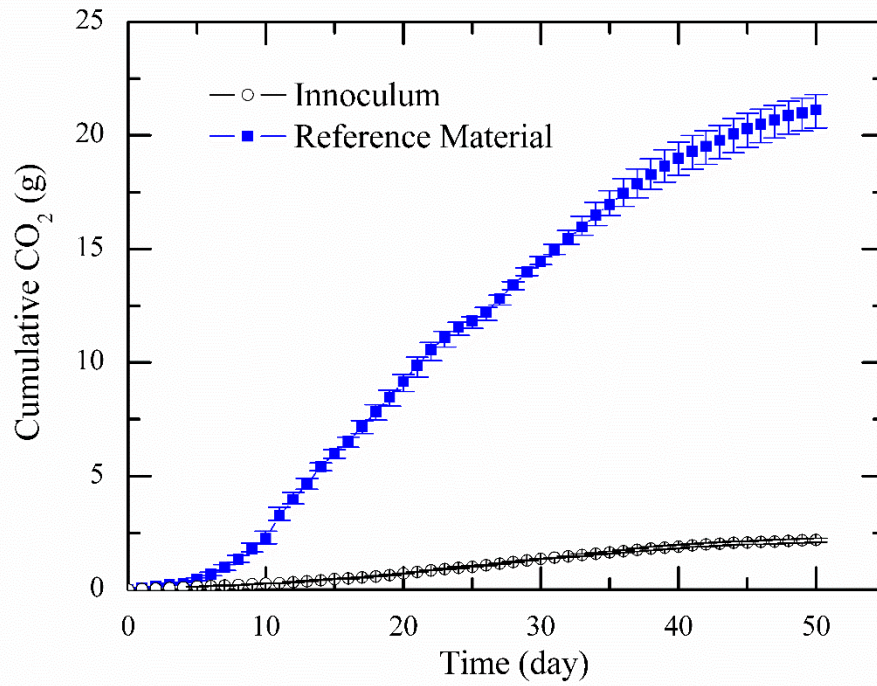


Figure 6.4. Cumulative CO₂ evolution of cellulose bioreactor.

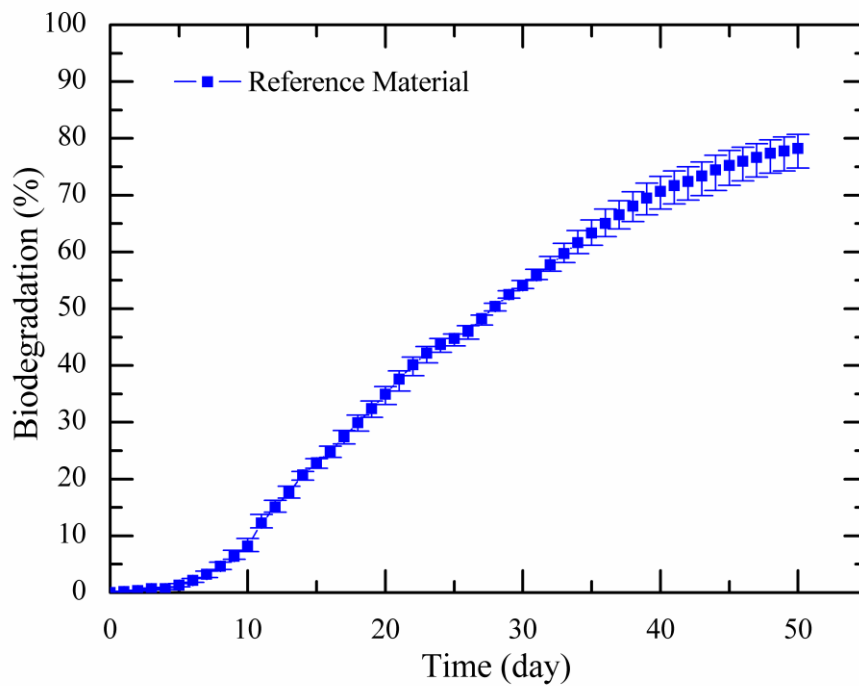


Figure 6.5. Biodegradation of cellulose bioreactor

Samples of both bio-based polymeric materials (PC-ELO and PC-ESO) tested in this study was partially synthesised from ELO and ESO respectively. Herein, the comparison between the cumulative CO₂ evolved and percentage degradation of both polymeric materials and their precursors are presented. Figure 6.6 and Figure 6.7 illustrate the cumulative CO₂ and % biodegradation by LO, ELO and PC-ELO. LO bioreactors produced 45.1 g CO₂ and reached a 100% of mineralization after 50 days of testing. Meanwhile, at the end of trial period a cumulated CO₂ emission equivalent to 37.9 g CO₂ per vessel and 15.2 g CO₂ per vessel was recorded for samples ELO and PC-ELO respectively. This corresponds to 92.7% and 44.6% of biodegradation.

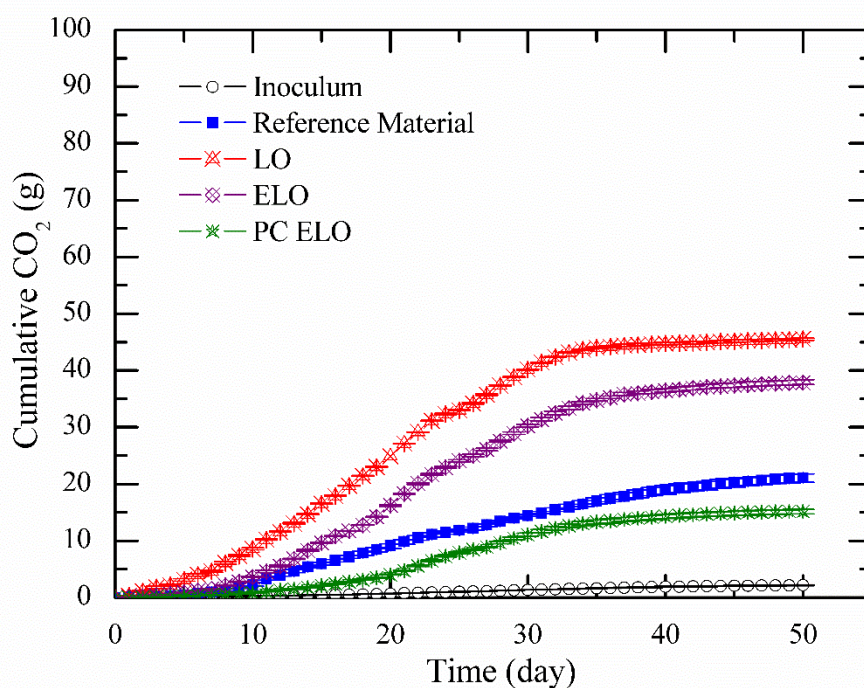


Figure 6.6. Cumulative CO₂ evolution of LO, ELO and PC-ELO test materials

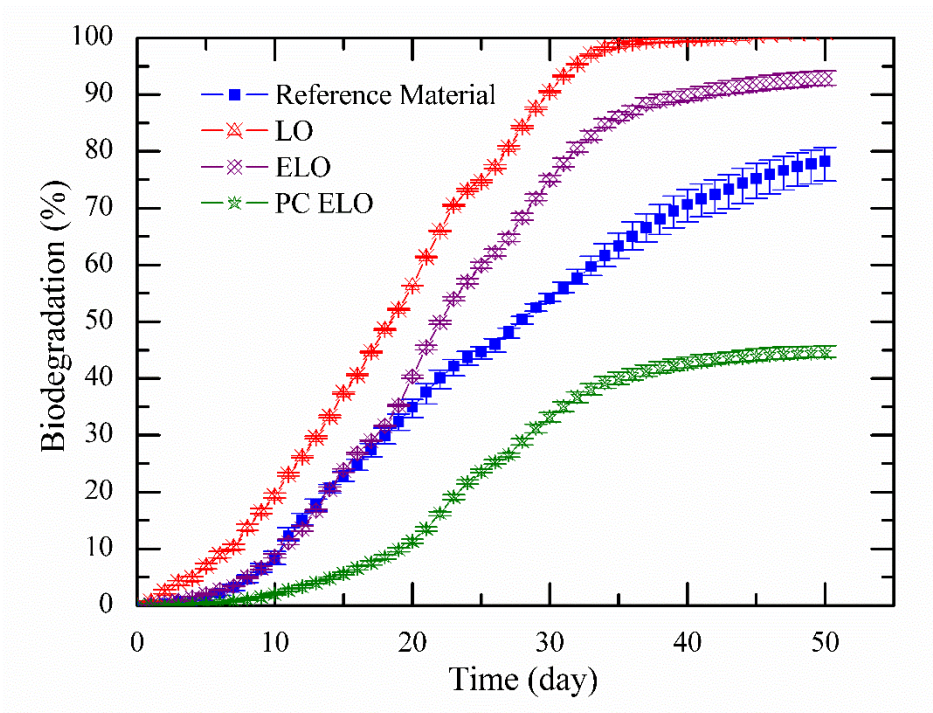


Figure 6.7. Biodegradation of LO, ELO and PC-ELO test materials

Figure 6.8 and Figure 6.9 demonstrate the cumulative CO₂ and % biodegradation by SO, ESO and PC-ESO. Similar trend was observed for SO based samples, whereby the percentage biodegradation recorded at the end of the trial for SO was the highest among the all followed by ESO and PC-ESO with 90.1%, 81.9% and 51.8% correspondingly. In terms of cumulative CO₂ emission, this is equivalent to 45.2 g of CO₂ evolved in SO bioreactor, 37.9 g of CO₂ evolved in ESO bioreactor and 15.2 g of CO₂ evolved in PC-ESO bioreactor. According to Broekhuizen et al. (2003) under both aerobic and anaerobic conditions, vegetable oils and synthetic esters have a much better biodegradation capacity than mineral oil.

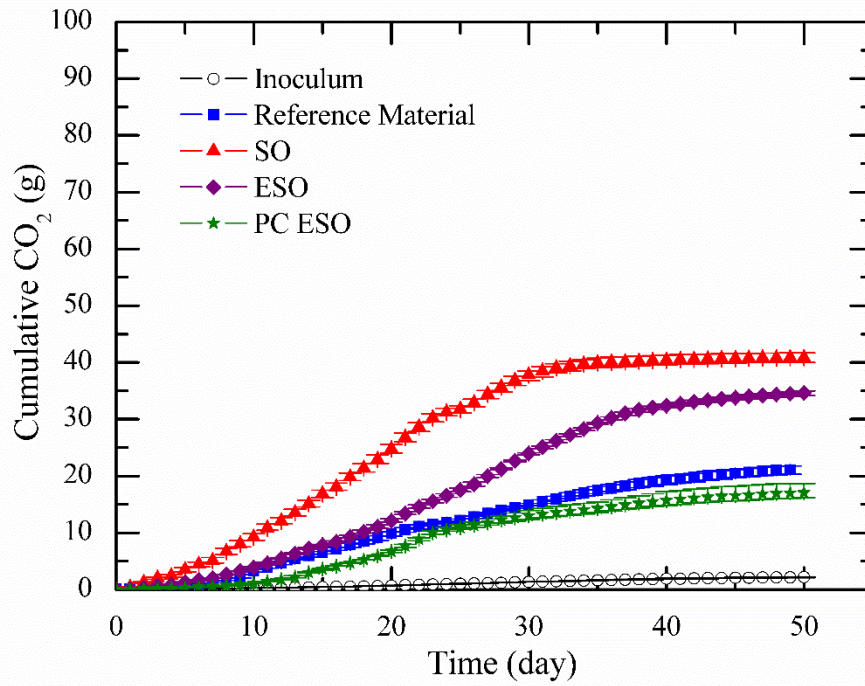


Figure 6.8. Cumulative CO₂ evolution of SO, ESO and PC-ESO test materials

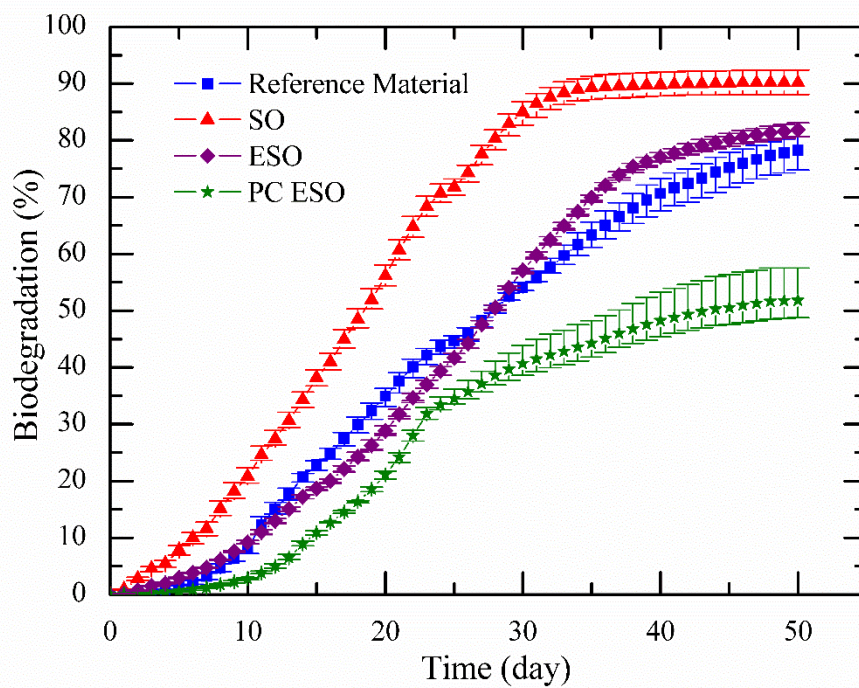
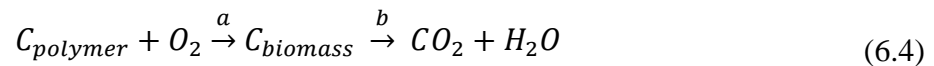


Figure 6.9. Mineralization of SO, ESO and PC-ESO test materials

Aluyor and co-worker (2009) stated that from several tests conducted, vegetable oils can undergo about 70 to 100% biodegradation in a period of 28 days. This statement is in accordance with the results obtain from this study which showed that after 28 days, both vegetable oils used underwent approximately 70% of degradation. The degradation of vegetable-based oils firstly took place when the enzyme-catalyzed cleavage of the ester bond to fatty acids. Esterases and lipases are the enzymes which catalyze this biodegradation reaction and these two enzymes are synthesized by a wide range of microorganisms including the one commonly found in compost.

For all samples tested in this study, biodegradation took place in aerobic condition. Before mineralization took place, the carbon in polymers ($C_{polymer}$) is converted to carbon biomass ($C_{biomass}$), which later being used by microorganisms for growth and reproduction as illustrated in equation 6.4



where reaction a is the biodegradation process and reaction b is the mineralization process.

For both polymeric samples tested in this study, the reaction is considered as heterogenous since it takes place at the solid/liquid interface of the polymer, by which the biodegraded polymer surface is the solid phase and the microbial enzyme is the liquid phase. According to Gu et al. (2000), there are two groups of enzymes which actively involved in biological degradation of polymers: extracellular and intracellular depolymerases (Gu et al., 2000). Intracellular degradation is the hydrolysis of an endogenous carbon reservoir by the accumulating bacteria themselves while extracellular degradation is the utilization of an

exogenous carbon source not necessarily by the accumulating microorganisms (Tokiwa and Calabia, 2007).

Finding from present work showed that the percentage biodegradation for PC-ELO was slightly lower than PC-ESO. A possible explanation for this result might be to the fact that PC-ELO sample has higher molecular weight in comparison to PC-ESO. According to Kale et al. (2007), the biodegradation rate of a polymeric material is very much affected by its molecular weight. The polymer's T_g (glass transition temperature) increases as the molecular weight increases and as a result the polymer become more glassier and less flexible. Moreover, commonly a higher molecular weight polymer also has a longer chain length, which means that there are more bonds that must be cleaved in order to release the water-soluble oligomers or monomers that are small enough to be consumed by microorganisms. Table 6.4 gives the values of T_g and T_m for both PC-ELO and PC-ESO.

Table 6.4. Properties of PC-ELO and PC-ESO

Parameters	PC-ELO	PC-ESO
$T_{g,1}$ (°C)	21.75	-1.69
$T_{g,2}$ (°C)	n/a	24.53
$T_{m,p1}$ (°C)	261.32	163.67
$T_{m,p2}$ (°C)	n/a	185
M_n (g.mol ⁻¹)	6.21 x 10 ⁵	1.02 x 10 ⁴
M_w (g.mol ⁻¹)	6.54 x10 ⁵	1.04 x 10 ⁴

** T_g and T_m obtained from DSC

**Number average molecular weight (M_n), number weight average molecular weight (M_w) and polydispersity index ratio (PDI) were measured using GPC

Kale et al. (2007) reported that the irregularity of the polymer chains may increase when a comonomers are introduced into a polymer structure. As a result, the polymer's crystallinity is lessened, and subsequently increase the biodegradability of the said polymer. Nevertheless, this is highly dependent on the type of comonomer. The biodegradability of a copolymer may increase if the comonomer contains hydrolyzable groups such as ether, ester, amide, or carbonate (Figure 6.10). On the contrary, if the comonomer contains aromatic structures, or other groups that provide rigidity to the polymer chain, and no hydrolyzable groups, the copolymer will generally have lower biodegradability or may not even biodegrade at all. This is certainly true in the case of the two polymeric samples tested in this study. Since both polymeric samples tested in this study are made up from more than one monomer and contain hydrolyzable groups in their polymeric chain (i.e., ether, ester, and carbonate) thus under the conditions applied, these two polymeric samples are easily degraded.

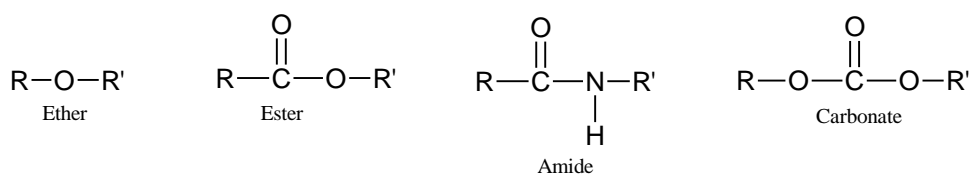


Figure 6.10. Hydrolyzable functional groups commonly found in biodegradable polymers
(Kale et al., 2007)

6.5. Conclusions

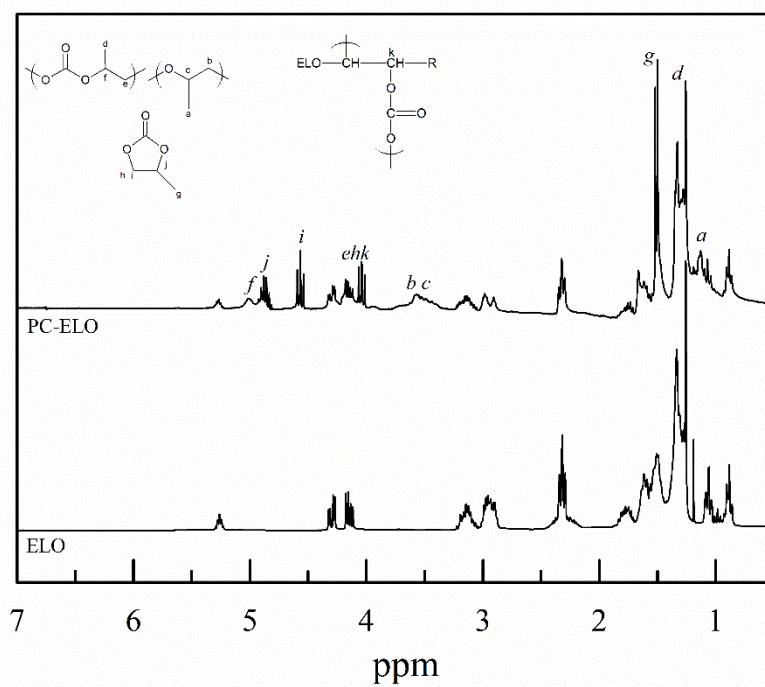
In this study, two products from catalytic copolymerization of EVO, PO and CO₂ that is poly(carbonate)-co-ether along with its precursor underwent aerobic biodegradation study using standard respirometric test. Results from the present study reveals that, under the conditions applied 44.6% of PC-ELO and 51.8% of PC-ESO were degraded at the end of trial period. As foreseen, these polymers easily underwent biodegradation since the co-monomer

used in their production are renewable and bio-based. Additionally, the comonomer contains hydrolyzable groups which contribute to acceleration of the process. The small different of percentage biodegradation recorded between these polymers was attributed to the physical properties of the individual polymer.

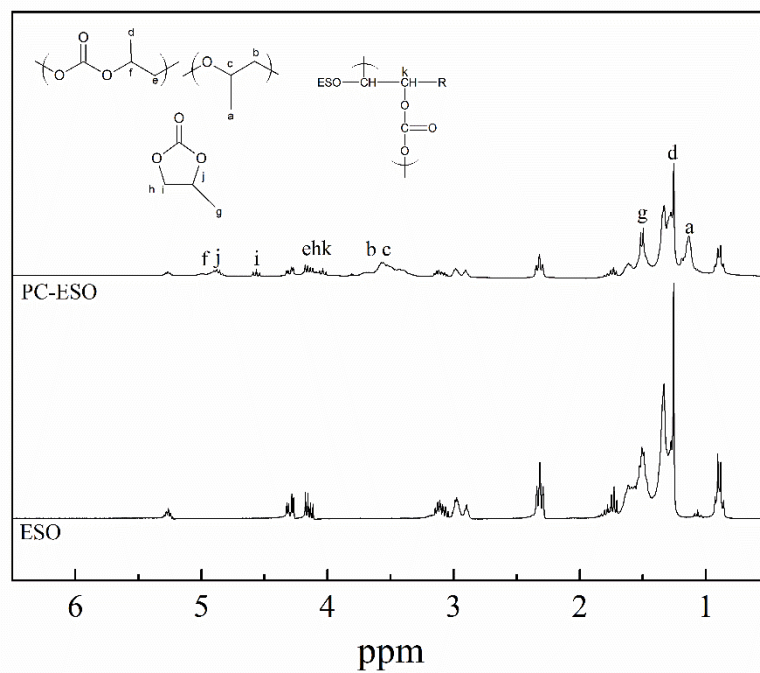
Acknowledgement

The authors gratefully acknowledge the financial support by the Spanish Ministry of Economy and Competitiveness (Program RETOS, Grant No. PID2019-106518RB-I00). Majlis Amanah Rakyat and Universiti Kuala Lumpur, Malaysia are both acknowledged for funding a fellowship to make this study possible.

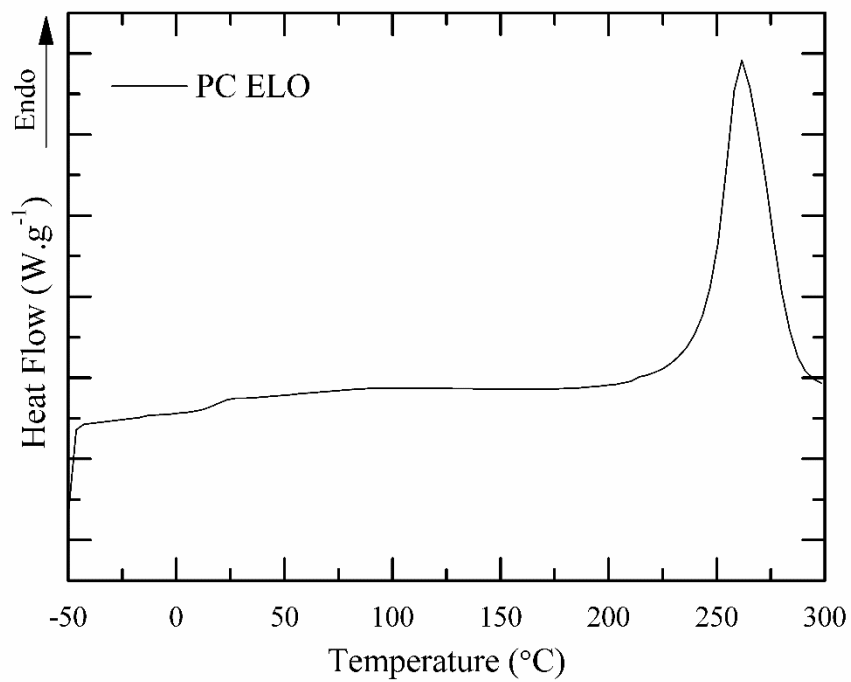
Appendix C6. Supplementary material



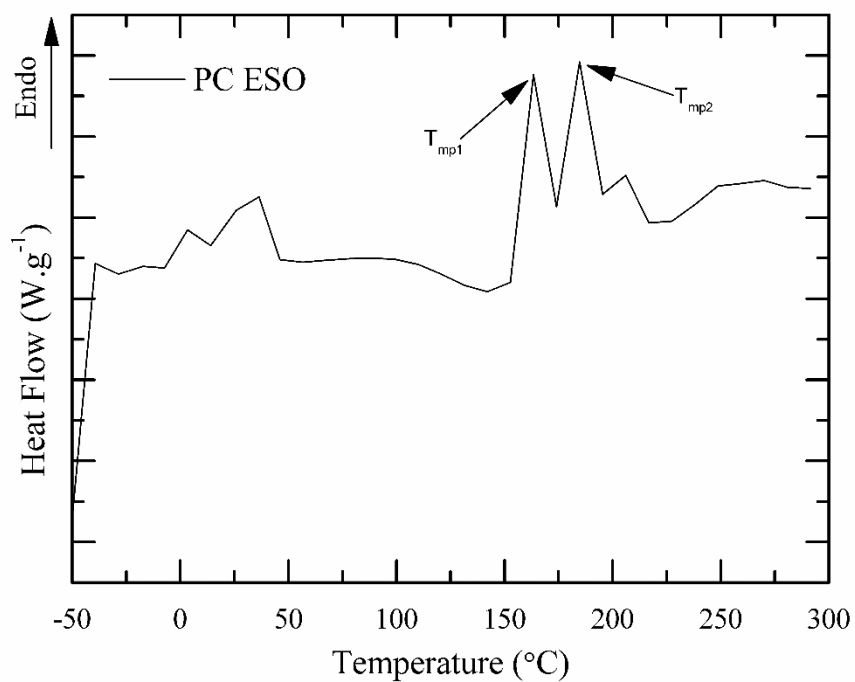
Appendix C6.1. ¹H NMR spectra for PC-ELO and ELO



Appendix C6.2. ¹H NMR spectra for PC-ESO and ESO



Appendix C6.3. DSC spectrum for PC-ELO



Appendix C6.4. DSC spectrum for PC-ESO

CHAPTER 7 : CONCLUSIONS AND RECOMMENDATIONS

7.1 Conclusions

1. Co-Zn DMC catalyst was found to be feasible for the copolymerization reaction of CHO/CO₂ and PO/CO₂. The yield and molecular weight of PCHC1 and PPC1 obtained are satisfactorily moderate and this implies the reliability of Co-Zn DMC for the copolymerization reaction. The application of this heterogenous catalyst was further extended in the terpolymerization reaction of PO, VO and CO₂. The in-situ epoxidation reaction of selected VOs has successfully transformed the VO into EVO. Nevertheless, no polymer obtained from the terpolymerization reactions performed using the EVO prepared owing to the low content of epoxy group of the oils used hence reducing the sites for the reaction to takes place. On the contrary, results from the preliminary studies indicate the potential of both ELO and ESO to be employed as the co-monomer in the copolymerization reaction to manufacture polycarbonate.
2. Utilization of ESO as the co-monomer in the catalytic copolymerization reaction with CO₂ has successfully synthesized products comprises of mixture of poly(propylene carbonate), cyclic carbonate and polyether unit. The presence of each individual component has been validated by means of FTIR and ¹H NMR analysis. At the reaction time of 80°C, reaction time of 6h and CO₂ pressure of 4 MPa, the M_n of the polymeric products recorded is 6498 g. mol⁻¹ with the percentage incorporation of ESO in the polymer is only 7.8%. Also notable are two samples prepared at reaction temperature of 90°C and 100°C whose unable to be characterized by GPC most likely due to the formation of a cross-linked material. Results from a simple solubility test also signify that the two samples were insoluble and strongly suggest the development of a cross-linked polymer.

3. Poly(carbonate-co-ether) was successfully synthesized via catalytic polymerization of ELO, PO and CO₂. FTIR and ¹H NMR spectroscopic methods affirm the formation of poly(carbonate-co-ether) bonded to the triglyceride chain of the ELO. The effects of the reaction temperature, reaction time and catalyst loading on the physical properties of the resultant polymers were also studied. Herein, the resultant polymer with maximum M_n of 6.21×10^5 g.mol⁻¹ and PDI of 1.05 was obtained using 0.2 g of Co-Zn DMC catalyst at reaction temperature, reaction time and CO₂ pressure of 60 °C, 24 h and 5 MPa respectively.
4. Finding from the aerobic biodegradation study reveals that at 45 days, the degradation of cellulose has exceeded 70% and this is in accordance with the ISO 14855-1:2012 which confirm the validity of the trial conducted. Both VOs employed in this study effortlessly degraded with nearly 100% of degradation at the end of the trial period meanwhile ELO and ESO showed 92.7% and 81.9% of degradation correspondingly. Due to the co-monomer used in the production of both PC-ELO and PC-ESO are renewable and bio-based, these two polymers naturally underwent biodegradation. Additionally, the comonomer contains hydrolyzable groups which contribute to acceleration of the process. After 50 days of trials periods, 44.6% of PC-ELO and 51.8% of PC-ESO were degraded.
5. The vegetable oil-based polycarbonate synthesized are still at the infant stage whereby a lot of improvement needs to be done in terms of increasing the percentage incorporation of renewable monomer in the polymeric material and making sure that it has an attractive properties at least equivalent to the commercial polycarbonate available in the market. It is crucial to remember that sustainable polymers are fairly new when compared to petroleum-based polymers. The outstanding performance of polymers derived from fossil fuels is the outcome of many years of intensive research

and commercial scale optimisation. This will come for the next generation of renewably derived polymers but will require significant and concerted academic and industrial research in the coming decades.

7.2 Recommendations

1. Different type of catalysts should be employed in the copolymerization reaction including homogeneous catalysts and new heterogeneous composite catalyst (for instance ZnGA/DMC catalyst).
2. The choice of vegetable oils as co-monomer could be extended to several other types especially with oil that contain high number of double bonds per triglyceride molecules such as corn oil (4.5 double bond) , cottonseed oil (3.9 double bond), jatropha oil (3.0 double bond) and rapeseed oil (3.8 double bond).
3. Explore the potential of utilizing terpenes (an organic compounds produced by a variety of plants) as the monomer in copolymerization with CO₂. These molecules are hydrocarbons that contain one or more carbon-carbon double bonds and exhibit a carbon skeleton of isoprene (2-methyl-1,4-butadiene) units with a large variety of structures and (bio)activities.
4. With respect to the operating conditions applied during the copolymerization reaction (temperature, time, catalyst loading, CO₂ pressure), optimization should be carried out in the future studies using response surface methodology (RSM) as it reduces the number of experimental trials needed to evaluate the interaction between multiple factors, thereby making process more authentic and rapid.
5. Microwave-assisted copolymerization could be employed for forthcoming studies as this method helps to minimize the reaction time compared to the conventional heating method which requires long hours to complete.

6. Additional characterizations on the polymers obtained from the copolymerization can be studied such as the glass transition temperature (T_g) and melting temperature (T_m).
7. The method for biodegradation study may be change to other approach such as soil burial degradation study or enzymatic degradation study.

List of Publications and Conferences

1. Shaarani, F.W. and J.J. Bou, Synthesis of vegetable-oil based polymer by terpolymerization of epoxidized soybean oil, propylene oxide and carbon dioxide. *Science of The Total Environment*, 2017. 598: p. 931-936.
2. Shaarani, F.W. and J.J. Bou, Synthesis of vegetable-oil based polymer by terpolymerization of epoxidized soybean oil, propylene oxide and carbon dioxide. Poster presentation at the 10th International Society for Environmental Biotechnology (ISEB) Conference, Barcelona, June 1st to 3rd, 2016.
3. Shaarani, F.W., J.J. Bou, and R.N. Hakim, Production of Poly(carbonate-co-ether) via Catalytic Polymerization of Epoxidized Linseed Oil, Propylene Oxide and Carbon Dioxide. *IOP Conference Series: Materials Science and Engineering*, 2019. 548: p. 012019.
4. Shaarani, F.W., J.J. Bou, and R.N. Hakim. Production of Poly(carbonate-co-ether) via Catalytic Polymerization of Epoxidized Linseed Oil, Propylene Oxide and Carbon Dioxide. *National Symposium of Polymeric Materials 2018 (NSPM2018)* on 6th September 2018 at Kuala Lumpur Convention Centre.
5. Shaarani, F.W. and J.J. Bou, Synthesis of Bio-based Poly(carbonate-co-ether) with Epoxidized Linseed Oil. Poster presentation at the 68th Canadian Chemical Engineering Conference (CSCHE2018), Oct 28th to 31st, 2018.
6. Farra Wahida Saarani, Laura de Sousa Serrano, Jordi J Bou, 2020. Aerobic Biodegradation of Polycarbonates based on vegetable oils. 14th Mediterranean Congress of Chemical Engineering, Barcelona, November 16th to 20th, 2020. doi.org/10.48158/MeCCE-14.DG.09.01

Articles under review:

1. Shaarani, F.W. and J.J. Bou, Synthesis of Bio-based Poly(carbonate-co-ether) by means of Catalytic Polymerization of Epoxidized Linseed Oil, Propylene Oxide and Carbon Dioxide (Journal of Industrial and Engineering Chemistry).
2. Farra Wahida Saarani, Laura de Sousa Serrano, Jordi J Bou, Aerobic Biodegradation of Bio-based Poly(carbonate)-co-ether (Journal of Polymers and the Environment).

References

- Abbasi A, Nasef MM, Yahya WZN. Copolymerization of vegetable oils and bio-based monomers with elemental sulfur: A new promising route for bio-based polymers. *Sustainable Chemistry and Pharmacy* 2019; 13: 100158.
- Acik G, Kamaci M, Altinkok C, Karabulut HRF, Tasdelen MA. Synthesis and properties of soybean oil-based biodegradable polyurethane films. *Progress in Organic Coatings* 2018; 123: 261-266.
- Adekunle K. A Review of Vegetable Oil-Based Polymers: Synthesis and Applications. *Open Journal of Polymer Chemistry* 2015; 5: 34-40.
- Alagi P, Ghorpade R, Jang JH, Patil C, Jirimali H, Gite V, et al. Functional soybean oil-based polyols as sustainable feedstocks for polyurethane coatings. *Industrial Crops and Products* 2018; 113: 249-258.
- Albarrán-Preza E, Corona-Becerril D, Viguera-Santiago E, Hernández-López S. Sweet polymers: Synthesis and characterization of xylitol-based epoxidized linseed oil resins. *European Polymer Journal* 2016; 75: 539-551.
- Aluyor E, Obahiagbon K, Ori-Jesu M. Biodegradation of Vegetable Oils: A Review. Vol 4, 2009.
- Anastas P, Eghbali N. Green Chemistry: Principles and Practice. *Chemical Society Reviews* 2010; 39: 301-312.
- Anderson TS, Kozak CM. Ring-opening polymerization of epoxides and ring-opening copolymerization of CO₂ with epoxides by a zinc amino-bis(phenolate) catalyst. *European Polymer Journal* 2019; 120: 109237.
- Ang R-R, Tin Sin L, Bee S-T, Tee T-T, Kadhum AAH, Rahmat AR, et al. A review of copolymerization of green house gas carbon dioxide and oxiranes to produce polycarbonate. *Journal of Cleaner Production* 2015; 102: 1-17.

- Artham T, Doble M. Biodegradation of Aliphatic and Aromatic Polycarbonates. *Macromolecular Bioscience* 2008; 8: 14-24.
- Ashter SA. 5 - Types of Biodegradable Polymers. In: Ashter SA, editor. *Introduction to Bioplastics Engineering*. William Andrew Publishing, Oxford, 2016, pp. 81-151.
- ASTM International. ASTM D5338 - 15 Standard Test Method for Determining Aerobic Biodegradation of Plastic Materials Under Controlled Composting Conditions, Incorporating Thermophilic Temperatures. ASTM International, West Conshohocken, PA, 2015.
- ASTM International. ASTM D883 Standard Terminology Relating to Plastics, 2019.
- Babu RP, O'Connor K, Seeram R. Current progress on bio-based polymers and their future trends. *Progress in Biomaterials* 2013; 2: 8.
- Badia JD, Gil-Castell O, Ribes-Greus A. Long-term properties and end-of-life of polymers from renewable resources. *Polymer Degradation and Stability* 2017; 137: 35-57.
- Baekeland LH. The Synthesis, Constitution, and Uses of Bakelite. *Journal of Industrial & Engineering Chemistry* 1909; 1: 149-161.
- Bahramian B, Dehghani F. New Catalytic Systems for Fixation of Carbon Dioxide into Valuable Poly(Alkylene Carbonates). In: Wang LENA-J-A, editor. *Advanced Catalytic Materials - Photocatalysis and Other Current Trends*. IntechOpen, 2016.
- Belgacem MN, Gandini A. *Monomers, Polymers and Composites from Renewable Resources*: Elsevier, 2008.
- Bellia G, Tosin M, Degli-Innocenti F. The test method of composting in vermiculite is unaffected by the priming effect. *Polymer Degradation and Stability* 2000; 69: 113-120.
- Bhalerao MS, Kulkarni VM, Patwardhan AV. Ultrasound-assisted chemoenzymatic epoxidation of soybean oil by using lipase as biocatalyst. *Ultrasonics Sonochemistry* 2018; 40: 912-920.

- Bickel S. Ölpflanzen in Europa. 2012; 42: 222-231.
- Briassoulis D, Dejean C. Critical Review of Norms and Standards for Biodegradable Agricultural Plastics Part I. Biodegradation in Soil. *Journal of Polymers and the Environment* 2010; 18: 384-400.
- Brodin M, Vallejos M, Opedal MT, Area MC, Chinga-Carrasco G. Lignocellulosics as sustainable resources for production of bioplastics – A review. *Journal of Cleaner Production* 2017; 162: 646-664.
- Castro-Aguirre E, Auras R, Selke S, Rubino M, Marsh T. Insights on the aerobic biodegradation of polymers by analysis of evolved carbon dioxide in simulated composting conditions. *Polymer Degradation and Stability* 2017; 137: 251-271.
- Chang C, Qin Y, Luo X, Li Y. Synthesis and process optimization of soybean oil-based terminal epoxides for the production of new biodegradable polycarbonates via the intergration of CO₂. *Industrial Crops and Products* 2017; 99: 34-40.
- Changmai B, Sudarsanam P, Rokhum L. Biodiesel production using a renewable mesoporous solid catalyst. *Industrial Crops and Products* 2020; 145: 111911.
- Chauhan P, Chen H, Roy Goswami S, Yan N. Improved mechanical properties of flexible bio-based polymeric materials derived from epoxy mono/di-abietic acid and soyabean oil. *Industrial Crops and Products* 2019; 138: 111437.
- Chavan AP, Gogate PR. Ultrasound assisted synthesis of epoxidized sunflower oil and application as plasticizer. *Journal of Industrial and Engineering Chemistry* 2015; 21: 842-850.
- Chavan VP, Patwardhan AV, Gogate PR. Intensification of epoxidation of soybean oil using sonochemical reactors. *Chemical Engineering and Processing: Process Intensification* 2012; 54: 22-28.

- Chen S, Wei X, Luo Y, Chen Y, Li Y, Zhuo D. Relative reactivities of epoxide monomers during copolymerization with carbon dioxide. *Advanced Industrial and Engineering Polymer Research* 2019; 2: 178-185.
- Cheng R, Zhou Y, Hou Q, Liu B. ZnO/SiO₂-modified rare-earth-metal ternary catalyst bearing quaternary ammonium salts for synthesis of high molecular weight poly(propylene carbonate). *Chinese Journal of Catalysis* 2018; 39: 1303-1310.
- Clark AJ, Hoong SS. Copolymers of tetrahydrofuran and epoxidized vegetable oils: application to elastomeric polyurethanes. *Polymer Chemistry* 2014; 5: 3238-3244.
- Coates GW, Moore DR. Discrete Metal-Based Catalysts for the Copolymerization of CO₂ and Epoxides: Discovery, Reactivity, Optimization, and Mechanism. *Angewandte Chemie International Edition* 2004a; 43: 6618-6639.
- Coates GW, Moore DR. Discrete Metal-Based Catalysts for the Copolymerization of CO₂ and Epoxides: Discovery, Reactivity, Optimization, and Mechanism. *Angewandte Chemie International Edition* 2004b; 43: 6618-6639.
- Cohen CT, Chu T, Coates GW. Cobalt Catalysts for the Alternating Copolymerization of Propylene Oxide and Carbon Dioxide: Combining High Activity and Selectivity. *Journal of the American Chemical Society* 2005; 127: 10869-10878.
- Colombo K, Ender L, Santos MM, Chivanga Barros AA. Production of biodiesel from Soybean Oil and Methanol, catalyzed by calcium oxide in a recycle reactor. *South African Journal of Chemical Engineering* 2019; 28: 19-25.
- Correia Diogo A. Polymers in Building and Construction. In: Gonçalves MC, Margarido F, editors. *Materials for Construction and Civil Engineering: Science, Processing, and Design*. Springer International Publishing, Cham, 2015, pp. 447-499.

- Costa CSMF, Fonseca AC, Moniz J, Godinho M, Serra AC, Coelho JFJ. Soybean and coconut oil based unsaturated polyester resins: Thermomechanical characterization. *Industrial Crops and Products* 2016; 85: 403-411.
- Coutris C, Macken AL, Collins AR, El Yamani N, Brooks SJ. Marine ecotoxicity of nitramines, transformation products of amine-based carbon capture technology. *Science of The Total Environment* 2015; 527–528: 211-219.
- Cuéllar-Franca RM, Azapagic A. Carbon capture, storage and utilisation technologies: A critical analysis and comparison of their life cycle environmental impacts. *Journal of CO2 Utilization* 2015; 9: 82-102.
- Cui S, Borgemenke J, Qin Y, Liu Z, Li Y. Chapter Five - Bio-based polycarbonates from renewable feedstocks and carbon dioxide. In: Li Y, Ge X, editors. *Advances in Bioenergy*. 4. Elsevier, 2019, pp. 183-208.
- Dai C, Zhu Q, Pang H, Zhu L, Lin Q. Rapid copolymerization of carbon dioxide and propylene oxide catalyzed by double metal cyanide complexes in an ultrasonic field. *Materials Letters* 2016; 180: 89-92.
- Dai Z, Jiang P, Lou W, Zhang P, Bao Y, Gao X, et al. Preparation of degradable vegetable oil-based waterborne polyurethane with tunable mechanical and thermal properties. *European Polymer Journal* 2020; 139: 109994.
- Darensbourg DJ, Chung W-C. Availability of Other Aliphatic Polycarbonates Derived from Geometric Isomers of Butene Oxide and Carbon Dioxide Coupling Reactions. *Macromolecules* 2014; 47: 4943-4948.
- Darensbourg DJ, Wildeson JR, Yarbrough JC, Reibenspies JH. Bis 2,6-difluorophenoxide Dimeric Complexes of Zinc and Cadmium and Their Phosphine Adducts: Lessons Learned Relative to Carbon Dioxide/Cyclohexene Oxide Alternating Copolymerization

- Processes Catalyzed by Zinc Phenoxides. *Journal of the American Chemical Society* 2000; 122: 12487-12496.
- Das R, Banerjee SL, Kumar R, Kundu PP. Development of sustainable elastomeric engineering nanocomposites from linseed oil with improved mechanical stability and thermally induced shape memory properties. *Journal of Industrial and Engineering Chemistry* 2016; 35: 388-399.
- Deacy AC, Kilpatrick AFR, Regoutz A, Williams CK. Understanding metal synergy in heterodinuclear catalysts for the copolymerization of CO₂ and epoxides. *Nature Chemistry* 2020; 12: 372-380.
- Dharman MM, Ahn J-Y, Lee M-K, Shim H-L, Kim K-H, Kim I, et al. Moderate route for the utilization of CO₂-microwave induced copolymerization with cyclohexene oxide using highly efficient double metal cyanide complex catalysts based on Zn₃[Co(CN)₆]. *Green Chemistry* 2008; 10: 678-684.
- Dinda S, Patwardhan AV, Goud VV, Pradhan NC. Epoxidation of cottonseed oil by aqueous hydrogen peroxide catalysed by liquid inorganic acids. *Bioresource Technology* 2008; 99: 3737-3744.
- Du L, Wang C, Zhu W, Zhang J. Copolymerization of carbon dioxide and propylene oxide catalyzed by two kinds of bifunctional salen-cobalt(III) complexes bearing four quaternary ammonium salts. *Journal of the Chinese Chemical Society* 2020; 67: 72-79.
- Erlandsson B, Karlsson S, Albertsson A-C. The mode of action of corn starch and a pro-oxidant system in LDPE: influence of thermo-oxidation and UV-irradiation on the molecular weight changes. *Polymer Degradation and Stability* 1997; 55: 237-245.
- Eubeler JP, Zok S, Bernhard M, Knepper T. Environmental biodegradation of synthetic polymers I. Test methodologies and procedures. *TrAC Trends in Analytical Chemistry* 2009; 28: 1057-1072.

- European Bioplastics n-I. Bioplastics market data. 2020, 2019.
- Fan L, Qin G, Cao S. Synthesis of Polycarbonates by Copolymerization of Carbon Dioxide and Cyclohexene Oxide Using Schiff Base Complex as Catalyst. *Arabian Journal for Science and Engineering* 2015; 40: 2861-2866.
- Farhadian A, Gol Afshani MB, Babaei Miyardan A, Nabid MR, Safari N. A Facile and Green Route for Conversion of Bifunctional Epoxide and Vegetable Oils to Cyclic Carbonate: A Green Route to CO₂ Fixation. *ChemistrySelect* 2017; 2: 1431-1435.
- Faria DN, Cipriano DF, Schettino MA, Neto AC, Cunha AG, Freitas JCC. Na,Ca-based catalysts supported on activated carbon for synthesis of biodiesel from soybean oil. *Materials Chemistry and Physics* 2020; 249: 123173.
- Food and Agriculture Organizations of the United Nations. Production quantities of Linseed by country 2018. 2020, 2020.
- Frances M, Gardere Y, Duret E, Leroyer L, Cabaret T, Rubini M, et al. Effect of heat treatment on Pinus pinaster rosin: A study of physico chemical changes and influence on the quality of rosin linseed oil varnish. *Industrial Crops and Products* 2020; 155: 112789.
- Funabashi M, Ninomiya F, Kunioka M. Biodegradability evaluation of polymers by ISO 14855-2. *International journal of molecular sciences* 2009; 10: 3635-3654.
- Gandini A. Polymers from Renewable Resources: A Challenge for the Future of Macromolecular Materials. *Macromolecules* 2008; 41: 9491-9504.
- Gandini A. The irruption of polymers from renewable resources on the scene of macromolecular science and technology. *Green Chemistry* 2011; 13: 1061-1083.
- Gerbase AE, Gregório JR, Martinelli M, Brasil MC, Mendes ANF. Epoxidation of soybean oil by the methyltrioxorhenium-CH₂Cl₂/H₂O₂ catalytic biphasic system. *Journal of the American Oil Chemists' Society* 2002; 79: 179-181.

- Geyer R, Jambeck JR, Law KL. Production, use, and fate of all plastics ever made. *Science Advances* 2017; 3: e1700782.
- Ghasemlou M, Daver F, Ivanova EP, Adhikari B. Polyurethanes from seed oil-based polyols: A review of synthesis, mechanical and thermal properties. *Industrial Crops and Products* 2019; 142: 111841.
- Goud VV, Patwardhan AV, Pradhan NC. Studies on the epoxidation of mahua oil (*Madhumica indica*) by hydrogen peroxide. *Bioresource Technology* 2006; 97: 1365-1371.
- Grima S, Bellon-Maurel V, Feuilloley P, Silvestre F. Aerobic Biodegradation of Polymers in Solid-State Conditions: A Review of Environmental and Physicochemical Parameter Settings in Laboratory Simulations. *Journal of Polymers and the Environment* 2000; 8: 183-195.
- Gu J-D, Ford T, Mitton DB, Mitchell R. Microbial degradation and deterioration of polymeric materials. *The Uhlig Corrosion Handbook* 2000: 439-460.
- Gu L, Gao Y, Qin Y, Chen X, Wang X, Wang F. Biodegradable poly(carbonate-ether)s with thermoresponsive feature at body temperature. *Vol 51*, 2013.
- Guo Z, Lin Q. Coupling reaction of CO₂ and propylene oxide catalyzed by DMC with co-complexing agents incorporated via ball milling. *Journal of Molecular Catalysis A: Chemical* 2014; 390: 63-68.
- Gupta SK. *Technological Innovations in Major World Oil Crops, Volume 1: Breeding*: Springer New York, 2011.
- Hartweg M, Sundermeyer J. Quinoline-8-olato-chromium catalysts with pseudohalogen effects for the CO₂/cyclohexene epoxide copolymerization. *European Polymer Journal* 2019; 120: 109245.

- Hauenstein O, Reiter M, Agarwal S, Rieger B, Greiner A. Bio-based polycarbonate from limonene oxide and CO₂ with high molecular weight, excellent thermal resistance, hardness and transparency. *Green Chemistry* 2016; 18: 760-770.
- Hazmi ASA, Aung MM, Abdullah LC, Salleh MZ, Mahmood MH. Producing Jatropha oil-based polyol via epoxidation and ring opening. *Industrial Crops and Products* 2013; 50: 563-567.
- Honda M, Ebihara T, Ohkawa T, Sugimoto H. Alternating terpolymerization of carbon dioxide, propylene oxide, and various epoxides with bulky side groups for the tuning of thermal properties. *Polymer Journal* 2020.
- Hosseini S, Moradi GR, Bahrami K. Synthesis of a novel stabilized basic ionic liquid through immobilization on boehmite nanoparticles: A robust nanocatalyst for biodiesel production from soybean oil. *Renewable Energy* 2019; 138: 70-78.
- Huang J, Xu Y, Wang M, Duan Z. Copolymerization of propylene oxide and CO₂ catalyzed by dinuclear salicyl-CoCl complex. *Journal of Macromolecular Science, Part A* 2020; 57: 131-138.
- Ingrao C, Tricase C, Cholewa-Wójcik A, Kawecka A, Rana R, Siracusa V. Polylactic acid trays for fresh-food packaging: A Carbon Footprint assessment. *Science of The Total Environment* 2015; 537: 385-398.
- Inoue S, Koinuma H, Tsuruta T. Copolymerization of carbon dioxide and epoxide. *Journal of Polymer Science Part B: Polymer Letters* 1969; 7: 287-292.
- International Organization for Standardization. International Standard ISO 14855-1:2005(E), Determination of the ultimate aerobic biodegradability of plastic materials under controlled composting conditions - Method by analysis of evolved carbon dioxide - Part 1: General Method, Geneva, Switzerland, 2005.

- International Organization for Standardization. ISO 14855-2 Determination of the ultimate aerobic biodegradability of plastic materials under controlled composting conditions – method by analysis of evolved carbon dioxide. Part 2: Gravimetric measurement of carbon dioxide evolved in a laboratory scale test (under development), ISO/TC61/SC5. International Organization for Standardization, Geneva, 2006.
- International Organization for Standardization. ISO 14855-1:2012, Determination of the ultimate aerobic biodegradability of plastic materials under controlled composting conditions - method by analysis of evolved carbon dioxide, Part 1: General method, 2012.
- International Organization for Standardization. ISO 472:2013 Plastics — Vocabulary, 2013.
- International Organization for Standardization. ISO 14855-2:2018 Determination of the ultimate aerobic biodegradability of plastic materials under controlled composting conditions — Method by analysis of evolved carbon dioxide — Part 2: Gravimetric measurement of carbon dioxide evolved in a laboratory-scale test. 2018.
- Ionescu M. Chemistry and Technology of Polyols for Polyurethanes: Rapra Technology, 2005.
- İşeri-Çağlar D, Baştürk E, Oktay B, Kahraman MV. Preparation and evaluation of linseed oil based alkyd paints. *Progress in Organic Coatings* 2014; 77: 81-86.
- Jebrane M, Cai S, Sandstrom C, Terziev N. The reactivity of linseed and soybean oil with different epoxidation degree towards vinyl acetate and impact of the resulting copolymer on the wood durability. *Express Polymer Letters* 2017; 11: 383-395.
- Jin L, Zeng H, Ullah A. Rapid copolymerization of canola oil derived epoxide monomers with anhydrides and carbon dioxide (CO₂). *Polymer Chemistry* 2017; 8: 6431-6442.
- Kale G, Kijchavengkul T, Auras R, Rubino M, Selke SE, Singh SP. Compostability of Bioplastic Packaging Materials: An Overview. *Macromolecular Bioscience* 2007; 7: 255-277.

- Karak N. *Vegetable Oil-Based Polymers: Properties, Processing and Applications*: Elsevier Science, 2012.
- Kember MR, Buchard A, Williams CK. Catalysts for CO₂/epoxide copolymerisation. *Chemical Communications* 2011; 47: 141-163.
- Kernbichl S, Rieger B. Aliphatic polycarbonates derived from epoxides and CO₂: A comparative study of poly(cyclohexene carbonate) and poly(limonene carbonate). *Polymer* 2020; 205: 122667.
- Khandelwal V, Sahoo SK, Kumar A, Manik G. Electrically conductive green composites based on epoxidized linseed oil and polyaniline: An insight into electrical, thermal and mechanical properties. *Composites Part B: Engineering* 2018; 136: 149-157.
- Kijchavengkul T, Auras R. Compostability of polymers. 2008; 57: 793-804.
- Kim N, Li Y, Sun XS. Epoxidation of *Camelina sativa* oil and peel adhesion properties. *Industrial Crops and Products* 2015; 64: 1-8.
- Klaus S, Lehenmeier MW, Herdtweck E, Deglmann P, Ott AK, Rieger B. Mechanistic Insights into Heterogeneous Zinc Dicarboxylates and Theoretical Considerations for CO₂-Epoxide Copolymerization. *Journal of the American Chemical Society* 2011; 133: 13151-13161.
- Konyalı S. *Sunflower Production, Consumption, Foreign Trade and Agricultural Policies in Turkey*. 2017.
- Kothandaraman J, Zhang J, Glezakou V-A, Mock MT, Heldebrant DJ. Chemical transformations of captured CO₂ into cyclic and polymeric carbonates. *Journal of CO₂ Utilization* 2019; 32: 196-201.
- Krist S, Bauer B. *Vegetable Fats and Oils*: Springer International Publishing, 2020.
- Kruper WJ, Swart DJ. Carbon dioxide oxirane copolymers prepared using double metal cyanide complexes. US Patent 4, 500, 704, 1985 1985.

- Kumar AP, Depan D, Singh Tomer N, Singh RP. Nanoscale particles for polymer degradation and stabilization—Trends and future perspectives. *Progress in Polymer Science* 2009; 34: 479-515.
- Lamm ME, Li P, Hankinson S, Zhu T, Tang C. Plant oil-derived copolymers with remarkable post-polymerization induced mechanical enhancement for high performance coating applications. *Polymer* 2019; 174: 170-177.
- Lamnatou C, Moreno A, Chemisana D, Reitsma F, Clariá F. Ethylene tetrafluoroethylene (ETFE) material: Critical issues and applications with emphasis on buildings. *Renewable and Sustainable Energy Reviews* 2018; 82: 2186-2201.
- Langanke J, Wolf A, Hofmann J, Böhm K, Subhani MA, Müller TE, et al. Carbon dioxide (CO₂) as sustainable feedstock for polyurethane production. *Green Chemistry* 2014; 16: 1865-1870.
- Laskar IB, Deshmukhya T, Bhanja P, Paul B, Gupta R, Chatterjee S. Transesterification of soybean oil at room temperature using biowaste as catalyst; an experimental investigation on the effect of co-solvent on biodiesel yield. *Renewable Energy* 2020; 162: 98-111.
- Lauber CL, Hamady M, Knight R, Fierer N. Pyrosequencing-Based Assessment of Soil pH as a Predictor of Soil Bacterial Community Structure at the Continental Scale. *Applied and Environmental Microbiology* 2009; 75: 5111-5120.
- Laurentino LS, Medeiros AMMS, Machado F, Costa C, Araújo PHH, Sayer C. Synthesis of a biobased monomer derived from castor oil and copolymerization in aqueous medium. *Chemical Engineering Research and Design* 2018; 137: 213-220.
- Laurichesse S, Avérous L. Chemical modification of lignins: Towards biobased polymers. *Progress in Polymer Science* 2014; 39: 1266-1290.

- Lee A, Deng Y. Green polyurethane from lignin and soybean oil through non-isocyanate reactions. *European Polymer Journal* 2015; 63: 67-73.
- Lee IK, Ha JY, Cao C, Park D-W, Ha C-S, Kim I. Effect of complexing agents of double metal cyanide catalyst on the copolymerizations of cyclohexene oxide and carbon dioxide. *Catalysis Today* 2009; 148: 389-397.
- Lee SH, Cyriac A, Jeon JY, Lee BY. Preparation of thermoplastic polyurethanes using in situ generated poly(propylene carbonate)-diols. *Polymer Chemistry* 2012; 3: 1215-1220.
- Leejarkpai T, Suwanmanee U, Rudeekit Y, Mungcharoen T. Biodegradable kinetics of plastics under controlled composting conditions. *Waste Management* 2011; 31: 1153-1161.
- Li H, Niu Y. Alternating copolymerization of CO₂ with propylene oxide and terpolymerization with aliphatic epoxides by bifunctional cobalt Salen complex. *Polym J* 2011; 43: 121-125.
- Li S, Haufe J, Patel MK. Product overview and market projection of emerging bio-based plastics. 2019, 2009.
- Li Z, Qin Y, Zhao X, Wang F, Zhang S, Wang X. Synthesis and stabilization of high-molecular-weight poly(propylene carbonate) from ZnCo-based double metal cyanide catalyst. *European Polymer Journal* 2011; 47: 2152-2157.
- Liang H, Feng Y, Lu J, Liu L, Yang Z, Luo Y, et al. Bio-based cationic waterborne polyurethanes dispersions prepared from different vegetable oils. *Industrial Crops and Products* 2018; 122: 448-455.
- Liu B, Zhao X, Wang X, Wang F. Copolymerization of carbon dioxide and propylene oxide with Ln(CCl₃COO)₃-based catalyst: The role of rare-earth compound in the catalytic system. *Journal of Polymer Science Part A: Polymer Chemistry* 2001; 39: 2751-2754.
- Liu H, Wang X, Gu Y, Guo W. Preparation and Characterization of Double Metal Cyanide Complex Catalysts. *Molecules* 2003; 8: 67.

- Liu Y, Xiao M, Wang S, Xia L, Hang D, Cui G, et al. Mechanism studies of terpolymerization of phthalic anhydride, propylene epoxide, and carbon dioxide catalyzed by ZnGA. *RSC Advances* 2014; 4: 9503-9508.
- Liu Z-H, Li Y, Zhang C-J, Zhang Y-Y, Cao X-H, Zhang X-H. Synthesis of high-molecular-weight poly(ϵ -caprolactone) via heterogeneous zinc-cobalt(III) double metal cyanide complex. *Giant* 2020; 3: 100030.
- Liu Z, Shah SN, Evangelista RL, Isbell TA. Polymerization of euphorbia oil with Lewis acid in carbon dioxide media. *Industrial Crops and Products* 2013; 41: 10-16.
- Lligadas G, Ronda JC, Galià M, Cádiz V. Renewable polymeric materials from vegetable oils: a perspective. *Materials Today* 2013; 16: 337-343.
- Lu X-B, Darensbourg DJ. Cobalt catalysts for the coupling of CO₂ and epoxides to provide polycarbonates and cyclic carbonates. *Chemical Society Reviews* 2012; 41: 1462-1484.
- Luo M, Li Y, Zhang Y-Y, Zhang X-H. Using carbon dioxide and its sulfur analogues as monomers in polymer synthesis. *Polymer* 2016; 82: 406-431.
- Mandal M. Group 4 complexes as catalysts for the transformation of CO₂ into polycarbonates and cyclic carbonates. *Journal of Organometallic Chemistry* 2020; 907: 121067.
- Marbach J, Nornberg B, Rahlf AF, Luinstra GA. Zinc glutarate-mediated copolymerization of CO₂ and PO - parameter studies using design of experiments. *Catalysis Science & Technology* 2017; 7: 2897-2905.
- Marquez C, Rivera-Torrente M, Paalanen PP, Weckhuysen BM, Cirujano FG, De Vos D, et al. Increasing the availability of active sites in Zn-Co double metal cyanides by dispersion onto a SiO₂ support. *Journal of Catalysis* 2017; 354: 92-99.
- Menczel JD, Judovits L, Prime RB, Bair HE, Reading M, Swier S. Differential Scanning Calorimetry (DSC). *Thermal Analysis of Polymers*. John Wiley & Sons, Inc., 2008, pp. 7-239.

- Meng Q, Cheng R, Li J, Wang T, Liu B. Copolymerization of CO₂ and propylene oxide using ZnGA/DMC composite catalyst for high molecular weight poly(propylene carbonate). *Journal of CO₂ Utilization* 2016; 16: 86-96.
- Miao S, Callow N, Wang P, Liu Y, Su Z, Zhang S. Soybean Oil-Based Polyurethane Networks: Shape-Memory Effects and Surface Morphologies. *Journal of the American Oil Chemists' Society* 2013; 90: 1415-1421.
- Miao S, Wang P, Su Z, Zhang S. Vegetable-oil-based polymers as future polymeric biomaterials. *Acta Biomaterialia* 2014; 10: 1692-1704.
- Michelle. Why coconut oil is the best hair oil (and how to use it) 2020, 2020.
- Milios L, Holm Christensen L, McKinnon D, Christensen C, Rasch MK, Hallstrøm Eriksen M. Plastic recycling in the Nordics: A value chain market analysis. *Waste Management* 2018; 76: 180-189.
- Mittal V. *Characterization Techniques for Polymer Nanocomposites*: Wiley, 2012.
- Mizera K, Ryszkowska J. Polyurethane elastomers from polyols based on soybean oil with a different molar ratio. *Polymer Degradation and Stability* 2016; 132: 21-31.
- Moharir RV, Kumar S. Challenges associated with plastic waste disposal and allied microbial routes for its effective degradation: A comprehensive review. *Journal of Cleaner Production* 2019; 208: 65-76.
- Molekuul.be. Olive oil triglyceride (glyceryl trioleate, triolein). Example of an olive oil triglyceride, containing 3 oleic acid moieties. Skeletal formula. 2020, 2020.
- Monroe K, Kirk T, Hull V, Biswas E, Murawski A, Quirino RL. *Vegetable Oil-Based Polymeric Materials: Synthesis, Properties, and Applications*. Reference Module in *Materials Science and Materials Engineering*. Elsevier, 2019.
- Montero de Espinosa L, Meier MAR. Plant oils: The perfect renewable resource for polymer science?! *European Polymer Journal* 2011; 47: 837-852.

MPOB. About Palm Oil. 2020, 2011.

Murillo G, Ali SS, Sun J, Yan Y, Bartocci P, El-Zawawy N, et al. Ultrasonic emulsification assisted immobilized *Burkholderia cepacia* lipase catalyzed transesterification of soybean oil for biodiesel production in a novel reactor design. *Renewable Energy* 2019; 135: 1025-1034.

Muthuraj R, Mekonnen T. Recent progress in carbon dioxide (CO₂) as feedstock for sustainable materials development: Co-polymers and polymer blends. *Polymer* 2018; 145: 348-373.

Ni K, Kozak CM. Kinetic Studies of Copolymerization of Cyclohexene Oxide with CO₂ by a Diamino-bis(phenolate) Chromium(III) Complex. *Inorganic Chemistry* 2018; 57: 3097-3106.

Oh HJ, Ko YS. Effect of polymerization conditions on the polymer properties of CO₂-cyclohexene oxide copolymer prepared by double metal cyanide catalyst. *Journal of Industrial and Engineering Chemistry* 2013; 19: 1939-1943.

Otabor GO, Ifijen IH, Mohammed FU, Aigbodion AI, Ikhuoria EU. Alkyd resin from rubber seed oil/linseed oil blend: A comparative study of the physiochemical properties. *Heliyon* 2019; 5: e01621.

Pagga U. Testing biodegradability with standardized methods. *Chemosphere* 1997; 35: 2953-2972.

Parada Hernandez NL, Bahú JO, Schiavon MIRB, Bonon AJ, Benites CI, Jardini AL, et al. (Epoxidized castor oil – citric acid) copolyester as a candidate polymer for biomedical applications. *Journal of Polymer Research* 2019; 26: 149.

Patil A, Patel A, Purohit R. An overview of Polymeric Materials for Automotive Applications. *Materials Today: Proceedings* 2017; 4: 3807-3815.

- Patil MV, Yadav MK, Jasra RV. Prins condensation for synthesis of nopol from β -pinene and paraformaldehyde on novel Fe–Zn double metal cyanide solid acid catalyst. *Journal of Molecular Catalysis A: Chemical* 2007; 273: 39-47.
- Peeters A, Valvekens P, Ameloot R, Sankar G, Kirschhock CEA, De Vos DE. Zn–Co Double Metal Cyanides as Heterogeneous Catalysts for Hydroamination: A Structure–Activity Relationship. *ACS Catalysis* 2013; 3: 597-607.
- Pescarmona PP, Taherimehr M. Challenges in the catalytic synthesis of cyclic and polymeric carbonates from epoxides and CO₂. *Catalysis Science & Technology* 2012; 2: 2169-2187.
- Petrović ZS. Polyurethanes from Vegetable Oils. *Polymer Reviews* 2008; 48: 109-155.
- Petrović ZS, Zlatanić A, Lava CC, Sinadinović-Fišer S. Epoxidation of soybean oil in toluene with peroxyacetic and peroxyformic acids — kinetics and side reactions. *European Journal of Lipid Science and Technology* 2002; 104: 293-299.
- Piccolo D, Vianello C, Lorenzetti A, Maschio G. Epoxidation of soybean oil enhanced by microwave radiation. *Chemical Engineering Journal* 2019; 377: 120113.
- Pinilla-de Dios M, Andrés-Iglesias C, Fernández A, Salmi T, Galdámez JR, García-Serna J. Effect of Zn/Co initial preparation ratio in the activity of double metal cyanide catalysts for propylene oxide and CO₂ copolymerization. *European Polymer Journal* 2017; 88: 280-291.
- PlasticsEurope. *Plastics – the Facts 2018: An analysis of European plastics production, demand and waste data*. 2019. PlasticsEurope, Brussels – Belgium, 2018.
- Poland SJ, Darensbourg DJ. A quest for polycarbonates provided via sustainable epoxide/CO₂ copolymerization processes. *Green Chemistry* 2017; 19: 4990-5011.
- Qiang L, Zhifang G, Lisha P, Xue X. Zn–Cr double metal cyanide catalysts synthesized by ball milling for the copolymerization of CO₂/propylene oxide, phthalic

- anhydride/propylene oxide, and CO₂/propylene oxide/phthalic anhydride. *Catalysis Communications* 2015; 64: 114-118.
- Raman SK, Deacy AC, Pena Carrodegua L, Reis NV, Kerr RWF, Phanopoulos A, et al. Ti(IV)–Tris(phenolate) Catalyst Systems for the Ring-Opening Copolymerization of Cyclohexene Oxide and Carbon Dioxide. *Organometallics* 2020; 39: 1619-1627.
- Raupach MR, Marland G, Ciais P, Le Quéré C, Canadell JG, Klepper G, et al. Global and regional drivers of accelerating CO₂ emissions. *Proc Natl Acad Sci U S A* 2007; 104: 10288-93.
- Rebecca Lindsey. *Climate Change: Atmospheric Carbon Dioxide*. 2020. Climate.gov, 2020.
- Ree M, Bae JY, Jung JH, Shin TJ, Hwang Y-T, Chang T. Copolymerization of carbon dioxide and propylene oxide using various zinc glutarate derivatives as catalysts. *Polymer Engineering & Science* 2000; 40: 1542-1552.
- Ren W-M, Liu Y, Xin A-X, Fu S, Lu X-B. Single-Site Bifunctional Catalysts for COX (X = O or S)/Epoxides Copolymerization: Combining High Activity, Selectivity, and Durability. *Macromolecules* 2015; 48: 8445-8450.
- Ren WM, Liu ZW, Wen YQ, Zhang R, Lu XB. Mechanistic aspects of the copolymerization of CO₂ with epoxides using a thermally stable single-site cobalt(III) catalyst. *J. Am. Chem. Soc.* 2009; 131.
- Rokaya D, Srimaneepong V, Sapkota J, Qin J, Siraleartmukul K, Siriwongrungson V. Polymeric Materials and Films in Dentistry: An overview. *Journal of Advanced Research* 2018.
- Ronda JC, Lligadas G, Galià M, Cádiz V. Vegetable oils as platform chemicals for polymer synthesis. *European Journal of Lipid Science and Technology* 2011; 113: 46-58.

- Rudnik E. Chapter 6 - Biodegradability testing of compostable polymer materials under laboratory conditions. In: Rudnik E, editor. *Compostable Polymer Materials (Second Edition)*. Elsevier, Boston, 2019, pp. 163-237.
- Rüsch gen. Klaas M, Warwel S. Complete and partial epoxidation of plant oils by lipase-catalyzed perhydrolysis. Based partly on a lecture at the International Conference of the Association for the Advancement of Industrial Crops, Saltillo, Mexico, September 14–18, 1997. *Industrial Crops and Products* 1999; 9: 125-132.
- Saeidi S, Amin NAS, Rahimpour MR. Hydrogenation of CO₂ to value-added products—A review and potential future developments. *Journal of CO₂ Utilization* 2014; 5: 66-81.
- Sahoo Sushanta K, Khandelwal V, Manik G. Development of toughened bio-based epoxy with epoxidized linseed oil as reactive diluent and cured with bio-renewable crosslinker. *Polymers for Advanced Technologies* 2017; 29: 565-574.
- Sakakura T, Choi J-C, Yasuda H. Transformation of Carbon Dioxide. *Chemical Reviews* 2007; 107: 2365-2387.
- Salih A, Ahmad M, Ibrahim N, Dahlan K, Tajau R, Mahmood M, et al. Synthesis of Radiation Curable Palm Oil-Based Epoxy Acrylate: NMR and FTIR Spectroscopic Investigations. *Molecules* 2015; 20: 14191.
- Sankar M, Ajithkumar TG, Sankar G, Manikandan P. Supported imidazole as heterogeneous catalyst for the synthesis of cyclic carbonates from epoxides and CO₂. *Catalysis Communications* 2015; 59: 201-205.
- Satyarthi JK, Srinivas D, Ratnasamy P. Hydrolysis of vegetable oils and fats to fatty acids over solid acid catalysts. *Applied Catalysis A: General* 2011; 391: 427-435.
- Schneider D. *Culinary Herbs & Spices Illustrations Available for Stock Use*. 2014.

- Sebastian J, Darbha S. Structure-induced catalytic activity of Co–Zn double-metal cyanide complexes for terpolymerization of propylene oxide, cyclohexene oxide and CO₂. *RSC Advances* 2015; 5: 18196-18203.
- Sebastian J, Srinivas D. Effects of method of preparation on catalytic activity of Co–Zn double-metal cyanide catalysts for copolymerization of CO₂ and epoxide. *Applied Catalysis A: General* 2014; 482: 300-308.
- Sebastian J, Srinivas D. Factors influencing catalytic activity of Co–Zn double-metal cyanide complexes for alternating polymerization of epoxides and CO₂. *Applied Catalysis A: General* 2015; 506: 163-172.
- Seniha Güner F, Yağcı Y, Tuncer Erciyes A. Polymers from triglyceride oils. *Progress in Polymer Science* 2006; 31: 633-670.
- Shah AA, Hasan F, Hameed A, Ahmed S. Biological degradation of plastics: A comprehensive review. *Biotechnology Advances* 2008; 26: 246-265.
- Shahbandeh M. Olive oil: global production volume 2012/13-2019/20. 2020, 2020.
- Shao H, Reddi Y, Cramer CJ. Modeling the Mechanism of CO₂/Cyclohexene Oxide Copolymerization Catalyzed by Chiral Zinc β-Diiminates: Factors Affecting Reactivity and Isotacticity. *ACS Catalysis* 2020; 10: 8870-8879.
- Sheng X, Wu W, Qin Y, Wang X, Wang F. Efficient synthesis and stabilization of poly(propylene carbonate) from delicately designed bifunctional aluminum porphyrin complexes. *Polymer Chemistry* 2015; 6: 4719-4724.
- Shi J, Shi Z, Yan H, Wang X, Zhang X, Lin Q, et al. Synthesis of Zn–Fe double metal cyanide complexes with imidazolium-based ionic liquid cocatalysts via ball milling for copolymerization of CO₂ and propylene oxide. *RSC Advances* 2018; 8: 6565-6571.

- Sienkiewicz AM, Czub P. The unique activity of catalyst in the epoxidation of soybean oil and following reaction of epoxidized product with bisphenol A. *Industrial Crops and Products* 2016; 83: 755-773.
- Srivastava R, Srinivas D, Ratnasamy P. Fe–Zn double-metal cyanide complexes as novel, solid transesterification catalysts. *Journal of Catalysis* 2006; 241: 34-44.
- Stoffella PJ, Kahn BA. *Compost Utilization In Horticultural Cropping Systems*: CRC Press, 2001.
- Subhani MA, Gürtler C, Leitner W, Müller TE. Nanoparticulate TiO₂-Supported Double Metal Cyanide Catalyst for the Copolymerization of CO₂ with Propylene Oxide. *European Journal of Inorganic Chemistry* 2016; 2016: 1944-1949.
- Sudakar P, Sivanesan D, Yoon S. Copolymerization of Epichlorohydrin and CO₂ Using Zinc Glutarate: An Additional Application of ZnGA in Polycarbonate Synthesis. *Macromolecular Rapid Communications* 2016; 37: 788-793.
- Suh HS, Ha JY, Yoon JH, Ha C-S, Suh H, Kim I. Polyester polyol synthesis by alternating copolymerization of propylene oxide with cyclic acid anhydrides by using double metal cyanide catalyst. *Reactive and Functional Polymers* 2010; 70: 288-293.
- Sun X-K, Zhang X-H, Chen S, Du B-Y, Wang Q, Fan Z-Q, et al. One-pot terpolymerization of CO₂, cyclohexene oxide and maleic anhydride using a highly active heterogeneous double metal cyanide complex catalyst. *Polymer* 2010; 51: 5719-5725.
- Sun X-K, Zhang X-H, Wei R-J, Du B-Y, Wang Q, Fan Z-Q, et al. Mechanistic insight into initiation and chain transfer reaction of CO₂/cyclohexene oxide copolymerization catalyzed by zinc–cobalt double metal cyanide complex catalysts. 2012; 50: 2924-2934.
- Sundberg C, Jönsson H. Higher pH and faster decomposition in biowaste composting by increased aeration. *Waste Management* 2008; 28: 518-526.

- Taherimehr M, Pescarmona PP. Green polycarbonates prepared by the copolymerization of CO₂ with epoxides. 2014; 131: 41141.
- Tang L, Xiao M, Xu Y, Wang S, Meng Y. Zinc adipate/tertiary amine catalytic system: efficient synthesis of high molecular weight poly(propylene carbonate). Journal of Polymer Research 2013; 20: 1-9.
- Taşcı Z, Ulusoy M. Efficient pathway for CO₂ transformation to cyclic carbonates by heterogeneous Cu and Zn salen complexes. Journal of Organometallic Chemistry 2012; 713: 104-111.
- Teo AJT, Mishra A, Park I, Kim Y-J, Park W-T, Yoon Y-J. Polymeric Biomaterials for Medical Implants and Devices. ACS Biomaterials Science & Engineering 2016; 2: 454-472.
- Tharun J, Dharman MM, Hwang Y, Roshan R, Park MS, Park D-W. Tuning double metal cyanide catalysts with complexing agents for the selective production of cyclic carbonates over polycarbonates. Applied Catalysis A: General 2012; 419–420: 178-184.
- The American Soybean Association. SoyStats® 2020 International : World Soybean Production. 2020, 2020.
- Tokiwa Y, Calabia BP. Biodegradability and Biodegradation of Polyesters. Journal of Polymers and the Environment 2007; 15: 259-267.
- Tomlinson EP, Hay ME, Boudouris BW. Radical Polymers and Their Application to Organic Electronic Devices. Macromolecules 2014; 47: 6145-6158.
- Tosin M, Degli-Innocenti F, Bastioli C. Detection of a Toxic Product Released by a Polyurethane-Containing Film Using a Composting Test Method Based on a Mineral Bed. Journal of environmental polymer degradation 1998; 6: 79-90.

- Tran CH, Kim SA, Moon Y, Lee Y, Ryu HM, Baik JH, et al. Effect of dicarbonyl complexing agents on double metal cyanide catalysts toward copolymerization of CO₂ and propylene oxide. *Catalysis Today* 2020.
- Trott G, Garden JA, Williams CK. Heterodinuclear zinc and magnesium catalysts for epoxide/CO₂ ring opening copolymerizations. *Chemical Science* 2019; 10: 4618-4627.
- Trott G, Saini PK, Williams CK. Catalysts for CO₂/epoxide ring-opening copolymerization. *Philosophical Transactions of the Royal Society A: Mathematical, Physical and Engineering Sciences* 2016; 374.
- Tuomela M, Hatakka A, Karjomaa S, Itävaara M. Priming effect as determined by adding ¹⁴C-glucose to modified controlled composting test. *Biodegradation* 2002; 13: 131-40.
- US Food and Drug Administration. Bisphenol A (BPA): Use in Food Contact Application. US Food and Drug Administration,, 2014.
- van Broekhuizen P, Theodori D, Blansch KL, Ullmer S. *Lubrication in Inland and Coastal Water Activities*: Taylor & Francis, 2003.
- Varghese JK, Park DS, Jeon JY, Lee BY. Double metal cyanide catalyst prepared using H₃Co(CN)₆ for high carbonate fraction and molecular weight control in carbon dioxide/propylene oxide copolymerization. 2013; 51: 4811-4818.
- Veronese L, Brivio M, Biagini P, Po R, Tritto I, Losio S, et al. Effect of Quaternary Phosphonium Salts as Cocatalysts on Epoxide/CO₂ Copolymerization Catalyzed by salen-Type Cr(III) Complexes. *Organometallics* 2020; 39: 2653-2664.
- Wang C-S, Yang L-T, Ni B-L, Shi G. Polyurethane networks from different soy-based polyols by the ring opening of epoxidized soybean oil with methanol, glycol, and 1,2-propanediol. 2009; 114: 125-131.
- Wang JT, Shu D, Xiao M, Meng YZ. Copolymerization of carbon dioxide and propylene oxide using zinc adipate as catalyst. *Journal of Applied Polymer Science* 2006; 99: 200-206.

- Wang Z, Bu Z, Cao T, Ren T, Yang L, Li W. A novel and recyclable catalytic system for propylene carbonate synthesis from propylene oxide and CO₂. *Polyhedron* 2012; 32: 86-89.
- Way C, Wu DY, Dean K, Palombo E. Design considerations for high-temperature respirometric biodegradation of polymers in compost. *Polymer Testing* 2010; 29: 147-157.
- Wei R-J, Zhang X-H, Du B-Y, Fan Z-Q, Qi G-R. Selective production of poly(carbonate-co-ether) over cyclic carbonate for epichlorohydrin and CO₂ copolymerization via heterogeneous catalysis of Zn-Co (III) double metal cyanide complex. *Polymer* 2013; 54: 6357-6362.
- Woods End Laboratories Incorporated. *Interpreting Waste & Compost Tests Vol 2.* . Woods End Research Laboratory, Mt Vernon, ME, 2005, pp. 6.
- World Economic Forum LLC. World Economic Forum. *The New Plastics Economy: Rethinking the future of plastics.* Industry Agenda. 2019, Geneva, Switzerland, 2016.
- Wu G-P, Wei S-H, Ren W-M, Lu X-B, Li B, Zu Y-P, et al. Alternating copolymerization of CO₂ and styrene oxide with Co(III)-based catalyst systems: differences between styrene oxide and propylene oxide. *Energy & Environmental Science* 2011; 4: 5084-5092.
- Wu G-P, Xu P-X, Zu Y-P, Ren W-M, Lu X-B. Cobalt(III)-complex-mediated terpolymerization of CO₂, styrene oxide, and epoxides with an electron-donating group. *Journal of Polymer Science Part A: Polymer Chemistry* 2013; 51: 874-879.
- Wulf C, Doering U, Werner T. Copolymerization of CO₂ and epoxides mediated by zinc organyls. *RSC Advances* 2018; 8: 3673-3679.
- Xia Y, Larock RC. Vegetable oil-based polymeric materials: synthesis, properties, and applications. *Green Chemistry* 2010; 12: 1893-1909.

- Xu Y, Lin L, He C-T, Qin J, Li Z, Wang S, et al. Kinetic and mechanistic investigation for the copolymerization of CO₂ and cyclohexene oxide catalyzed by trizinc complexes. *Polymer Chemistry* 2017; 8: 3632-3640.
- Yongphet P, Wang J, Kiatsiriroat T, Wang D, Deethayat T, Quaye EK, et al. Enhancement of biodiesel production from soybean oil by electric field and its chemical kinetics. *Chemical Engineering and Processing - Process Intensification* 2020; 153: 107997.
- Yu SJ, Liu Y, Byeon SJ, Park DW, Kim I. Ring-opening polymerization of propylene oxide by double metal cyanide catalysts prepared by reacting CoCl₂ with various metal cyanide salts. *Catalysis Today* 2014; 232: 75-81.
- Zainal NA, Zulkifli NWM, Gulzar M, Masjuki HH. A review on the chemistry, production, and technological potential of bio-based lubricants. *Renewable and Sustainable Energy Reviews* 2018; 82: 80-102.
- Zhang C, Garrison TF, Madbouly SA, Kessler MR. Recent advances in vegetable oil-based polymers and their composites. *Progress in Polymer Science* 2017; 71: 91-143.
- Zhang J, Tang JJ, Zhang JX. Polyols Prepared from Ring-Opening Epoxidized Soybean Oil by a Castor Oil-Based Fatty Diol. *International Journal of Polymer Science* 2015a; 2015: 8.
- Zhang M, Yang Y, Chen L. Preparation of crown ether complexing highly active double metal cyanide catalysts and copolymerization of CO₂ and propylene oxide. *Chinese Journal of Catalysis* 2015b; 36: 1304-1311.
- Zhang X-H, Hua Z-J, Chen S, Liu F, Sun X-K, Qi G-R. Role of zinc chloride and complexing agents in highly active double metal cyanide catalysts for ring-opening polymerization of propylene oxide. *Applied Catalysis A: General* 2007; 325: 91-98.

- Zhang X-H, Liu F, Sun X-K, Chen S, Du B-Y, Qi G-R, et al. Atom-Exchange Coordination Polymerization of Carbon Disulfide and Propylene Oxide by a Highly Effective Double-Metal Cyanide Complex. *Macromolecules* 2008; 41: 1587-1590.
- Zhang X-H, Wei R-J, Sun X-K, Zhang J-F, Du B-Y, Fan Z-Q, et al. Selective copolymerization of carbon dioxide with propylene oxide catalyzed by a nanolamellar double metal cyanide complex catalyst at low polymerization temperatures. *Polymer* 2011.
- Zhang X-H, Wei R-J, Zhang YY, Du B-Y, Fan Z-Q. Carbon Dioxide/Epoxy Copolymerization via a Nanosized Zinc–Cobalt(III) Double Metal Cyanide Complex: Substituent Effects of Epoxides on Polycarbonate Selectivity, Regioselectivity and Glass Transition Temperatures. *Macromolecules* 2015c; 48: 536-544.
- Zhang Y-Y, Zhang X-H, Wei R-J, Du B-Y, Fan Z-Q, Qi G-R. Synthesis of fully alternating polycarbonate with low T_g from carbon dioxide and bio-based fatty acid. *RSC Advances* 2014; 4: 36183-36188.
- Zhi Y, Miao Y, Zhao W, Wang J, Zheng Y, Su H, et al. Simultaneous terpolymerization of CO₂/SO₂ with epoxide and mechanistic understanding. Vol 165, 2019.
- Zhi Y, Shan X, Shan S, Jia Q, Ni Y, Zeng G. Synthesis and thermal degradation kinetics of new terpolymer of carbon dioxide, cyclohexene oxide and alpha-pinene oxide. *Journal of CO₂ Utilization* 2017; 22: 299-306.
- Zhu W, Du L, Qian S, Yang Q, Song W. Copolymerization of carbon dioxide and propylene oxide by several metallosalen-based bifunctional catalysts. *Journal of the Chinese Chemical Society* 2018; 65: 841-849.
- Zia F, Zia KM, Zuber M, Kamal S, Aslam N. Starch based polyurethanes: A critical review updating recent literature. *Carbohydrate Polymers* 2015; 134: 784-798.
- Zuk M, Richter D, Matuła J, Szopa J. Linseed, the multipurpose plant. *Industrial Crops and Products* 2015; 75: 165-177.